Technische Universität München
Fakultät für Medizin

Expression of human endogenous retrovirus type K HML2 in hepatitis C patients treated with direct acting antiviral therapy

Melanie Maria Weber

Vollständiger Abdruck der von der Fakultät für Medizin der Technischen Universität München zur Erlangung des akademischen Grades einer Doktorin der Medizinischen Wissenschaft (Dr. med. sci.) genehmigten Dissertation.

Vorsitzende: Prof. Dr. Angela Krackhardt

Prüferinnen der Dissertation:

1. Prof. Dr. Ulrike Protzer
2. Priv.-Doz. Dr. Martina Anton
3. Priv.-Doz. Dr. Ursula Ehmer

Die Dissertation wurde am 07.05.2021 bei der Technischen Universität eingereicht und durch die Fakultät für Medizin am 08.12.2021 angenommen.

Zusammenfassung

Humane endogene Retroviren (HERVs) haben sich vor über 40 Millionen Jahren in die menschliche DNA integriert und haben einen Anteil von bis zu acht Prozent am menschlichen Genom. Obwohl jene normalerweise still sind, können sie reaktiviert werden und die Genexpression beeinflussen. Die Expression von HERV-K Untertyp HML2 wurde beispielsweise bei Leberzirrhose oder hepatozellulärem Karzinom als signifikant erhöht beschrieben. Jedoch muss die Rolle von HERV-K HML2 in Hepatitis C erst noch geklärt werden.

In dieser Studie wurden 42 Hepatitis C Patienten mit einer direkt agierenden antiviralen (DAA) Kombinationstherapie behandelt. Klinische und experimentelle Parameter wurden zu Therapiebeginn (baseline), in Woche 2 und Woche 4, am Ende der Behandlung sowie 12 Wochen nach Ende der DAA-Therapie, was als anhaltendes virologisches Ansprechen 12 (SVR 12) bezeichnet wird, gesammelt. Zusätzlich wurden vier gesunde Probanden eingeschlossen, um die HERV-K HML2 Expression mit der gesunder Erwachsener zu vergleichen. Das Blut der Hepatitis C Patienten und der gesunden Kontrollen wurde auf die Expression von HERV-K HML2 sowie der Entzündungsmarker tumor necrosis factor alpha-induced protein 3 (A20), interferon gamma-induced protein 10 (IP-10), interleukin-6 und interleukin-10 untersucht.

93% der Patienten konnten ein anhaltendes virologisches Ansprechen erreichen. Die Leberfunktion der Patienten verbesserte sich, was sich laborchemisch durch eine signifikante Verbesserung der Gamma-Glutamyltransferase, Aspartat-Aminotransferase und Alanin-Aminotransferase zeigte. Leberzirrhose und ein Albuminspiegel von $\leq$ 35 g/l zeigten eine signifikante Korrelation mit klinischen Parametern einer schlechteren Leberfunktion.
Eine erhöhte HERV-K HML2 Expression war stark mit niedrigem Albumin und Leberzirrhose in Hepatitis C Patienten assoziiert. Die HERV-K HML2 Expression zu Therapiebeginn korrelierte mit der quantitativen Hepatitis C Virus RNA zum Zeitpunkt SVR 12.
Hepatitis C Patienten ohne Leberzirrhose sowie diejenigen mit einem Albuminspiegel über 35 g/l zeigten signifikant niedrigere Expression von HERV-K HML2 und gleichzeitig signifikant höhere Expression von IP-10 verglichen mit den gesunden Kontrollen. Die Höhe der IP-10 Expression nahm nach Beginn der DAA-Therapie ab und zum Zeitpunkt SVR 12 konnte kein signifikanter Unterschied in der Höhe der Genexpression von IP-10 zwischen den Hepatitis C Patienten und den gesunden Probanden festgestellt werden.

Diese Arbeit zeigt den Zusammenhang zwischen HERV-K HML2 und Leberzirrhose sowie niedrigen Albuminwerten in Hepatitis C Patienten zum ersten Mal. Darüber hinaus zeigten Patienten, die kein anhaltendes virologisches Ansprechen erreichen konnten, signifikant höhere Expression von HERV-K HML2 zu Behandlungsbeginn, was darauf hinweist, dass HERV-K HML2 als Kandidat für einen Biomarker zur Evaluation von Therapieerfolg herangezogen werden könnte. Die Daten zeigen eine klare Notwendigkeit, die funktionelle Rolle von HERVs in der Pathogenese des Hepatitis C Virus zu verstehen, um die antivirale Therapie zu verbessern.

Abstract

Human endogenous retroviruses (HERVs) integrated into the human DNA over 40 million years ago and make up eight percent of the human genome. Even though they are usually silenced, they can be reactivated in diseases and consequently modify gene expression. Expression of HERV-K subtype HML2 has been shown to be significantly increased in liver cirrhosis and hepatocellular carcinoma. However, the role of HERV-K HML2 in hepatitis C has yet to be elucidated.

In this study, 42 hepatitis C patients were treated with direct acting antiviral (DAA) combination therapy. Clinical and experimental parameters were monitored at baseline, week 2, week 4, end of treatment and 12 weeks after completion of DAA treatment, referred to as sustained virologic response 12 (SVR 12). To compare HERV-K HML2 levels with those of healthy adults, four healthy controls were included. Patients as well as healthy controls were screened for expression of HERV-K HML2 as well as four inflammation markers: tumor necrosis factor alpha-induced protein 3 (A20), interferon gamma-induced protein 10 (IP-10), interleukin-6 (IL-6) and interleukin-10 (IL-10).

93 % of patients achieved sustained viral respons. Liver function improved throughout treatment as alanin-aminotransferase, aspartate-aminotransferase and gamma-glutamyl transferase decreased significantly. Liver cirrhosis and albumin levels of $\leq$ 35 g/l significantly correlated with clinical parameters indicating worse liver function.
Higher HERV-K HML2 expression levels were strongly associated with lower albumin levels and with the presence of liver cirrhosis in HCV positive patients. HERV-K HML2 levels at baseline were significantly correlated with quantitative hepatitis C virus RNA at SVR 12.
Hepatitis C patients without liver cirrhosis as well as those with baseline albumin levels of > 35 g/l showed significantly lower HERV-K HML2 levels and significantly higher IP-10 expression at baseline than healthy controls. IP-10 expression levels declined after start of DAA treatment and at SVR 12 no significant difference of IP-10 levels between hepatitis C patients and healthy controls could be detected.

This thesis provides the first evidence of an association of HERV-K HML2 and hepatitis C patients with liver cirrhosis as well as low albumin levels. Above, the patients who failed to achieve sustained viral response showed significantly higher expression levels of HERV-K HML2 at baseline indicating that HERV-K HML2 might be considered as a biomarker candidate for

successful treatment. These data clearly highlight the necessity to understand the functional role of HERVs in HCV pathogenesis to improve antiviral treatment.

Nomenclature

$A20$ Tumor necrosis factor alpha-induced protein 3

$ADAMTS$ A disintegrin and metalloproteinase with thrombospondin motifs

AKT Protein kinase B

$ALAT$ Alanin amino transferase

ALS Amyotrophic lateral sclerosis

$ASAT$ Aspartate amino transferase

CD Cluster of differentiation

CMV Cytomegalovirus

CRP C-reactive protein

DAA Direct acting antivirals

DNA Deoxyribonucleic acid

EBV Ebstein Barr virus

$EGRF$ Epidermal growth factor receptor

EOT End of treatment

ERK Extracellular signal-regulated kinases

GGT Gamma-glutamyl transferase

HC Healthy control

HCC Hepatocellular carcinoma

HCV Hepatitis C virus

$HERV$ Human endogenous retrovirus

HHV Human herpes virus

HIV Human immunodeficiency virus

HML Human endogenous murine mammary tumor virus (MMTV)-like

IL Interleukin

INR International Normalized Ratio

$IP-10$ Interferon-gamma induced protein 10

$IRAK4$ Interleukin-1 receptor-associated kinase 4

IRF Interferon regulatory factor

LC Liver cirrhosis

LTR Long terminal repeats

$MAPK$ Mitogen-activated protein kinase

MEK Mitogen-activated protein kinase kinase

$MMTV$ Murine mammary tumor virus

$mTOR$ Mammalian target of rapamycin

$Myd88$ Myeloid differentiation primary response 88

$NF-kB$ Nuclear factor kappa-light-chain-enhancer of activated B cells

NS Non-structural

NTR Non translated regions

ORF Open reading frame

$p70S6K$ Ribosomal protein S6 kinase beta-1

PAH Pulmonal arterial hypertension

$PBMC$ Peripheral blood mononuclear cells

PCR Polymerase chain reaction

$PI3K$ Phosphoinositide3-kinase

RA Rheumatoid arthritis

RF Rheumatoid factor

RNA Ribonucleic acid

RT Reverse transcriptase

$SARM1$ Sterile alpha and TIR motif containing 1

SVR Sustained viral response

TLR Toll like receptor

$VEGF(R)$ Vascular endothelial growth factor(receptor)

Contents

1 Introduction

1.1 Hepatitis C

1.1.1 Hepatitis C - a global burden

Worldwide 71 million people were chronically infected with hepatitis C virus (HCV) in 2019 (World Health Organization, 2020). With anti-HCV seroprevalence of 2.4 % in Central and Western Europe and 2.9 % in Eastern Europe hepatitis C affected millions of people in Europe alone. Anti-HCV seropositivity was most prevalent in North Africa and the Middle East (3.6 %) as well as Asia with an estimate of 3.5 % in 2005 (Mohd Hanafiah et al., 2013). In Germany the incidence of hepatitis C had been increasing since the second half of 2017. In 2018 there were 7.1 new infections per 100,000 inhabitants (Robert Koch Institut, 2019). The virus is contracted parenterally, e.g. by contaminated needles via tattooing, intravenous drug consumption or injuries in a health care setting (Alter et al., 1992). Vertical transmission from mother to child is yet another important, but less common, possibility. The risk of this way of transmission is 5.8 % for children of anti-HCV and HCV RNA positive mothers and 10.8 % of mothers co-infected with HIV (Benova et al., 2014). High risk groups can be derived from the most prevalent ways of infection. Up to around 50 years ago blood transfusions were a relevant risk factor for contraction of the virus in countries with high medical standards. Due to hygienic improvements blood transfusions no longer pose a high risk of contracting HCV in these regions. However, this is not necessarily true for resource limited countries. Egypt serves as an example as a big part of the population was infected through mass vaccination against shistosomiasis in the 1960s (Rao et al., 2002). While in 2005 14.2 % were anti-HCV positive (El-Zanaty & Way, 2009), 6.3 % of the 1 - 59 year old were seropositive in 2014 (Ministry of Health and Population, Cairo, Egypt et al., 2015), which is far above the global average. Additionally, blood transfusion protocols there only mandated anti-HCV antibodies which may remain negative for several weeks after infection, whereas HCV RNA is detectable much earlier by PCR (Abdelrazik et al., 2018). The combination of these factors contributes to a high risk of further transmission in countries like Egypt.

Symptoms of acute hepatitis C are unspecific. They may include, but are not limited to, jaundice, fatigue, abdominal pain in the right upper quadrant, ALAT and bilirubin elevation (Gerlach et al., 2003; Wiegand et al., 2006). As the incubation time is eight weeks and many patients are asymptomatic (Cox et al., 2005), diagnosis of acute hepatitis C is not rarely missed. Some of

the infected clear the virus spontaneously, however in 75 - 85 % the infection leads to chronic disease (Rustgi, 2007).

Nowadays the vast majority of patients can be cured as new antiviral medications, direct acting antivirals (DAA), were developed. If left untreated or treated unsuccessfully, chronic hepatitis C can lead to liver cirrhosis responsible for 720,000 deaths each year and eventually liver cancer causing approximately 470,000 deaths per year (Colombo et al., 1989; World Health Organization, 2017). Viral hepatitis, especially caused by HCV and HBV infection, is one of the leading causes of hepatocellular carcinoma (HCC) (de Martel et al., 2015). Thus, prevention and treatment of viral hepatitis are key factors for effective reduction of this global burden (Wedemeyer et al., 2015).

1.1.2 Hepatitis C virus

Hepatitis C virus is a hepacivirus within the flaviviridae family. It is a positive-sense single stranded RNA virus of 9.6 kb and a diameter of 50 - 65 mm.
In figure 1.1 the viral structure consisting of single-stranded RNA surrounded by the core protein and a lipid bilayer with envelope proteins E1 and E2 is depicted.

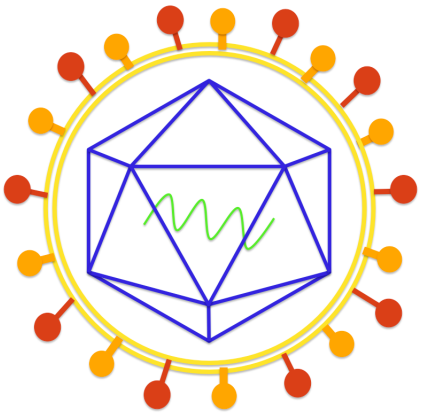

Figure 1.1 Hepatitis C virus: green = single-stranded RNA, blue = core, yellow = lipid bilayer, orange = E1, marroon = E2.

Distribution of HCV genotypes

Seven HCV genotypes are known. Above that high replication rates (Neumann et al., 1998) and the lack of a functioning proof reading system cause high genetic variability in HCV leading to quasispecies within an infected person (Moradpour et al., 2007). There are geographical differences in the distribution of genotypes. In Europe genotype 1 was most prevalent (64.4 %, worldwide 46.2 %) followed by genotype 3 making up 25.5 % (worldwide 30.1 %) of HCV infections (Petruzziello et al., 2016; Messina et al., 2015). In other regions genotype 2 was second most prevalent instead (Central Latin America 19.3 %, Western sub-Saharan Africa 23.0 %, Southeast Asia 18.2 %). In South Asia genotype 3 made up 71.6 %, in Eastern sub-Saharan Africa genotype 4 came in second with 30.7 % while this genotype took the first place in North Africa and Middle East with 65.3 %. In Southern sub-Saharan Africa genotype 5 made up 58.8 % and in East Asia genotype 6 was the second most prevalent genotype (16.2 %) after genotype 1 with 58.0 % (Messina et al., 2015). Genotype seven has been discovered in patients in Africa recently and seems not to have spread widely by this point in time (Murphy et al., 2015). Determination of the HCV genotype is not only important for therapeutic planning, but some genotypes showed

clinically relevant peculiarities. Genotype 3 for example has been shown to be associated with a higher score of steatosis (Rubbia-Brandt et al., 2000), which may be due to an interaction of HCV core with lipid droplets affecting lipid metabolism (Moradpour et al., 2007). Thus, knowledge about the genotype is important for patient assessment after diagnosis.

Structure of the HCV genome

Structurally, HCV consists of a 5' non translated region (NTR), an open reading frame (ORF) encoding for structural and non-structural (NS) proteins and a 3'NTR. Especially the non-structural proteins serve as targets for antiviral treatment as HCV replication can be interrupted by inhibiting parts of these proteins. Therefore the HCV genome and its function, mainly focusing on viral replication, is summarized here (figure 1.2).

The 5'NTR is highly preserved between genotypes and contains an internal ribosome entry site (IRES). IRES has an important role in high-level viral replication, but without the first 125 of 5'NTR which are located upstream of IRES replication itself is not achievable (Friebe et al., 2001).
The other end of the viral genome, 3'NTR, is mainly made up of short and variable sequences. Here, a 98 nucleotide element also known as 3'X or X-tail which is highly conserved is indispensable for replication (Friebe & Bartenschlager, 2002).

Core, the envelope proteins and p7 can be classified as structural HCV proteins. Core encodes for the viral nucleocapsid. It is an alpha helical protein found in ER membranes and membranous webs - distinct membrane alterations aiding viral replication by hosting replication complexes (Egger et al., 2002). The n-terminal domain is involved in RNA-binding and homo-oligomerization (Moradpour et al., 2007). The region between core and E1 is responsible for targeting the viral genome to the membrane of the endoplasmatic reticulum (ER), so E1 can translocate into its lumen (McLauchlan et al., 2002). E1 and E2 serve as building block for the viral envelope. p7 is also konwn as viroporin. This is due to its function as ion channel with two transmembrane domains (Griffin et al., 2003; Pavlovic et al., 2003). Additionally, it controls levels of E2 and is involved in viral particle maturation, packaging and release (Denolly et al., 2017).

Non-structural proteins NS2-5 are essential for viral replication. The c-terminal of NS2 in combination with the n-terminal third of NS3 form an autoprotease containing two composite active sites. NS3 surface patch is critical for the activation of the NS2 protease as well as NS5A hyperphosphorylation and thus may regulate active HCV replication (Isken et al., 2015). NS4A serves as co-factor of the NS3 serine protease with its center being integrated as component into the enzyme core (Shiryaev et al., 2012; Lin et al., 1995). The n-terminal of NS4A is responsible for the formation of the replication complex and NS3 harbors residues involved in membrane asso-

ciation of the NS3-4 complex (Brass et al., 2008). The two thirds of NS3 on the c-terminal side unwind RNA as RNA helicase and NTPase (Wardell et al., 1999). The complex as a whole inactivates proteins provoking a detection by the innate immune response (K. Li et al., 2005; Meylan et al., 2005). For replication positive-strand RNA viruses alter membranes. A specific one of these membrane alterations is called membranous web and is prompted by NS4B. HCV most likely modifies ER membranes for its membranous web (Gosert et al., 2003; Neufeldt et al., 2016).
NS5A is a phosphoprotein whose phosphorylation state of certain serine residues determines the efficiency of viral replication (Chong et al., 2016). Phosphorylation of NS5A is not only found in HCV, but also other hepaci- and flaviviridae. NS5A is responsible for binding the viral RNA to intracellular membranes. This tethering process results in the creation of a track for RNA to slide along (Moradpour et al., 2007). Other NS5A regions act as guardians of the viral RNA protecting it from being degraded by cellular RNAses or being detected by defense mechanisms (Moradpour et al., 2007).
NS5B produces a negative strand copy of the original HCV RNA and uses it as a template for the synthesis of the new positive strand RNA (Moradpour et al., 2007). RNA dependent RNA polymerase is the enzyme playing the main role in the process (Lohmann et al., 1997; Behrens et al., 1996). As it is essential for replication and shares motifs with RNA dependent RNA polymerases of other viruses, it serves as a candidate target for antiviral therapy. Apart from that NS5B also contains a cis-acting replication element in its c-terminal region (You et al., 2004).

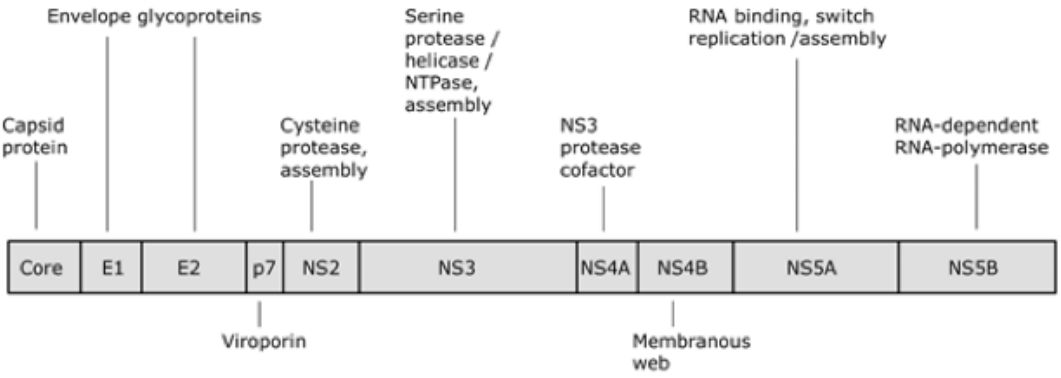

Figure 1.2 An overview of the functional proteins of the hepatitis C virus.

1.1.3 Diagnosis and current treatment schemes for hepatitis C

To diagnose hepatitis C, the level of anti-HCV antibodies is measured. If these antibodies are positive, a RT-PCR to measure HCV RNA is carried out as second step. Negative HCV RNA in combination with positive anti-HCV antibodies is a sign for healed acute HCV infection. In immunosuppressed patients anti-HCV antibodies may be falsely negative.
HCV RNA is measured by RT-PCR. The result of this test is called viral load and used as a parameter for infectiousness as well as treatment outcome. HCV RNA can be detectable 1 - 2

weeks after infection, whereas it takes 7 - 8 weeks until anti-HCV antibodies can be detected in blood samples (Pawlotsky, 2002). Consequently HCV RNA can also be used to detect acute HCV infection. Once HCV infection is confirmed the genotype is determined.
To get a clinical grasp of the state of disease, blood analyses and an HCC-screening consisting of abdominal sonography and an elastography of the liver will be performed. Blood analyses are used to determine if liver synthesis is impaired and if there are co-infections with HBV, HAV or HIV. Imaging methods help detect and monitor liver steatosis, fibrosis, or cirrhosis. Knowledge about these liver conditions is important for the assessment of the patients' risk to develop HCC (Sarrazin et al., 2018).

Acute hepatitis C generally is not an indication to start antiviral treatment, though it may be treated in individual cases. Yet, chronic HCV infection is an indication to start antiviral treatment irrespective of the absence of complications. First line therapy in Germany (Sarrazin et al., 2018) involves a combination of direct acting antivirals (DAAs) with a possible addition of the nucleoside analogon ribavirin. The selection of the preferable DAAs mainly depends on the HCV genotype. In some cases comorbidities, prior treatment and other factors have to be taken into account as well to choose the right agents.
Before DAAs revolutionized hepatitis C treatment in 2015, a combination of PEG IFN alpha and ribavarin had been used. Severity of adverse effects was an important issue and viral clearance was only achieved in less than half of the monoinfected patients and even less often in patients with complications or co-infections (Moreno et al., 2005). Thanks to advancements in the understanding of the HCV replication cycle and non-structural proteins the development of DAAs as drugs targeted at specific parts of the virus was possible. Nomenclature of these drugs is simple. Protease inhibitors end in "-previr" and target NS3/4. NS5A inhibitors are named "-asvir". The polymerase is located in NS5B and is the aim of drugs ending in "-buvir" (Zeuzem, 2017). With the combination of different DAAs and in some cases addition of ribavirin an overall sustained viral response of > 90 % can be achieved (Suwanthawornkul et al., 2015; Wei et al., 2018). As they are well tolerated, DAAs can be offered almost any patient irrespective of their comorbidities. However, due to the high cost of DAAs global accessibility remains an issue to be tackled.
Table 1.1 provides an overview of antiviral drugs used in this study. It defines the targets of the DAAs as well as the HCV genotypes the respective medication can be used against.

Targets of antiviral drugs applied in this study		
Drug	Target / mechanism	Genotype
Simeprevir	NS3 4	1
Daclatasvir	NS5A	1, 3
Ledipasvir	NS5A	1a, 1b, 4a, 5a, less activity: 2a, 3a
Exviera = Dasabuvir	NS5B	1
Viekirax	NS5A (ombitasvir) + NS3 4 (paritaprevir) and CYP3A4 (ritonavir)	1
Sofosbuvir	NS5B (in combination with other DAAs)	1 - 6
Ribavirin	Nucleoside analog	1 - 6

Table 1.1 Antiviral treatment: DAAs used in this study with their respective targets and suitable HCV genotypes (Spengler, 2018). Ribavirin is a nucleoside analog which can be used in addition to a combination therapy of two or more DAAs. Viekirax is a drug combination consisting of two DAAs and ritonavir, a CYP3A4 inhibitor.

In this study patients with genotypes 1, 3 and 4 were included. According to current German guidelines (Sarrazin et al., 2018) the following drug combinations can be applied in clinical routine for the respective genotypes:

Genotype 1	Genotype 3	Genotype 4
Ledipasvir + Sofosbuvir $\pm$ Ribavirin	Velpatasvir + Sofosbuvir	Velpatasvir + Sofosbuvir
Velpatasvir + Sofosbuvir	Daclatasvir + Sofosbuvir	Paritaprevir + Ombitasvir + Ribavirin
Grazoprevir + Elbasvir $\pm$ Ribavirin		Ledipasvir + Sofosbuvir $\pm$ Ribavirin
Paritaprevir + Ombitasvir + Dasabuvir $\pm$ Ribavirin		Grazoprevir + Elbasvir $\pm$ Ribavirin
Simeprevir + Sofosbuvir $\pm$ Ribavirin		Simeprevir + Sofosbuvir $\pm$ Ribavirin
Daclatasvir + Sofosbuvir $\pm$ Ribavirin		Daclatasvir + Sofosbuvir $\pm$ Ribavirin

Table 1.2 Antiviral combination treatment for different genotypes of HCV according to German guidelines (Sarrazin et al., 2018).

Notably, treatment approaches for genotype 1 are more diverse than for genotypes 3 and 4. For genotype 3 a NS5A-inhibitor is combined with a NS5B inhibitor and no ribavirin is added. For genotype 4 a protease inhibitor is included in any possible scheme.

1.2 Retroviruses

Retroviruses consist of a single stranded RNA genome that is reversely transcribed into a double stranded DNA by their reverse transcriptase. The produced DNA integrates into the genome of the host cell as a provirus.

There are three major coding sequences, gag, pol and env, within the genome (figure 1.3). Gag is responsible for synthesis of structural proteins, the matrix, and the capsid. Pol contains information for the polymerase which is a reverse transcriptase in retroviruses and env synthesizes the envelope. These sequences are surrounded by long terminal repeat (LTR) regions at the 3' and 5' ends (Coffin et al., 1997).

Figure 1.3 Genomic organization of the DNA of retroviruses (Coffin et al., 1997).

There are two subfamilies of retroviridae - Spumaretrovirinae and Orthoretroviridae (table 1.3). Spumaretrovirinae consist of a single genus whereas Orthoretroviridae consist of six genera. Some retroviruses are known to cause disease in humans, mammals or birds.

Family	Subfamily	Genus	Example
Retroviridae	Orthoretroviridae	Alpharetrovirus	Avian sarcoma virus
		Betaretrovirus	Mouse mammary tumor virus
		Gammaretrovirus	Feline leukemia virus
		Deltaretrovirus	Human T-cell leukemia virus
		Epsilonretrovirus	Walleye epidermal hyperplasia virus
		Lentivirus	Human immunodeficiency virus
	Spumaretrovirinae	Spumaretrovirus	Human foamy virus

Table 1.3 Classification of retroviridae (King et al., 2012).

Apart from exogenous retroviruses which contain all information needed to form infectious viral cycle and thus infectious particles there are endogenous retroviruses.

1.3 Human endogenous retroviruses

Human endogenous retroviruses (HERVs) are retroviral elements that first integrated into the human DNA over 40 million years ago (Mager & Freeman, 1995). These elements make up 8 % of the human genome (Lander et al., 2001).
There are three classes of HERVs (figure 1.4) according to their sequence homologies to exogenous retroviruses within the pol-gene. Class I are gamma-retrovirus related, class II are beta-retrovirus related and class III are spumavirus-related elements (Seifarth et al., 2005). Subdivision into viral families is based on sequence similarity of their putative tRNA primer binding site specificity. For example, the primer binding site for HERV-K matches the end of the tRNA of K, lysine (Ono et al., 1986). As oftentimes HERVs are primed by the same tRNA, pol sequence similarities and other structural traits are used for phylogenetic classification (Jern et al., 2005).

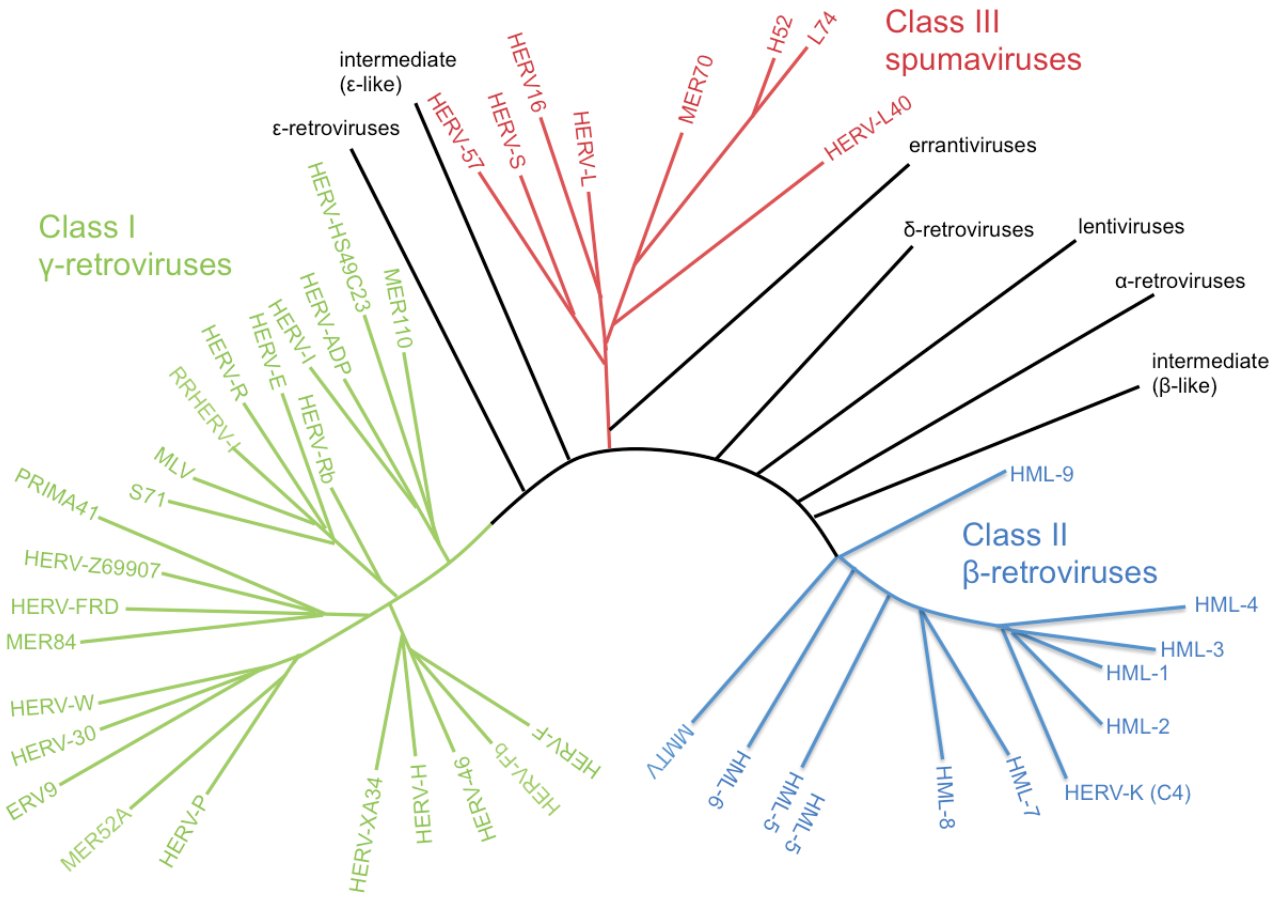

Figure 1.4 Classification of human endogenous retroviruses. HERV-K HML2 belongs to Class II or beta-retroviruses. Information in graph extracted from (Jern et al., 2005) and (Leib-Mösch & Seifarth, 1996)

The first invasion of HERVs into the primate genome took place before the separation of the lineage of old (catarrhine) and new world monkeys (platyrrhine) more than 40 million years ago (Mager & Freeman, 1995; Takahata & Satta, 1997). The majority of identified HERVs was found in old world monkeys only. As germline cells were infected, HERVs are passed to subsequent generations by vertical transmission. Proliferation was mainly achieved by retrotransposition as in HERV-H or reinfection as in HERV-K HML2. Within new world monkeys a wide range of amplification and distribution took place. The youngest amplification event occured after the separation of chimpanzees from humans which happened about 5 - 7 million years ago (Glazko, 2003). Insertion polymorphisms found in HERV-K HML2 hint at recent or even ongoing reinfections (Mamedov et al., 2004). Due to their early integration into the primate genome HERVs represent millions of years of primate and human evolution.

HERVs are structured similarly to exogenous retroviruses with retroviral protein genes surrounded by long terminal repeat (LTR) regions (Yu et al., 2013). The LTR regions at the 3' and 5' ends may function as promoter or enhancer regions crucial for retroviral transcription. The 3' LTR region consists of U3 containing promoters, enhancer-elements and transcription factor binding sites. The 5' LTR consists of R, defined as the starting point of transcription within the 5' LTR. R con-

tains a polyadenylation site at the border to U5 (Baust et al., 2001; Lania et al., 1992). These elements may affect the expression of neighboring genes and thus the activation of oncogenes or inactivation of tumor suppressor genes. HERV-K HML2 expresses spliced RNA encoding Np9 (Armbruester et al., 2002) and Rec (Löwer et al., 1995), proteins involved in oncogenesis, that are shown to be elevated in cancerous tissue compared to non-pathological cells of the same cell type (Büscher et al., 2006; Tavakolian, Goudarzi, & Faghihloo, 2019; Tavakolian, Goudarzi, Lak, & Faghihloo, 2019; Chen et al., 2013; Chan et al., 2019), but also in some healthy tissues (Schmitt et al., 2015). Gag, pol and env often contain mutations and deletions. Subsequently, HERVs do not have the capacity to replicate and infect independently. As LTR retrotransposons some of them posses the ability to generate mRNA from intact open reading frames (ORF) and translate this mRNA into cDNA. Generated cDNA has the ability to reintegrate into the host DNA. For this process a reverse transcriptase and an integrase are needed that HERVs either code themselves or borrow from other retroelements. There are only three HERVs with intact ORFs for gag, pol and env, all of which belong to HERV-K HML2 (Dewannieux et al., 2005; Mayer et al., 1999). However, these HERVs contain point mutations within critical parts of RT as well. Through retrotransposition thousands of HERV copies were spread throughout all human chromosomes (Fraser et al., 1988).

Most HERVs are silenced epigenetically, but reactivation through radiation, chemicals, internal signals (Schanab et al., 2011; Hohenadl et al., 1999; Ono et al., 1987) or a wide range of other viruses, e.g. HIV, HSV-1, HHV-6, EBV and CMV (Contreras-Galindo et al., 2007; Nellåker et al., 2006; Sutkowski et al., 2001; Tai et al., 2009; Hsiao et al., 2009), is possible. Reactivation can increase the level of transcript, lead to the expression of env or gag, or even to a formation of retroviral particles. HERV-K HML2 and HML4 have been shown to be stimulated by steroids by cause of their glucocorticoid responsive element (Ono et al., 1987; Seifarth et al., 1995). Furthermore, activity of HERV-K has been shown to be influenced by EBV and CMV (Freimanis et al., 2010; Nelson et al., 1999).

As highly mutated, non-infectious, and replication deficient elements HERVs have long been considered junk DNA. Reactivation of the normally suppressed HERVs may play a key role in the development of certain diseases and thus needs to be studied more extensively.

1.3.1 Human endogenous retrovirus type K HML2

HERV-K subtype HML2 is a beta-class human endogenous retrovirus. The subtype HML means human endogenous murine mammary tumor virus (MMTV)-like.

HERV-K is considered to be the youngest and most active HERV (Subramanian et al., 2011). It is the only subtype known to have members specific for humans (Medstrand & Mager, 1998; Buzdin et al., 2003) and slight differences within gag sequences in HERV-K hint at this subtype being transcriptionally active (Lower et al., 1993). In vitro the production of infectious virions could be achieved by combinination of several HERV-K proviruses (Dewannieux et al., 2006)

suggesting that under certain circumstances there is a possibility of viral particle production in vivo. HML2 transcripts as well as proteins could be detected in healthy tissues (Mehraein et al., 2006) to a certain extent, but especially in embryonic cells (Fuchs et al., 2013), and in malignancies (Büscher et al., 2006).
HERV-K HML2 plays a role in embryogenesis and human stem cell development. It is expressed early in embryonic development up to the blastocyste stage, but in contrast to other HERVs downregulated later in the process. Upregulation of HERV-K HML2 in human stem cells could be observed throughout various genetic backgrounds (Grow et al., 2015). HERV-K HML2 is involved in the maintenance of pluripotency of cells. Differentiation of stem cells induced downregulation of HERV-K HML2 (Fuchs et al., 2013) and HERV-K expression was highly correlated with several pluripotency biomarkers (Mareschi et al., 2019). These findings are congruent with the role of HERV-K HML2 in embryogenesis as well as its possible contribution to the development of associated diseases.

HERV-K in disease

Examples of cancers associated with HERV-K are liver cancer, teratocarcinoma, germ cell tumors, melanoma, ovarian, breast, and prostate cancer (Löwer et al., 1984; Herbst et al., 1998; Muster et al., 2003; Büscher et al., 2005; Wallace et al., 2014; Wang-Johanning et al., 2007, 2008; Kurth & Bannert, 2010). Androgens had the ability to stimulate HERV-K HML2 expression (Hanke et al., 2013) and thus might be mechanistically involved in its role in prostate cancer. In teratocarcinomas and melanomas viral like particles played an important role (Löwer et al., 1984; Büscher et al., 2005; Schmitt et al., 2013). Furthermore, the HERV-K accessory protein Np9 has been found to be expressed in various tumor tissues such as in breast and ovarian cancer as well as leukemia cells (Armbruester et al., 2002; Chen et al., 2013). Even though HERV-K HML2 was correlated with prognosis and progress of HCC (Ma et al., 2016), studies examining HERV-K HML2 and the factors leading to HCC, e.g. viral hepatitis, are missing.

Of autoimmune diseases the association between HERVs and amyotrophic lateral sclerosis (ALS) has been studied the most thoroughly. The viral proteins gag, pol and env of the HML2 subgroup could be detected in brains of ALS patients. Additionally, RT and env protein expression was found in cortical neurons (Douville et al., 2011; W. Li et al., 2015). Induced expression of HML2 in neurons lead to neuronal injury and cell death. This was achieved either by transfection with the complete consensus sequence or by targeting HML2 LTRs with the CRISPR technology. Transgenic mice in which HML2 Env was expressed under a neuronal promoter developed progressive motor dysfunction with specific loss of neurons in the motor cortex and the anterior horn of the spinal cord (W. Li et al., 2015). RT activity in the blood and cerebrospinal fluid of ALS patients could be detected in various studies (Viola et al., 1975; Steele et al., 2005; McCormick et al., 2008). At the same time, the use of reverse transcriptase inhibitors as antiviral drugs in

HIV patients with ALS could reverse or slow down neurological symptoms in some patients, especially early after the symptomatic onset of the disease (Alfahad & Nath, 2013), leading to the assumption that this may be due to the association of ALS with human endogenous retroviruses and a consecutive antiviral effect on HERV activity.
Sequence variations and polymorphisms within HERVs are linked to autoimmune disease and diabetes. Immunosuppressive properties were characteristic of many retroviruses and HML2 had retained this feature (Denner, 1998). HML2 particles released from a human teratocarcinoma cell line, a recombinant Env transmembrane (TM) protein, and a peptide corresponding to a highly-conserved region of the TM were able to inhibit human immune cell proliferation, change the expression of numerous cytokines, such as increasing IL-10, and affect gene expression (Morozov et al., 2013). HERVs also showed interaction with beta-catenin, a protein involved in the wnt pathway (Chen et al., 2013). Activation of this pathway contributes to tumorogenesis (reviewed by (Krishnamurthy & Kurzrock, 2018)). Apart from this, binding sites for pro-inflammatory transcription factors could be found within the HML2 LTR consensus sequence (Manghera & Douville, 2013).

HERVs share structural similarities with exogenous retroviruses. As infection with the retrovirus HIV is a global health issue, several studies looking for a link between HIV infection and HERV expression have been conducted. HIV infection was able to increase the levels of HML2 mRNA in PBMC (Contreras-Galindo et al., 2007; Ormsby et al., 2012; Bhardwaj et al., 2014) and the activation of certain HML2 loci was cell-type specific (Vincendeau et al., 2015). HERV-levels in PBMC of HIV-positive individuals were elevated in comparison to healthy controls, even when HML2 RNA could not be detected in plasma (Sugimoto et al., 2001; Bhardwaj et al., 2014; Brinzevich et al., 2014). When LC5-cells, a cell line frequently used for studying HIV, were persistently infected with HIV-1, HML2 transcript levels increased about 1.8-fold compared to uninfected cells. This effect was even higher in newly infected cells resulting in an approximately 8-fold increase (Vincendeau et al., 2015). Reverse transcriptase and integrase inhibitors are integral parts of antiviral treatment in HIV. In in-vitro studies, these drugs proved to be somewhat effective against HERV-K HML2 as well, yet to a much lesser extent than against HIV (Contreras-Galindo et al., 2017; Tyagi et al., 2017). This effect may, however, still be relevant to find treatment for HERV-K related diseases that are either badly or non-treatable.

Consequences of HERV-K HML2 reactivation for gene expression

As described in the previous section HERV-K is reactivated in various diseases. LTRs found within HERV-K HML2 can modify gene expression by acting as alternative promoters or as enhancers for other promoters in specific cell types. A HERV-K HML2 long terminal repeat (LTR) has been shown to induce the expression of a luciferase in certain cell lines. For example, in Tera-1, a human testicular embryonal carcinoma cell line, the LTR showed promoter as well as enhancer

activity compared to a control plasmid. Yet, these effects could not be achieved in NT2/D1, a cell line derived from the same carcinoma, possibly due to differences in protein interactions and thus distinct complexes formed between the LTR and the proteins of each cell line highlighting the cell type specificity (Ruda et al., 2004; Domanskiĭ et al., 2002). These effects on gene expression may contribute to disease progression and perhaps explain altered response to treatment in some individuals. However, this mechanism could also be exploited for new or additional treatment options in the future.

The potential link between HERV-K HML2 and hepatitis C

So far only one study screening for HERV-K HML2 in hepatits C patients has been conducted. Plasma of HCV-infected individuals was screened for HERV-K HML2 in Great Britain, but expression of HERV-K pol RNA was only detected in 1 out of 19 patients (Contreras-Galindo et al., 2006). As plasma samples were screened in this study, an intracellular upregulation of HERV-K HML2 expression possibly modifying downstream gene expression or other intracellular processes without release of HERV RNA may have been missed. Thus, it would make sense to screen cellular material of hepatitis C patients for HERV-K expression.
A different study linked intravenous drug abuse in hepatitis C patients to HERV-K HML2. In patients with ongoing long-term addictive behaviour of a duration of least two years a 3.5 fold higher frequency of HERV-K HML2 integration within RASGRF2, a gene related to addiction, was found (Karamitros et al., 2018). This study, however, did not show an association between HERV-K HML2 and HCV. The control group were hepatitis C patients who did not consume drugs intravenously. No other studies on RASGRF2 and hepatitis C or HCV have been published.

Even though HERV-K HML2 has been linked to many diseases, a possible association with hepatitis C has not been studied in depth yet. Hepatitis C is caused by viral infection and leads to liver cirrhosis and HCC. HERV-K HML2 has been shown to be associated with all of the latter, but to date there is low evidence for an association with hepatitis C. Additionally, hepatitis C is linked to cryoglobulinemia, a cutaneous as well as systemic autoimmune disease (Ramos-Casals et al., 2012) and HERV-K HML2 is associated with autoimmune diseases as well. Thus, it seems reasonable to investigate whether HERV-K HML2 is involved in the pathomechanisms of hepatitis C and its associated diseases as well as long-term complications.

1.4 Aim of the work

There are hints that HERV-K HML2 expression may play an important role in hepatitis C pathogenicity. To investigate a possible link between HERV-K HML2 levels and HCV infection and treatment, the following central hypotheses were addressed:

- DAA treatment leads to clearance of quantitative HCV RNA and to improvement of clinical parameters indicating impaired liver function.
- There is a difference in HERV-K HML2 expression between HCV infected patients and healthy controls.
- Patients with impaired liver function at baseline have different expression levels of HERV-K HML2 than the rest of the cohort.
- HERV-K HML2 expression levels change over the course of DAA treatment.
- HERV-K HML2 levels are different in patients who fail to achieve sustained viral response.
- There is an association between the level of HERV-K HML2 expression and clinical (leukocytes, CRP) as well as experimental (A20, IL-6, IL-10 and IP-10) inflammation markers in this cohort.

In order to shed light onto this possible association of HCV and HERV-K HML2, a cohort of 42 hepatitis C patients treated with direct acting antiviral therapy was analyzed. The primer used in this study binds to cDNA encoding for Gag, a functional protein responsible for antibody generation and encoding matrix, capsid or nucleocapsid proteins. These functions could imply that activation of this part of a HERV may be involved in autoantibody production or pathogenic processes. As patient samples were collected for various time points throughout antiviral treatment, a modulation of HERV-K HML2 expression over the course of treatment was identifiable.
The level of HERV-K HML2 expression was monitored over the course of treatment and associations with clinically relevant values and changes thereof were investigated. A comparison of HERV-K HML2 levels between baseline and end of treatment (EOT) as well as 12 weeks after EOT (SVR 12) is reasonable since patients with absence of detectable HCV RNA at SVR 12 are clinically considered as cured. To determine if there was a difference of HERV-K HML2 expression between healthy controls and patients infected with HCV, HERV-K HML2 levels at baseline were compared to those of healthy blood donors.
My results support an association between relative HERV-K HML2 expression levels and HCV infection that was affected by DAA treatment. They provide the foundation for the revelation of the role of HERV-K HML2 in pathogenesis, treatment outcome and progression of hepatitis C.

2 Material

2.1 Consumable material

Product	Manufacturer
Certified RNAse/DNAse and pyrogen safe pipette tips	VistaLab Technologies, USA
96 well plates	Nunc International, Wiesbaden
Eppendorf tubes 0,5 ml, 1,5 ml, 2 ml	Eppendorf, Hamburg
Falcon 10 ml and 20 ml tubes	Becton Dickinson, USA
Counting chamber Fast Read 102	Madaus Diagnostics, Cologne
FrameStar R 480/96 for Roche Lightcycler 480	Brooks Life Sciences, USA

2.2 Kits

Product	Manufacturer
SuperScript TM first-strand synthesis system	invitrogen, Karlsruhe
KAPA SYBR® FAST One-Step qRT-PCR Master Mix (2X) Kit	KAPA Biosystems Inc., USA
DNase Treatment Kit	Promega, USA

2.3 Chemicals

Product	Manufacturer
2-Propanol Rotipuran $\geq$ 99.8%	Carl Roth, Karlsruhe
Chloroform 99.8%	acros organics, USA
Dimethyl sulfoxide (DMSO)	Sigma Aldrich, USA
Ethanol absolute	Merck, Darmstadt
Fetal Bovine Serum (FBS)	Thermo Fisher, USA
Ficoll Solution	Sigma Aldrich, USA
LightCycler 480 SYBR Green I Master (LC)	Roche Diagnostics, Mannheim
Nuclease free water B1500S	New England BioLabs, United Kingdom
Phosphate buffered saline (PBS)	Thermo Fisher, USA
RPMI-1640	Thermo Fisher, USA
RQ1 RNAse-free DNAse	Promega, USA
RQ1 DNAse 10X reaction buffer	Promega, USA
RQ1 DNAse stop solution	Promega USA
TRIzol reagent	invitrogen, USA
Tuerk Solution	Sigma Aldrich, USA

2.4 Equipment

Product	Manufacturer
Eppendorf research plus pipettes	Eppendorf, Hamburg
Eppendorf centrifuge 5415 R	Eppendorf,
Eppendorf Thermomixer 5436	Eppendorf, Hamburg
Nanodrop	Thermo Fisher, USA
Roche Lightcycler 480 II	Roche, Switzerland
TB2 Thermoblock	Biometra, Göttingen
Thermo scientific Heraeus Pico 17	Thermo Fisher, USA
Vortex VF2	Janke & Kunkel (IKA) Labortechnik, Staufen

2.5 Primers

Primer sequences	
RPII forward	GCA CCA CGT CCA ATG ACA T
RPII reverse	GTC GGC TGC TTC CAT AA
HERV-K10 sense	GCA AGT AGC CTA TCA ATA CTG C
HERV-K10 antisense	GCA GCC CTA TTT CTT CGG ACC
IL-6 reverse	5'-GCT CCT CCT TGC TGC TTT CAC-3'
IL-6 forward	5'-GGT ACA TCC TCG ACG GCA TCT-3'
IL10 forward	CTGGAGGAGGTGATGCCCCAA
IL10 reverse	ACCTGCTCCACGGCCTTGCT
IP10 forward	5-ACTGTACGCTGTACCT-3
IP10 reverse	5-TGGCCTTCGATTCTGGA-3
TNFAIP3 forward	5'-TTTTGTACCCTTGGTGACCCTG-3'
TNFAIP3 reverse	5'-TTAGCTTCATCCAACTTTGCGG-3'

The final concentration of the primers used in this study was $20\ \frac{\mu mol}{L}$. Primers were manufactured by Metabion international AG, Germany.

2.6 Study population

42 hepatitis C patients and 4 healthy controls were included in the study. Ethical permission and informed consent for collection of blood and consecutive experiments as well as analyses were obtained.

2.7 Software

Product	Manufacturer
SPSS Version 26	IBM corp., USA
Roche Lightcycler 480 Software	Roche Diagnostics, Mannheim
Microsoft Word, Excel and Powerpoint for MAC	Microsoft Corp., USA
MAC OSX 10.15.4	Apple Inc., USA
Mendeley	Elsevier, Netherlands

3 Methods

3.1 Experimental methods

3.1.1 Isolation of peripheral blood mononuclear cells (PBMC)

Heparinized whole blood was collected by venipuncture and stored at room temperature. Within 8 h PBMC isolation was performed. After 1:2 dilution with PBS, whole blood was carefully transferred onto 15ml of Ficoll solution. A Ficoll density gradient was created by centrifugation (800 g, 15 min, $21\,$℃, brakes off). PBMC were separated and washed twice with RPMI-1640 (250 g, 10 min, $21\,$℃). Tuerk solution was used as stain to induce erythrocyte lysis for live/dead discrimination and viable PBMC were then counted under a light microscope. PBMC were chilled during the last centrifugation step (250 g, 10 min, $21\,$℃).

3.1.2 Cryoconservation and thawing of PBMC

For cryopreservation, PBMC were re-suspended in freezing medium containing FBS and 10 % DMSO at a concentration of one million cells per milliliter. Subsequently, PBMC were slowly frozen inside a controlled-grade freezing container at $-80\,$℃. PBMC stored at $-80\,$℃ were thawed partially in a water bath. After around 20 seconds, before the suspension becomes completely liquid, the PBMC suspension was transferred into 10 ml PBS.

3.1.3 Isolation of RNA using a Trizol gradient

PBMC were thawed and centrifuged (1200 rpm, 10 min, $21\,$℃). Supernatant was discarded. 1 mL of Trizol was added to the pellet and incubated for 5 min at room temperature. 0.2 mL of chloroform were added and after being mixed well the colloid was transferred to Eppendorf tubes. Tubes were centrifuged at 12,000 g for 15 min at $4\,$℃ to create a density gradient. The aqueous phase containing RNA was transferred to a new Eppendorf tube. 0.5 mL of 100 % isopropanol were added followed by a 10 min incubation at room temperature. Then, the mixture was centrifuged at 12,000 g for 10 min at $4\,$℃. Supernatant was discarded and 1 mL of 75 % ethanol was added. Another centrifugation step (7500 g, 5 min, $4\,$℃) followed. Supernatant was discarded again and the pellet was air-dried for 15 min. Afterwards, it was re-suspended in $30\,\mu\mathrm{L}$ of RNAse free water. RNA concentration and quality were verified by Nanodrop.

3.1.4 DNAse treatment

1000 ng of RNA were transferred into an Eppendorf tube. If the total volume was less than $8\,\mu L$, H_2O was added to even out the difference in volume. $1\,\mu L$ of DNAse as well as $1\,\mu L$ of DNAse buffer were added to each tube. Following an incubation of 30 min at 37℃ $1\,\mu L$ of RQ1 DNAse stop solution was added and the tubes were incubated for 10 min at 65℃.

3.1.5 First strand cDNA synthesis using random primers

After DNAse treatment $1\,\mu L$ of 10 m dNTP mix and $2\,\mu L$ of random hexamers ($50\,\frac{ng}{\mu L}$) were added to each tube. An incubation step of 5 min at 65℃ followed. Next, the samples were chilled on ice for at least 1 min. For the next step, a master mix was prepared consisting of the following:

Master mix per tube

Reagent	Amount
10X RT buffer	$2\,\mu L$
25 mM MgCl2	$4\,\mu L$
0.1 M DTT	$2\,\mu L$
RNAse OUT ($40\,\frac{U}{\mu L}$)	$1\,\mu L$

$9\,\mu L$ of the master mix were added to each tube and content was collected by brief centrifugation. This mixture was incubated for 2 min at room temperature. $1\,\mu L$ of Superscript 2 RT was added to each reaction. An incubation of 10 min at room temperature, 50 min at 42℃ and 15 min at 70℃ followed. Then, the reaction was chilled on ice and brief centrifugation was performed. $1\,\mu L$ of RNAse H was added per tube and the tubes were incubated for 20 min at 37℃. cDNA was stored at -20° C.

3.1.6 Quantitative polymerase chain reaction

Two step RT-qPCR

All parts of the procedure were executed on ice. Centrifuge was cooled down to 4℃. Primers were diluted to achieve a final concentration of $10\,\mu mol$. A master mix consisting of $10\,\mu L$ LC, $1\,\mu L$ each of the respective forward and reverse primer, and $6\,\mu L$ of H_2O per well was prepared. $18\,\mu L$ of the master mix were distributed into each well of a 96 well plate. RP2 was included as housekeeping gene on every plate. $2\,\mu L$ of cDNA were added to the respective wells and a control with $2\,\mu L$ of H_2O was included for every primer. The plate was centrifuged at 1500 rpm for 2 min at 4℃ and then put back onto ice. Afterwards, the plate was covered with transparent foil. Quantitative PCR was performed with Roche Light Cycler.
PCR conditions can be found in table 3.1.

	Temperature	Time [min:sec]
Pre-incubation	95 ℃	5:00
Amplification	95 ℃	0:10
	60 ℃	0:10
	72 ℃	0:10
Melting curve	95 ℃	0:05
	65 ℃	1:00
	97 ℃	5 acquisitions/℃
Cooling	40 ℃	0:30

Table 3.1 PCR conditions for SYBR green two step qPCR. 45 amplification cycles were carried out.

One-step RT-qPCR

	Temperature	Time [min:sec]
Reverse transcription	42 ℃	5:00
	95 ℃	3:00
Amplification	95 ℃	0:10
	60℃	0:20
	72 ℃	0:01
Melting curve	95 ℃	0:05
	65 ℃	1:00
	97 ℃	5 acquisitions/℃
Cooling	40 ℃	0:10

Table 3.2 PCR conditions for KAPA SYBR FAST one-Step RT-qPCR. 40 amplification cycles were performed.

As sufficiently low C_T-values could not be achieved for some samples using two step RT-qPCR, qRT-PCR using KAPA SYBR FAST One-Step was implemented. DNAse treatment was performed prior to qRT-PCR, but no cDNA synthesis was performed prior as cDNA synthesis took place inside the Light Cycler in this approach.

An amount of 20 ng of RNA suspended to a volume of $2.5\,\mu\mathrm{L}$ was used per well. A master mix consisting of $10\,\mu\mathrm{L}$ KAPA SYBR FAST qPCR Master Mix (2X), $0.4\,\mu\mathrm{L}$ 10 mM dUTP, $0.4\,\mu\mathrm{L}$ $10\,\mu$ forward primer, $0.4\,\mu\mathrm{L}$ $10\,\mu$ reverse primer, 0.4 $0.4\,\mu\mathrm{L}$ 50X KAPA RT Mix, and H_2O up to a total of $18.25\,\mu\mathrm{L}$ per well was prepared and plated onto a cooled 96 well plate. $2.75\,\mu\mathrm{L}$ of RNA mixture

was added to each well. RP2 was used as housekeeping gene on each plate. An H_2O control was included for every condition. The following steps were identical to the qPCR described above, but a different template was required.
PCR conditions can be found in table 3.2.

Analysis of qPCR results

On every plate a negative control for each primer and for the housekeeping gene RPII was included to rule out contamination of the reagents. RPII served as a reference gene to calculate relative expression of experimental parameters of interest. The fit point method was chosen to get C_T-values and values of ≥ 35 were discarded. ΔC_T-values were calculated as follows: ΔC_T = C_T(Primer) - C_T(RPII). The x-fold induction of experimental parameters relative to RPII was calculated by the $2^{-\Delta C_T}$ method (Livak & Schmittgen, 2001).
Due to a lack of sufficient patient material, it was not possible to use duplicates or triplicates. However, two exemplary probes that could be duplicated were be evaluated here (table 3.3). For both samples, standard deviation (SD) and coefficient of variation (CV) were calculated. Sample 1 had a SD of 0.0042 and a CV of 10.76 % and sample 2 had a SD of 0.0134 and a CV of 6.37 %.

Sample	C_T(RPII)	C_T(Primer)	ΔC_T	$2^{-\Delta C_T}$
Sample 1	27.77	32.33	4.56	0.042393885
Sample 1	28.47	33.25	4.78	0.036397925
Sample 2	27.77	29.96	2.19	0.21915143
Sample 2	28.47	30.79	2.32	0.200267469

Table 3.3 C_T-values obtained by qPCR and calculated respective ΔC_T and $2^{-\Delta C_T}$ of two duplicate samples.

3.2 Statisticical analysis

SPSS version 26 was used to complete statistical analysis and to generate graphs.
The level of significance was set to 5%. Thus, p-values of < 0.05 were considered statistically significant and $p < 0.01$ was considered highly significant. Bonferroni correction was applied as post-hoc test whenever pairwise comparisons or associations between more than two groups or time points were calculated. With this method, the level of significance is divided by the number of time points analyzed and adjusted accordingly (Curtin & Schulz, 1998). For example, when three time points were included in analysis, the calculation was 0.05/3 = 0.0167. Therefore, in that example $p < 0.017$ was considered statistically significant.

For pairwise comparison of different subgroups the independent samples t-test was used for

normally distributed data (clinical data) and Mann-Whitney U was used for non-parametric data (experimental data). To analyze if data for two different time points within the same subgroup significantly differed from each other, paired samples t-test was used for normally distributed data and the Wilcoxon-Sign test was used for data that did not show normal distribution.
In order to be able to interpret the development of parameters over time, one-way analysis of variance (ANOVA) was chosen for parameters which were normally distributed. Using this method an interpretation of significant differences between the mean value of each time point was possible and every time point got taken into account (Bender et al., 2007). For the experimental parameters which were not distributed normally, mixed model analysis was implemented (Cnaan et al., 1997). Subjects were defined by Patient ID, time points as the repeated measures. The repeated covariance type was set as unstructured as no specific structure within covariances could be identified. Restricted maximum likelihood and Satterwhaite approximation were used. The CI was set to 95 % according to the aforementioned level of significance in this study. The time points were set as fixed effects. No covariates were taken into account as neither gender, age nor liver cirrhosis had a significant influence on the fit of the curve. Mixed model analysis tries to find a converging non-linear line that fits the development of the parameter on the y-axis over - in this case - time represented on the x-axis. The y-intercept does not have to be equal for all subjects. So each subject has its own curve that may be shifted on the y-axis, but the shape of the curve is equal for all subjects (figure 3.1). So with this tool a non-linear development can be analyzed even if starting points differ per individual.

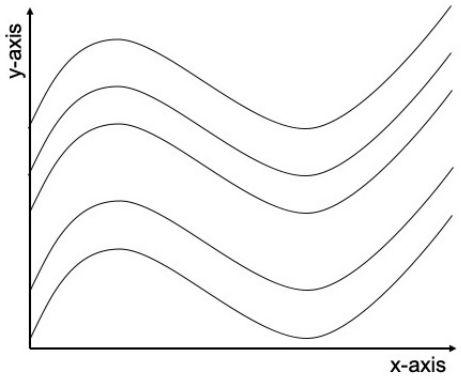

Figure 3.1 A simplified representation of mixed model analysis. Each curve represents the fitting line of one subject. Subjects may have different y-intercepts, but the shape of the curve does not differ between subjects.

Associations between binary variables were evaluated using the chi-square test. Higher values of chi-square correspond to higher association between the variables. For easier interpretation, the results were converted into Cramer's V. The output values of Cramer's V range from zero (no association) to 1, corresponding to perfect association. As the cohort could not be seen as representative of the population, the calculation of odds ratios were chosen over risk ratios.
For correlations between experimental and clinical data, a method to detect associations be-

tween parameters with non-parametrical distribution had to be used as experimental data were not distributed normally. Spearman's rho was considered. However, this method tends to overestimate correlations in small sample sizes, which I did not want to risk. Additionally, one value that behaves like a stray bullet can mess up the correlation coefficient. Kendall's tau, also known as Kendall Rank Correlation Coefficient, is less sensitive to such errors since its calculations are based on concordant and discordant pairs while Spearman's rho relies on deviations. Kendall's Tau is defined as the quotient of the difference of discordant (D) and concordant pairs (C) and the sum of concordant and discordant pairs (Liu et al., 2016).

$$Kendall's\ tau = \frac{(C - D)}{(C + D)}$$

Having juxtaposed the pros and cons, kendall's tau was chosen as the method of choice for this study.

To determine if a dichotomous variable had an effect on the odds of having a higher or lower value of a certain continuous variable, binary logistic regression was implemented. B was defined as the coefficient in the null model. Exp(B) is the exponentiation of B and can be more easily interpreted than the coefficient as Exp(B) it represents an odds ratio.

4 Results

4.1 Cohort characteristics

42 patients were treated with different combinations of DAAs and some additionally Ribavirin over the course of 8 – 24 weeks. 50 % (n = 21) of patients were female, 50 % (n = 21) male. The age ranged from 34 to 74 years with a median of 54 years. For most patients the way of infection was unknown (52.5 %, n = 23). 25 % (n = 10) were infected via intravenous drug abuse, 10.0 % (n = 4) via blood transfusion and 12.5 % (n = 5) are native of a high-risk country for hepatitis C. 71.4 % (n = 30) of patients were infected with HCV genotype 1, 23.8 % (n = 10) with genotype 3 and 4.8 % (n = 2) with genotype 4 (figure 4.1). For some patients, the subtype of genotype was known. The genotype distribution seen in the study cohort corresponded with genotype 1 being the most prevalent in Europe (Petruzziello et al., 2016). A complete table of patient characteristics and the respective drugs the patients were treated with is provided as supplementary material.

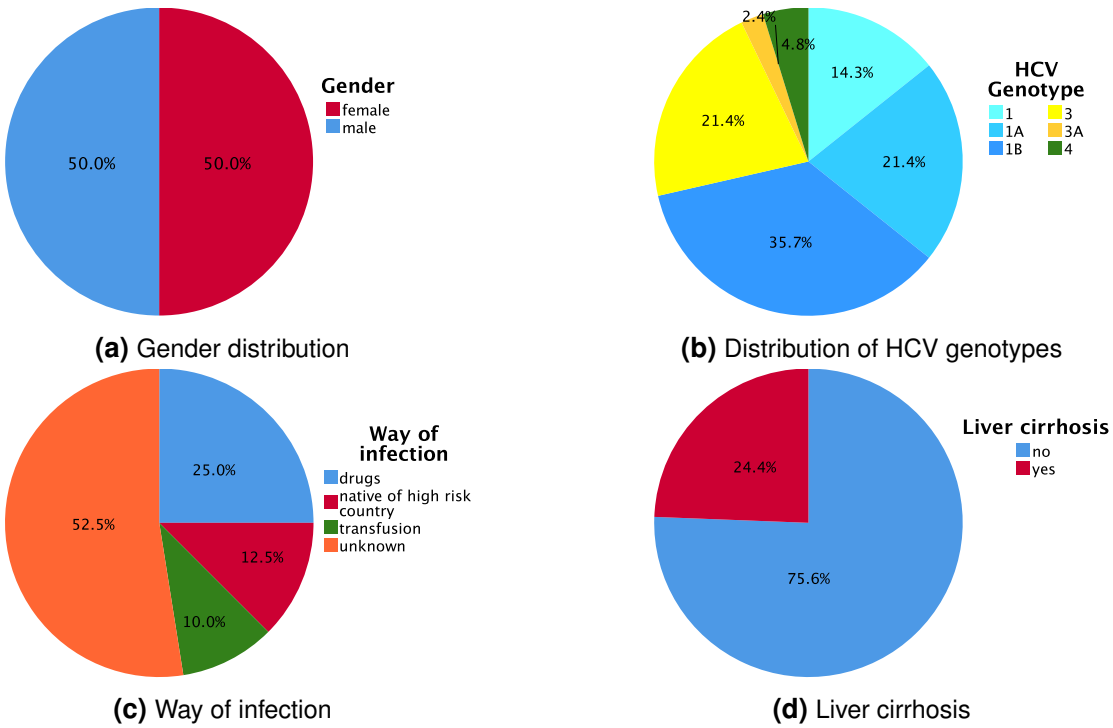

(a) Gender distribution

(b) Distribution of HCV genotypes

(c) Way of infection

(d) Liver cirrhosis

Figure 4.1 Distribution of descriptive parameters throughout the hepatitis C patient population (n = 42).

4.2 Monitored time points

Patients were treated over the course of 8 – 24 weeks depending on their drug scheme (figure 4.2). End of treatment marked the last day of DAA administration after 8 (n = 1), 12 (n = 34), or 24 (n = 6) weeks respectively. P08 died of a cardiovascular event before completion of treatment. Clinical data were collected for the following time points: baseline, week 2, week 4, end of treatment (EOT) and sustained viral response (SVR 12). To monitor treatment success, all patients were screened for sustained viral response 12 weeks after the end of treatment, some additionally 24 weeks after end of treatment. Data for time points week 8 and SVR 24 were available for a small number of patients only and therefore these time points were excluded from statistical analysis. As P08 died after week 8, this time point was included in descriptive analysis of experimental parameters in patients who failed to achieve SVR. Clinical parameters for the other time points were collected for every patient with few exceptions.

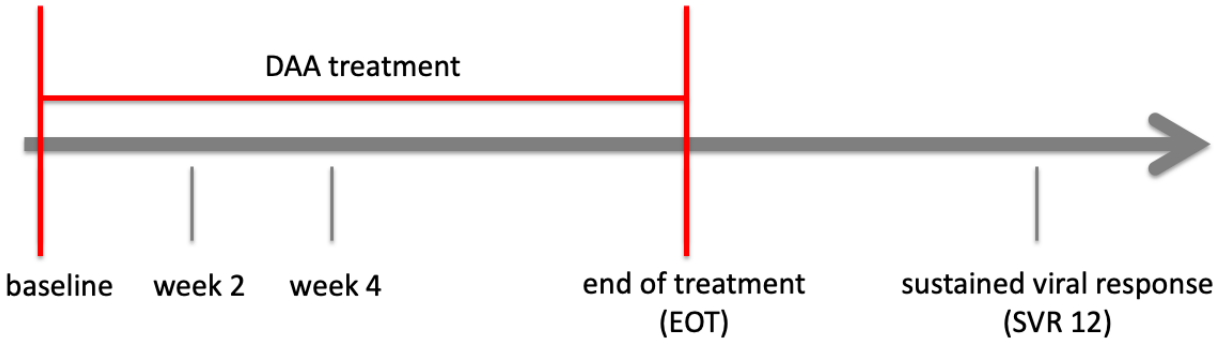

Figure 4.2 Time points of collection of clinical and experimental data. DAA treatment started at baseline and lasted until end of treatment (EOT). Twelve weeks after EOT sustained viral response was achieved if no quantitative HCV RNA could be detected at that time point.

4.3 Drug combinations

Treatment schemes depended on the HCV genotype the patients were infected with as well as their clinical status of the liver before the start of the treatment. All patients underwent combination therapy including one or more DAAs as well as an addition of Ribavirin for some patients. For genotype 1, any of the DAAs as well as Ribavirin is suitable. Sofosbuvir targets NS5B and can be applied for all 6 genotypes. It is always combined with other DAAs. Daclatasvir targets NS5A and works for genotypes 1 and 3. Ledipasvir also uses NS5A as target and can be used for genotypes 1a, 1b, 4a, and 5a. However, it shows less activity when applied to genotypes 2a or 3a. Exviera, also known as Dasabuvir, targets NS5B. Viekirax is a combination of Ombitasvir targeting NS5A and Paritaprevir (target: NS3/4) and Ritonavir (cytochrome P450 3A4 inhibitor). Ribavirin is a nucleoside analog which has been used for HCV treatment for a long time. DAAs were the first efficient HCV therapy which did not have to rely on Ribavirin. Yet, Ribavirin was

Drug combinations	
Simeprevir + Sofosbuvir + Ribavirin	5 patients
Simeprevir + Sofosbuvir	6 patients
Daclatasvir + Sofosbuvir	16 patients
Daclatasvir + Sofosbuvir + Ribavirin	3 patients
Ledipasvir + Sofosbuvir	5 patients
Ledipasvir + Sofosbuvir + Ribavirin	2 patients
Viekirax + Exviera	4 patients
Viekirax + Ribavirin	1 patient

Table 4.1 Drug combinations among the cohort of hepatitis C patients. Five direct acting antivirals (Simeprevir, Sofosbuvir, Daclatasvir, Ledipasvir, and Exviera) as well as Ribavirin, a nucleoside analogon, and Viekirax, a combination drug targeting NS5A, NS3-4 and CYP3A4, were used to treat the patients.

often applied in addition to DAAs in order to achieve a higher SVR in patients with previously unsuccessful treatment or advanced liver damage (Mathur et al., 2018).

The majority of patients (n = 37) received Sofosbuvir as part of their combination therapy. 19 patients were treated with Daclatasvir, 11 Simeprevir, 7 Ledipasvir, 5 Viekirax, and 4 Exviera (table 4.1).

There were 11 patients who received Ribavirin in addition to DAA treatment, whereas 31 patients completed a Ribavirin-free treatment scheme.

4.4 An overview of monitored clinical and experimental parameters

4.4.1 Clinical parameters

An overview of clinical parameters monitored in this study and their respective normal ranges (table 4.2) is provided in this section.
Aspartate amino transferase (ASAT) and Alanin amino transferase (ALAT) are transaminases used to quantify liver damage. While ASAT is a nearly ubiquitous enzyme which can be found in the liver, but also e.g. in erythrocytes as well as myocardial and skeletal muscle tissue (Gressner & Gressner, 2019c), ALAT is more liver specific (Gressner & Gressner, 2019a). A quotient of ASAT divided by ALAT can be calculated to estimate the type of the liver damage. This quotient is called De-Ritis quotient. A De-Ritis quotient below 1 is indicative of an inflammatation as found

in acute viral hepatitis, while values above 1 signal necrotic liver damage as seen in liver cirrhosis or chronically active as well as alcohol-toxic hepatitis (Gressner & Gressner, 2019f).
Gamma-Glutamyl-Transferase (GGT) and bilirubin are cholestasis markers. GGT is sensitive to alcohol abuse as well (Gressner & Arndt, 2019). Bilirubin is not only a marker for posthepatic icterus as in cholestasis, but can also be elevated due to pre- or intrahepatic icterus. Prehepatic icterus can be caused by hemolysis and intrahepatic icterus by disruption of absorption, conjugation or excretion of bilirubin in the liver (Gressner & Gressner, 2019d).
Albumin is synthesized in the liver and makes up around 60 % of plasma protein. Low albumin levels can occur due to - among others - impaired liver synthesis function, malnutrition or inflammation. Clinically, hypoalbuminemia may lead to a decline of oncotic pressure and consequently edema and ascites (Gressner & Gressner, 2019b).
Creatinine is an indirect, but widely used, indicator of kidney function. However, it is linearly dependent on the mass of muscle tissue. In patients with low muscle mass, creatinine levels only start to rise once glomerular filtration is highly reduced (Guder, 2019). So this parameter needs to be interpreted with caution.
Coagulation was monitored by Quick (Lichtman et al., 2000) and the international normalized ratio (INR) in this study. The INR is standardized and can therefore its results can be compared between different laboratories (Kirkwood, 1983).
Thrombocytes are blood platelets that are responsible for primary hemostasis by building aggregates and activating plasmatic coagulation (Baum, 2019). When thrombocyte levels drop below 50 - 80 /nl there is an increased likelihood of thrombopenic bleeding (Kreuzer et al., 2019).
Leukocytes are white blood cells whose count rises fast when inflammatory processes unfold. C-reactive protein (CRP) is an inflammation marker synthesized in hepatocytes that starts to rise four to six hours after onset of the inflammatory event (Gressner & Gressner, 2019e).
Viremia of HCV infection and therefore response to antiviral therapy can be monitored by quantitative HCV-RNA (Ehling et al., 2019). If HCV-RNA is undetectable at SVR 12, patients are considered healed.

Clinical parameter	Normal range
ASAT	male: < 50 U/l female: < 35 U/l
ALAT	male: 5 - 35 U/l female: 5 - 31 U/l
GGT	male: 12 - 64 U/l female: 9 - 36 U/l
Bilirubin	0.2 - 1.2 mg/dl
Albumin	34 - 48 g/l
Creatinine	male: 0.7 - 1.3 mg/dl female: 0.6 - 1.1 mg/dl
C-reactive protein	< 5 mg/l
Quick International normalized ratio (INR)	70 - 120 % < 1.1
Hemoglobin	male: 14 - 18 g/dl female: 12 - 16 g/dl
Leukocytes	3.5 - 10 /nl
Thrombocytes	150 - 360 /nl
quantitative HCV-RNA	non-detectable

Table 4.2 Normal ranges for clinical parameters as provided by the University of Mainz (Institut für klinische Chemie und Laboratoriumsmedizin, 2020)

4.4.2 Experimental parameters

HERV-K HML2 as well as inflammation markers A20, IP-10, IL-6 and IL-10 were monitored experimentally. A detailed description of HERV-K HML2, a human endogenous retrovirus involved associated with numerous diseases e.g. liver cirrhosis (Ma et al., 2016), can be found in the introduction of this thesis.

The remaining experimental parameters are involved in inflammation by either being part of or being regulated by NF-kB signalling. As HERV-K HML2 is associated with inflammatory processes, these parameters were taken a closer look at.

Interferon-gamma inducible protein (IP-10) or CXCL10 is secreted in response to interferon gamma (Luster & Ravetch, 1987) and acts as a chemokine. NF-kB can induce IP-10 expression (Nakamichi et al., 2005). Increased IP-10 expression compared to healthy controls has been

shown in chronic hepatitis C (Mihm et al., 2003) and IP-10 promotes HCC progression by attraction of protumorogenic macrophages (Liu et al., 2015).
IL-6 is an acute phase protein secreted by monocytes and macrophages (Bazin & Lemieux, 1987). It supports the growth of B cells (Tosato et al., 1988). As proinflammatory cytokine its expression is induced by NF-kB (Matsusaka et al., 1993; Ndlovu et al., 2009) and it leads to hypothalamic upregulation of body temperature resulting in fever (Evans et al., 2015). IL-6 serves as an essential part of the immune response to infection or trauma (Kopf et al., 1994). However, it can also contribute to diseases, e.g. to fatty liver disease (Miller et al., 2011) (Gavito et al., 2016) and HCC (Wan et al., 2015; Kong et al., 2016).
Both of these proteins contribute to systemic inflammation and have the ability to enhance disease progression or development.

In contrast, A20 as well as IL-10 serve as anti-inflammatory proteins. A20, also known as tumor necrosis factor alpha induced protein 3, inhibits NF-kB and TNF-induced apoptosis (Lee et al., 2000; He & Ting, 2002; Shembade et al., 2010; K. Z. Li et al., 2019), e.g. in acute liver failure (K. Z. Li et al., 2019). It helps prevent autoimmune conditions (Sokhi et al., 2018) like allergies (Schuijs et al., 2015), atopy (Devos et al., 2019) or inflammatory bowel disease (Zaidi et al., 2018). Loss of A20 expression is associated with the development B cell lymphomas (Kato et al., 2009; Novak et al., 2009).
IL-10 is an anti-inflammatory cytokine which blocks NF-kB activitation (Lentsch et al., 1997) and thus the production of pro-inflammatory agents (Fiorentino et al., 1989). Yet, the fact that high doses of IL-10 can also show pro-inflammatory effects (Lauw et al., 2000) needs to be taken into consideration when IL-10 is studied. In the liver, IL-10 shows hepatoprotective effects (Louis et al., 1997; Di Marco et al., 1999) and IL-10 therapy in hepatitis C patients has been shown to reduce hepatic inflammation and fibrosis (Nelson et al., 2000).

All of these proteins interact with NF-kB signaling and are capable of modulating immune response to viral infections.

4.5 Development of clinical parameters over time and treatment outcome

To evaluate the success of DAA treatment in this cohort, the development of clinical parameters throughout drug administration as well as at SVR 12 was observed. Ideally, clinical parameters normalized until the end of treatment and stayed within normal range at follow-up twelve weeks later as well. The absence of quantitative HCV RNA at SVR 12 was defined as treatment success. One way ANOVA was performed to determine significant differences of clinical parameters over time. For P39 no clinical data were available. Analysis of the whole cohort showed no significant

differences for albumin, creatinine, Quick, INR, leukocytes, thrombocytes and c-reactive protein. ASAT ($p < 0.001$, figure 4.3), ALAT ($p < 0.001$, figure 4.4) and GGT ($p = 0.001$, figure 4.5) decreased significantly over time suggesting a recovery of liver function. Quantitative HCV RNA showed a drastic decrease from baseline to week 2. At EOT, no HCV RNA was detectable in any patient and at SVR 12 in two patients only.

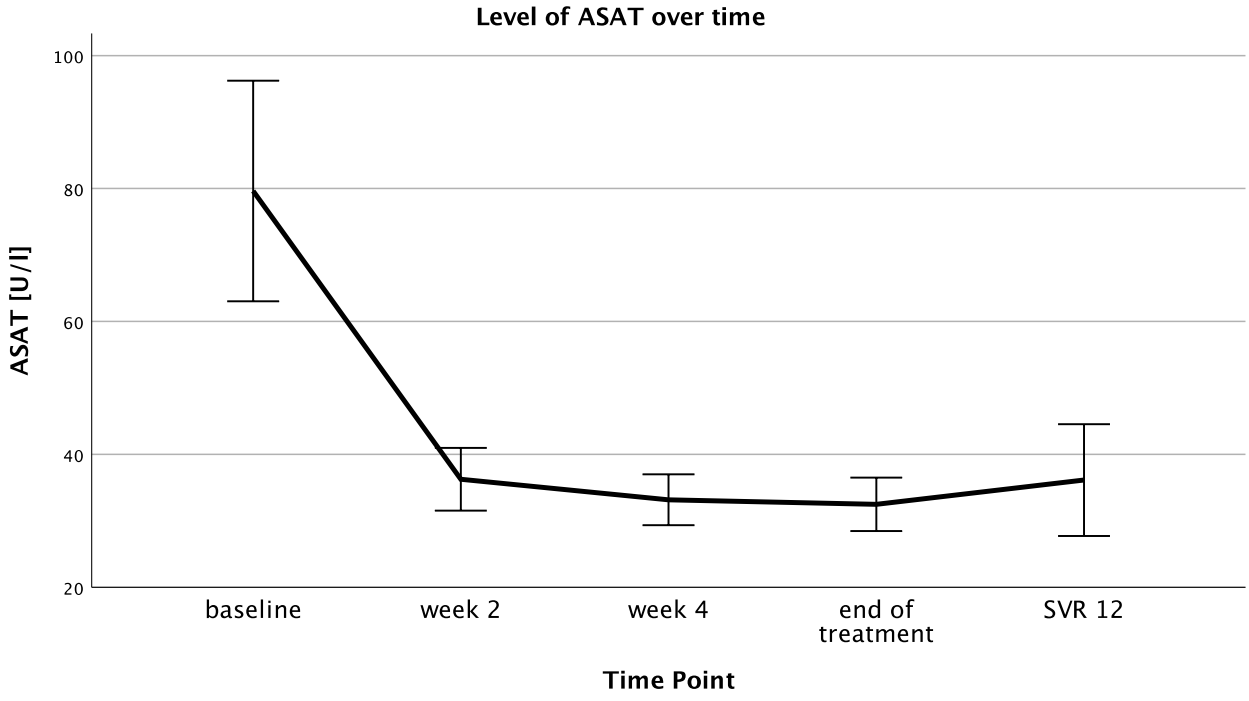

Figure 4.3 A drop in mean ASAT levels after the start of treatment could be observed ($p < 0.001$). Mean levels of ASAT in U/l over the course of time are shown. Error bars depict the 95% confidence intervals of the mean at each time point, n = 32.

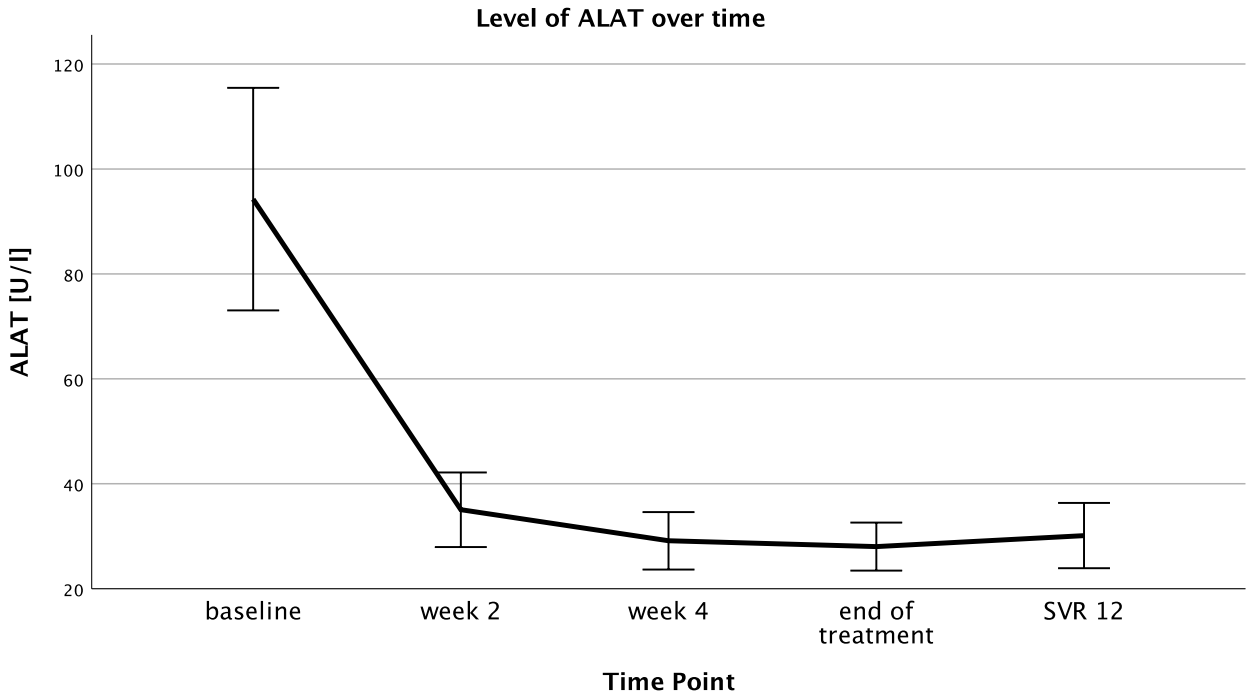

Figure 4.4 A decline of ALAT levels after the start of DAA treatment was observed ($p < 0.001$). The y-axis shows mean ALAT levels in U/l and the x-axis five distinct time points. Error bars depict the 95% confidence intervals of the mean at each time point, n = 32.

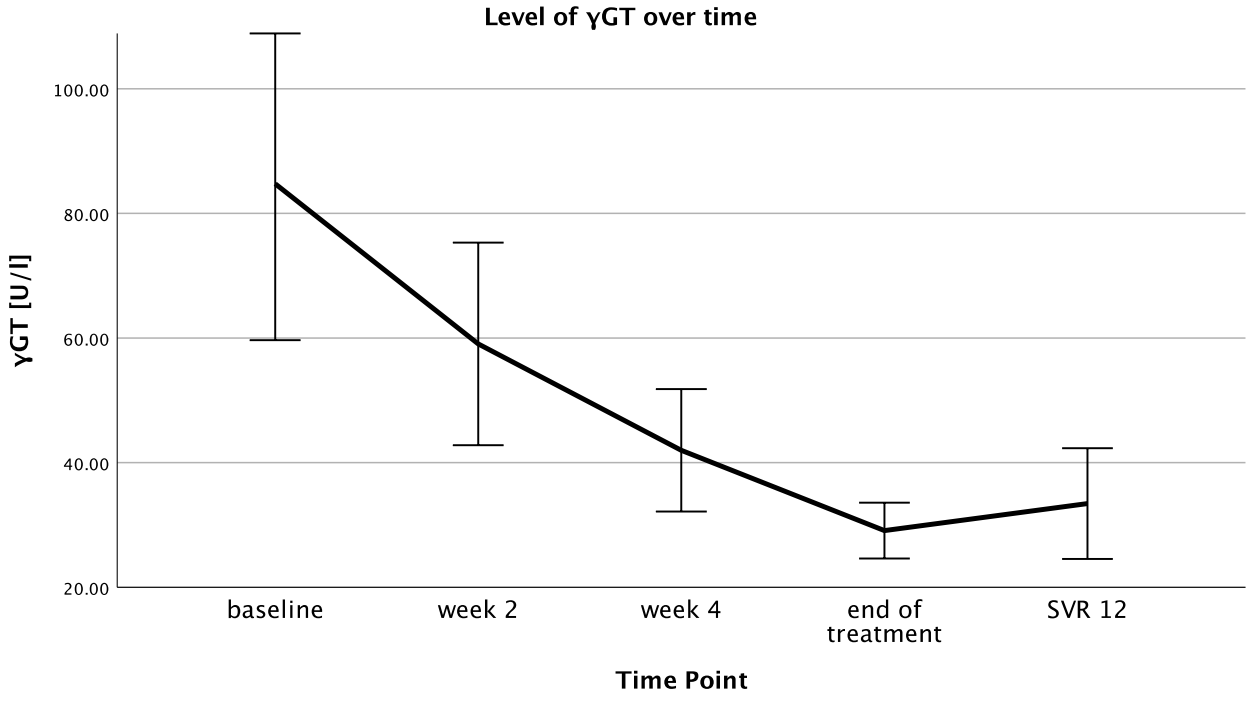

Figure 4.5 From baseline to EOT mean GGT levels declined ($p = 0.001$). Mean levels of GGT in U/l are shown on the y-axis and five time points on the x-axis. Error bars depict the 95% confidence intervals of the mean at each time point, n = 32.

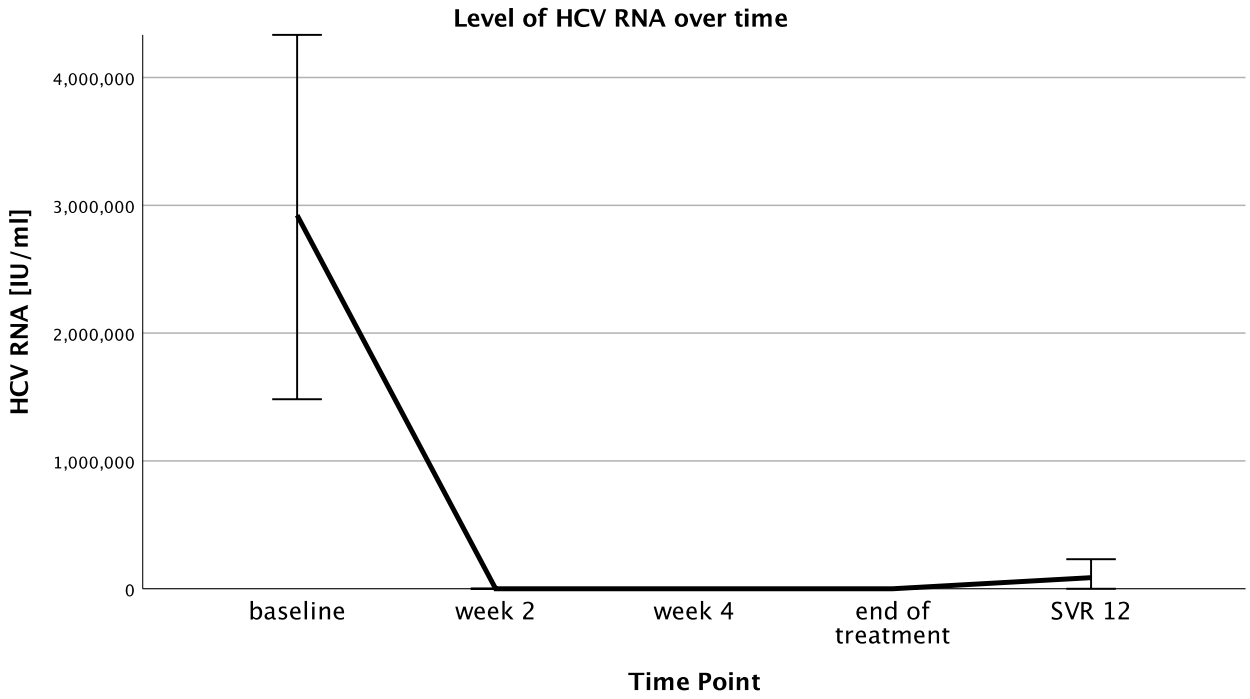

Figure 4.6 There was a decline of quantitative HCV RNA after the start of treatment. At EOT, HCV RNA was not detectable for any of the patients. At SVR 12, quantitative HCV RNA was detectable in two patients. Mean levels of quantitative HCV RNA over the course of time are depicted. Error bars depict the 95% confidence intervals of the mean at each time point, n = 34.

A pairwise comparison between baseline and SVR 12 confirmed the decrease of liver parameters ALAT, ASAT and GGT as seen over time (table 4.3). Additionally, a highly significant decrease in HCV-RNA ($p < 0.001$) could be detected meaning HCV-RNA stayed successfully suppressed 12 weeks after the end of treatment. Compared to baseline, mean hemoglobin was by 0.74 g/dl lower at EOT and by 0.51 g/dl at SVR 12. These differences were significant. The decrease of mean hemoglobin by almost one point from baseline to EOT and its recovery up to a mean of 14.27 g/dl after the end of treatment could infer that hemoglobin levels might have decreased due to DAA treatment.

To determine whether changes of experimental parameters at baseline compared with SVR 12 differed significantly, the sign test comparing the median of differences was applied.
IP-10 showed negative differences compared to baseline for patients who were not treated with Ledipasvir ($p = 0.017$) or took no Ribavirin ($p = 0.027$). This trend was also notable for the whole cohort, but it was not significant ($p = 0.054$). Patients treated with Simeprevir showed increased IL-10 levels at SVR 12 compared to baseline ($p = 0.031$).

Clinical Baseline vs. SVR12		
clinical parameter	p-value	n
ALAT	$p < 0.001$	n = 37
ASAT	$p < 0.001$	n = 37
GGT	$p < 0.001$	n = 37
Bilirubin	p = 0.036	n = 37
Albumin	p = 0.067	n = 37
Creatinine	p = 0.418	n = 37
Quick	p = 0.664	n = 37
INR	p = 0.078	n = 37
Hemoglobin	p = 0.003	n = 38
Leukocytes	p = 0.690	n = 38
Thrombocytes	p = 0.882	n = 38
HCV-RNA	$p < 0.001$	n = 39
C-reactive protein	p = 0.108	n = 36

Table 4.3 ALAT, ASAT, GGT, bilirubin, and HCV RNA were significantly lower at SVR 12 than at baseline, while hemoglobin was significantly higher. Paired samples t-tests of clinical parameters at baseline and SVR 12 were conducted.

4.6 Influence of medication on clinical and experimental parameters

As patients were treated with different DAAs and some patients were administered Ribavirin in addition to DAA treatment, the influence of these differences on clinical as well as experimental parameters was investigated. Ledipasvir as well as Daclatasvir inhibit NS5A and therefore they were not only analyzed separately, but also as group of NS5A inhibitors due to their common target.

For time points baseline, week 2, week 4, EOT and SVR 12 differences between patients receiving one specific drug and the rest of the cohort were analyzed. To avoid alpha error accumulation, p-values below 0.01 were considered significant to maintain a significance level of 0.05 (Bonferroni-correction).

Patients treated with Ribavirin showed differences in blood count. Their hemoglobin was about two points lower at week 4 (p = 0.008) and EOT (p = 0.002), thrombocyte count was significantly lower at all time points (see table 4.4) and leukocyte count was lower as well (baseline p = 0.015,

week 2 $p < 0.001$, week 4 $p = 0.002$, EOT $p = 0.001$, SVR 12 $p = 0.007$). Mean leukocyte count was within normal range for both groups, though, and CRP did not differ significantly.

Time point	mean thrombocyte count without Ribavirin	mean thrombocyte count with Ribavirin	p-value
baseline	214.5 /nl	105.0 /nl	$p < 0.001$
week 2	225.3 /nl	113.1 /nl	$p = 0.001$
week 4	228.0 /nl	114.6 /nl	$p = 0.001$
EOT	211.0 /nl	117.0 /nl	$p = 0.001$
SVR 12	213.9 /nl	115.6 /nl	$p = 0.001$

Table 4.4 Patients treated with Ribavirin showed significantly lower thrombocyte counts at all time points. P-values were calculated by independent samples t-tests.

Of the five patients who did not receive Sofosbuvir, four received Viekirax plus Exviera and one Viekirax only. Patients who did not take Sofosbuvir showed significantly lower mean ASAT (24.80 IU/l vs. 33.57 IU/l, $p = 0.001$) and ALAT (19.40 IU/l vs. 29.26 IU/l, $p = 0.009$) levels at end of treatment, even though there was no significant difference at baseline. No other significant differences could be detected for the rest of the clinical or experimental parameters.

Neither Sofosbuvir nor Ribavirin showed a significant influence on the expression level of HERV-K HML2, A20, IP-10, IL-6 or IL-10. Patients treated with Exviera and/or Viekirax did not show significant differences of these parameters, either.
Simeprevir is a NS3-4 inhibitor. Ledipasvir and Daclatasvir target NS5A. Baseline levels of HERV-K HML2 were significantly different between Ledipasvir and Daclatasvir as well as each of these drugs or both combined compared with Simeprevir (figure 4.7). However, the difference in HERV-K HML2 expression when comparing the two NS5A inhibitors was only significant at baseline, whereas it remained highly significant at EOT and SVR 12 for any of the aforementioned drug combinations in comparison with Simeprevir (Table 4.5). Simeprevir had a significant influence on the development of HERV-K HML2 levels over time when looking at patients treated with either Simeprevir or another NS5A inhibitor (mixed model analysis, Type III Test of fixed effects: $F = 50.703$, $p < 0.001$).

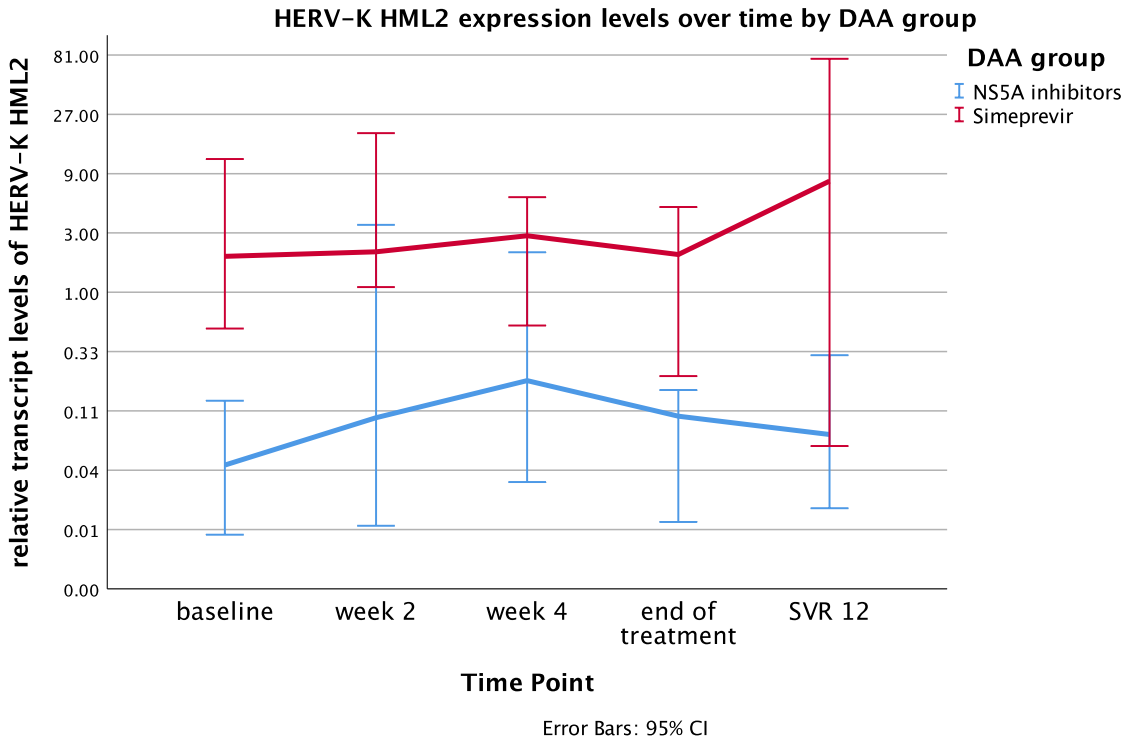

Figure 4.7 Patients treated with NS5A inhibitors show significantly lower HERV-K HML2 expression levels at baseline, EOT and SVR 12. The development of median HERV-K HML2 expression levels over time for patients treated with Simeprevir and patients treated with a NS5A inhibitor is outlined. Error bars show the 95 % confidence intervals and the y-axis is scaled logarithmically.

Median of HERV-K HML2 levels compared to Simeprevir				
Time point	Simeprevir	Ledipasvir (p-value)	Daclatasvir (p-value)	NS5A inhibitors (p-value)
baseline	1.945	0.007 (p = 0.001)	0.077 (p = 0.001)	0.041 ($p < 0.001$)
EOT	2.010	0.002 (p = 0.008)	0.102 (p = 0.001)	0.100 ($p < 0.001$)
SVR 12	7.835	0.004 (p = 0.008)	0.100 (p = 0.001)	0.072 ($p < 0.001$)

Table 4.5 Patients treated with Simeprevir showed significantly higher HERV-K HML2 expression levels at baseline, EOT and SVR 12 compared to any of the NS5A inhibitors used in this study. P-values were calculated by Mann-Whitney-U tests.

There was a significant difference in IL-6 expression levels between the group of NS5A inhibitors and Simeprevir at week 4 (p = 0.004) as well as Daclatasvir and Simeprevir (p = 0.008) at that time point. Comparing only Daclatasvir and Simeprevir patients, IL-6 levels were lower in Simeprevir patients at SVR 12 as well (median 0.254 vs. 0.049, p = 0.007). Patients receiving Simeprevir also showed significantly higher IP-10 levels at week 2 (median 3.25) compared with Daclatasvir or both NS5A inhibitors (both: median 0.032, p = 0.006). Ledipasvir patients neither showed differences in IL-6 nor in IP-10 expression levels compared with any of the other drugs used. However, patients receiving this DAA exhibited lower IL-10 levels at SVR 12 when compared with Daclatasvir (median Ledipasvir 0.076 vs. Daclatasvir 0.275,p = 0.015), even though

there was no significant difference between the groups at baseline or EOT.

Clinically, patients treated with NS5A inhibitors showed significantly lower levels of bilirubin than those treated with Simeprevir. When comparing Ledipasvir with Daclatasvir, no statistically significant difference in bilirubin levels was detectable, but if either drug was compared with Simeprevir, there was a clinically relevant difference. Yet, at SVR 12 the levels of bilirubin did not differ significantly between these groups anymore (table 4.6).

Mean bilirubin levels compared to Simeprevir				
Time point	Simeprevir	Ledipasvir (p-value)	Daclatasvir (p-value)	NS5A inhibitors (p-value)
baseline	1.44 mg/dl	0.64 mg/dl (p = 0.009)	0.95 mg/dl (p = 0.066)	0.86 mg/dl (p = 0.014)
week 2	1.82 mg/dl	0.61 mg/dl (p = 0.003)	0.91 mg/dl (p = 0.009)	0.81 mg/dl (p = 0.010)
week 4	1.86 mg/dl	0.60 mg/dl (p = 0.001)	0.72 mg/dl (p = 0.002)	0.68 mg/dl (p = 0.002)
EOT	2.08 mg/dl	0.55 mg/dl (p = 0.005)	0.72 mg/dl (p = 0.010)	0.67 mg/dl (p = 0.008)
SVR 12	1.36 mg/dl	0.60 mg/dl (p = 0.023)	0.72 mg/dl (p = 0.048)	0.69 mg/dl (p = 0.039)

Table 4.6 Simprevir patients showed higher bilirubin levels at all time points compared to patients treated with any of the NS5A inhibitors used in this study. P-values were calculated by independent samples t-tests.

There were differences in albumin levels between Simeprevir and any NS5A inhibitor (see table 4.7), but none of them were statistically significant at SVR 12. While mean albumin levels were above 35 g/l and thus within normal range for serum albumin in all groups except for patients who were treated with Simeprevir at all time points, mean albumin of Simeprevir patients recovered to 35.60 g/l at SVR 12. So it showed a tendency towards normalization of serum albumin.

Mean albumin levels compared to Simeprevir				
Time point	Simeprevir	Ledipasvir (p-value)	Daclatasvir (p-value)	NS5A inhibitors (p-value)
baseline	32.50 g/l	39.57 g/l (p = 0.004)	37.44 g/l (p = 0.031)	38.04 g/l (p = 0.017)
week 2	32.82 g/l	39.43 g/l (p = 0.003)	36.08g/l (p = 0.115)	37.25 g/l (p = 0.031)
week 4	33.36 g/l	39.86 g/l (p = 0.003)	37.33 g/l (p = 0.055)	38.26 g/l (p = 0.017)
EOT	33.60 g/l	39.57 g/l (p = 0.010)	37.61 g/l (p = 0.011)	38.16 g/l (p = 0.017)
SVR 12	35.60 g/l	39.33 g/l (p = 0.052)	38.33 g/l (p = 0.135)	38.58 g/l (p = 0.098)

Table 4.7 Patients treated with Simeprevir showed lower albumin levels than Ledipasvir patients. However, the observed difference was not significant anymore at SVR 12. P-values were calculated by independent samples t-tests.

Furthermore, Ledipasvir patients showed a lower De-Ritis quotient at baseline (p = 0.003) and EOT (p = 0.013) compared to patients receiving Daclatasvir. At SVR 12, however, the mean De-Ritis quotient was not significantly different. At baseline Simeprevir patients had a mean De-Ritis quotient of 1.19, which was significantly higher than in patients who received Ledipasvir (p =

0.008) or NS5A inhibitors (p = 0.015). Between Ledipasvir and Daclatasvir only the mean thrombocyte count at SVR 12 (Ledipasvir: 243.17 /nl, Daclatasvir: 184.50 /nl, p = 0.007) differed apart from that. For both groups, however, the mean was within normal range. Patients who received Simeprevir started out with a significantly lower mean Quick (78.40 %) than patients treated with Ledipasvir (p = 0.003, respective INR: p = 0.016). At SVR 12 this difference was still observable as the mean Quick of Simeprevir patients was 84.00 %, whereas it was 107.67 % for Ledipasvir patients (p = 0.010).

No influence by medication could be observed at baseline, which was as expected since baseline marked the start of drug administration.

4.7 Genotype specific differences

HCV genotype 3 is known to be associated with a higher score of steatosis (Rubbia-Brandt et al., 2000). Therefore, a comparison between patients infected with different HCV genotypes was conducted.

As there were only two patients, P28 and P30, with genotype 4, no statistical analysis between these two patients and the other genotypes could be conducted. For P28 no experimental data were available. Strikingly, quantitative HCV RNA was still detectable for both of these patients at week 4. Apart from this, none of the clinical values deviated markedly from the respective normal range for P28 or P30.

To evaluate if the genotype influences treatment outcome, SVR 12 was compared between patients infected with HCV genotypes 1 and 3.

Genotype 1 and 3 did not show significant differences in HERV-K HML2 expression levels. So HERV-K HML2 expression seemed to be independent of the HCV genotype in this cohort. There was, however, a significant difference in expression levels of IL-6 at SVR 12 (p = 0.037, figure 4.8). P30 who was infected with HCV genotype 4 had an IL-6 expression level of 0.1467 at SVR 12.

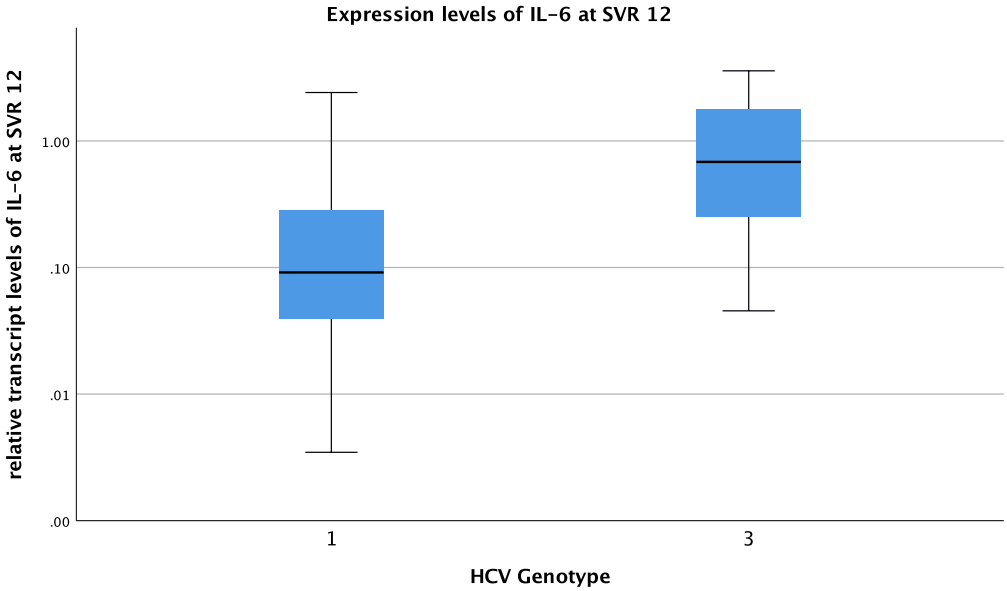

Figure 4.8 Patients with HCV genotype 3 (n = 7) showed higher median levels of IL-6 at SVR 12 than patients with HCV genotype 1 (n = 22) (p = 0.027, Mann-Whitney-U test). Boxplots comparing the expression levels of IL-6 at SVR 12 for genotypes 1 and 3 are depicted on a logarithmic scale.

As IL-6 is a pro-inflammatory marker, CRP and leukocytes at SVR 12 were compared between these groups. CRP and leukocyte count in patients infected with genotype 3 were higher at SVR 12, but the differences were not statistically significant. Inflammation could be involved in the development of liver steatosis and elevated IL-6 expression levels in HCV genotype 3 patients corresponded to that. Patients infected with genotype 3 had lower bilirubin levels at EOT (p = 0.001). All patients with liver cirrhosis were infected with HCV genotype 1, which might explain this difference since liver cirrhosis leads to elevated bilirubin levels and is thus included in clinical scores like the Child Pugh score (Child & Turcotte, 1964) (Pugh et al., 1973). As for the patients infected with genotype 4, P28 had a bilirubin level of 0.53 mg/dl and P30 of 1.04 mg/dl at EOT.

There were neither genotype-specific differences in clinical outcome nor in the development of clinical parameters except for bilirubin levels at EOT. The significantly higher expression levels of IL-6 in genotype 3 patients at SVR 12 may hint at liver inflammation which could be part of a steatotic transformation of liver tissue.

4.8 Analysis of patients without treatment success

To assess what might set patients with unsuccessful treatment apart from the rest of the cohort, they were analyzed in comparison with the rest of the cohort. In order to identify factors that may contribute to failure of viral clearance, baseline values of patients with and without successful treatment as well as the development of parameters over the course of time were compared.
In total, there were three patients without treatment success. P08 died after week 8. Two patients

did not reach a sustained viral response at time point SVR 12. This means that 39 out of 42 patients (92.86 %) achieved sustained viral response. A recent meta analysis shows that pooled sustained viral response in HCV patients treated with various DAAs was above 90 % (Zoratti et al., 2020), which was consistent with our cohort. All three of the patients whose treatment was unsuccessful were infected with HCV genotype 1.
Quantitative HCV RNA values at baseline were 320,000 IU/ml for P02, 500,000 IU/ml for P08 and 3,800,000 IU/ml for P10. At week 4 all three patients had a non-detectable level of HCV RNA which continued to be non-detectable at EOT for P02 and P10. At SVR 12 however, P02 had a rebound of HCV RNA to 660,000 IU/ml and P10 to 2,800,000 IU/ml, meaning they did not achieve sustained viral response (figure 4.9). P02 even exceeded its baseline value of quantitative HCV RNA. The mean levels of HCV RNA at SVR 12 were significantly higher than in the rest of the cohort ($p < 0.001$).

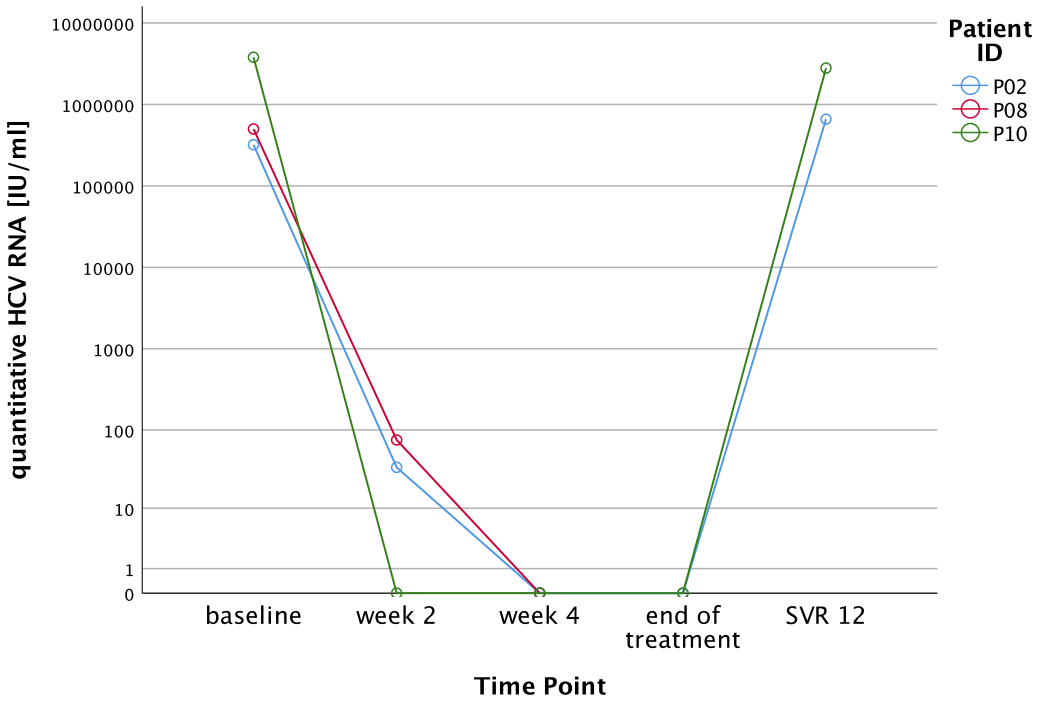

Figure 4.9 P02, P08 and P10 did not achieve sustained viral response. Level of quantitative HCV RNA over the course of time of each patient without treatment success is depicted on a logarithmic scale.

ASAT levels were much higher in the three patients with treatment failure than in the rest of the cohort at all time points. These three patients started out with a mean value of ASAT of 168.67 U/l (rest of the cohort: 72.41 U/l) decreasing to a mean value of 68.33 U/l at week 2 (rest of the cohort: 31.00 U/l). All three patients experienced a decrease of ASAT from baseline to week 2. There was an increase of ASAT between the respective last time points. For P08 this was from week 2 (62 U/l) to week 4 (65 U/l). For the remaining two patients there was an increase from EOT to SVR 12. P02's ASAT increased from 45 U/l to 153 U/l and P10 from 71 U/l to 123 U/l (figure 4.10).

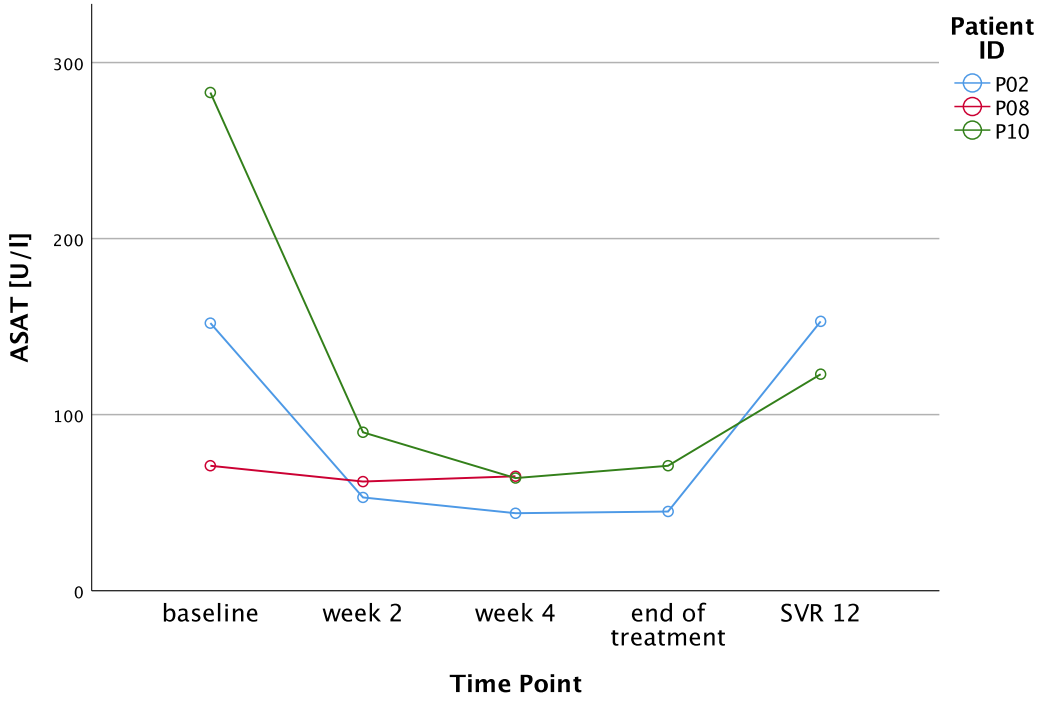

Figure 4.10 ASAT levels increased from EOT to SVR 12 for P02 and P10 and from week 2 to week 4 for P08. Levels of aspartate amino transaminase (ASAT) over the course of time of patients without treatment success are shown on a linear scale.

There was an increase of ALAT between the last two time point in all three patients (figure 4.11). P10 had a very high starting value of 273 U/l. From baseline to week 2 there was a decrease of ALAT levels in P02 and P10. ALAT levels significantly differed from the rest of the cohort at SVR 12 ($p < 0.001$) with a mean of 99.00 U/l for P02 and P10 and 26.41 U/l for the rest of the cohort.

ALAT and ASAT matched the development of HCV RNA levels of all three patients over time by decreasing after the start of treatment and increasing after EOT.
P10's baseline value of GGT at 431 U/l was distinctively high compared to the rest of the cohort. P08's GGT was at a steady level of right above 100 U/l, while P02's GGT levels were within normal range at all time points. There was an increase of GGT in P02 and P10 from EOT to SVR 12 (P02: 23 U/l to 41 U/l, P10: 77 U/l to 167 U/l). The mean of GGT of the patients without successful treatment was significantly higher than for the rest of the cohort at all time points.
Bilirubin values were within normal range for P08. P02 had an elevated starting value of 3.14 mg/dl. P02 and P10 showed a decrease of bilirubin from EOT to SVR 12. The mean of bilirubin was significantly higher than for the rest of the cohort at EOT ($p < 0.001$).
Albumin levels were significantly lower at baseline ($p = 0.001$), week 2 ($p = 0.004$) and week 4 ($p = 0.003$) compared to the rest of the cohort as P02 and P08 showed albumin levels below 30 g/l at all time points.
Creatinine levels of P02 and P10 were below 1. At baseline P08 had a creatinine of 1.74 mg/dl

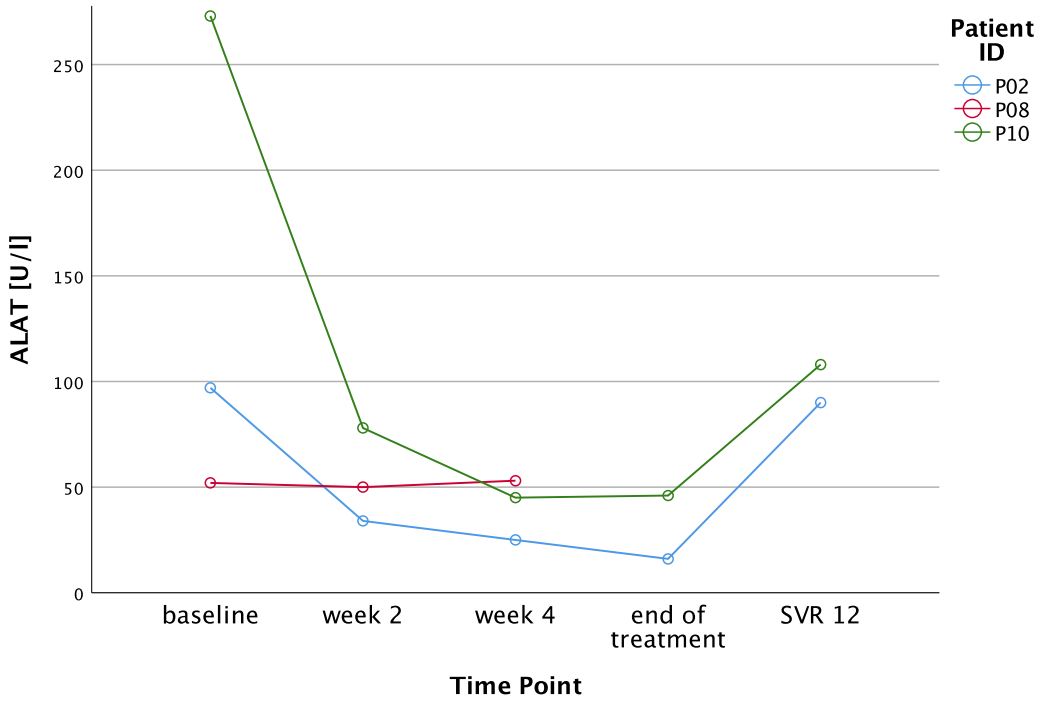

Figure 4.11 ALAT levels increased from EOT to SVR 12 for P02 and P10 and from week 2 to week 4 for P08. Levels of alanine amino transaminase (ALAT) over the course of time of patients without treatment success are shown on a linear scale.

which decreased slightly to 1.64 mg/dl at week 4. Both values were elevated indicating kidney damage.

Quick and INR were within normal range for P10 at all time points. P08 experienced a decrease of INR from 1.7 to 1.5 (Quick from 49 % to 59 %), while P02 experienced a continuous increase of INR from week 2 (INR 1.5, Quick 46 %) to SVR 12 (INR 1.9, Quick 42 %). The mean INR was not significantly different from the rest of the cohort.

P08 started out with a low hemoglobin level of 8.5 mg/dl at baseline increasing up to 9.8 mg/dl at week 4. For week 8 no hemoglobin value could be collected. P02 and P10 had hemoglobin levels within normal range at all time points.

Notably, all three patients had thrombocyte levels below the normal range of 150 - 360 /nl. P02's thrombocyte levels were below 50 /nl throughout the whole monitored time period. At SVR 12 thrombocyte count was even lower (39 /nl) than at baseline (46 /nl). Mean thrombocytes were lower than in the rest of the cohort at all time points. Even though this difference was not significant, it could be clinically relevant as thrombocyte levels below 50 - 80 /nl are clinically critical because of an increased likelihood of thrombopenic bleeding (Kreuzer et al., 2019).

Leukocytes and CRP did not show a clear tendency for the three patients without treatment success. CRP and lekocytes did not significantly differ from values of the rest of the cohort. This made inflammation unlikely to play an important role in treatment failure of these patients. However, due to the low number of patients without treatment success, no clear statement about this

could be made. Experimentally, IL-6 did not show a clear increase or decrease, either. The anti-inflammatory marker IL-10 increased over time in all three patients, however (figure 4.12). Median relative IL-10 transcript levels at baseline were higher than in patients whose treatment turned out to be successful. There was an increase of IL-10 in all three patients for the last two measured time points. P02 showed an increase from 0.21 at EOT to 0.38 at SVR 12, P08 had a baseline expression level of 0.00 which increased to 0.30 at week 2 and P10's IL-10 levels increased from 0.63 at EOT to 1.04 at SVR 12.

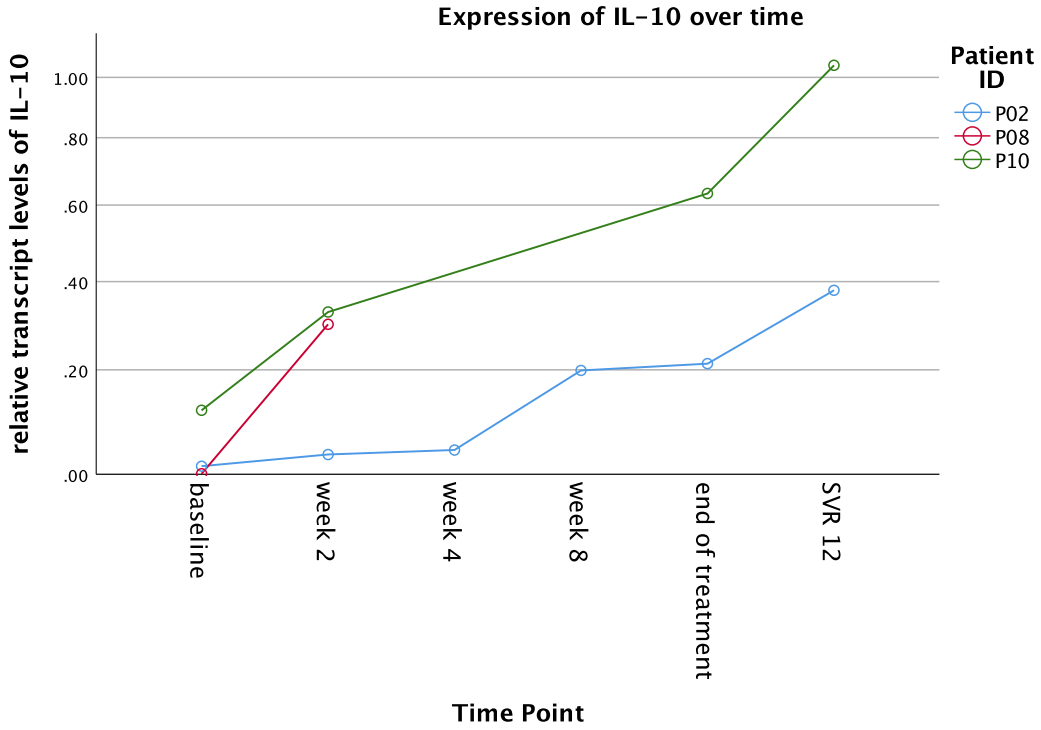

Figure 4.12 IL-10 expression increased for all three patients without successful treatment over time. Relative transcript levels of interleukin-10 (IL-10) relative to the house keeping gene RPII over the course of time of patients without treatment success are depicted on a linear scale.

The median baseline value of HERV-K HML2 (P02: 3.63, P08: 1.71, P10: 3.92) was significantly higher in patients without treatment success (U = 92, p = .029, n = 38). Only baseline values were compared as for P08 values for EOT and SVR 12 were not obtainable. There was an increase in relative transcript levels of HERV-K HML2 from week 2 to the last time point for each of the three patients (figure 4.13). P08 showed a drastic increase of HERV-K HML2 before death (week 2 2.17, week 8 16.91). The remaining patients P02 and P10 showed an increase in HERV-K HML2 expression after EOT (P02: EOT 1.34, SVR 12 7.26, P10 EOT 2.11, SVR 12 2.69). So, similar to IL-10 expression, there was an increase from the second-to-last to the very last time point in each patient.

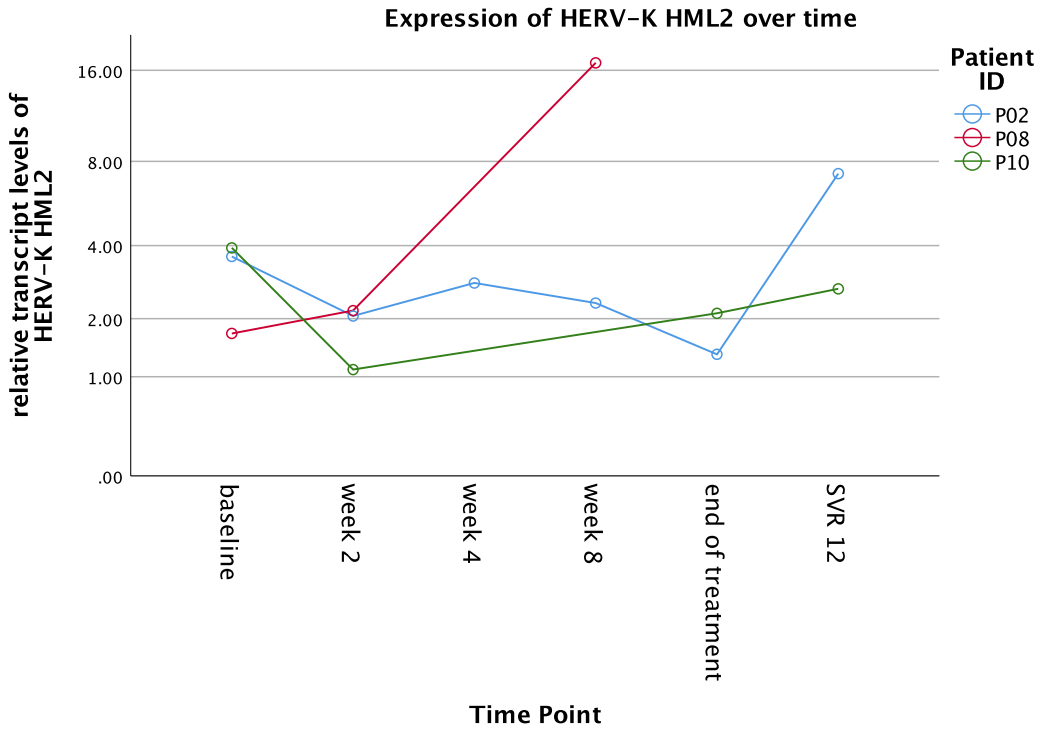

Figure 4.13 HERV-K HML2 expression levels increased from week 2 to week 8 for P08 and from EOT to SVR 12 for P02 and P10.Transcript levels of human endogenous retrovirus type k (HERV-K) HML2 relative to the house keeping gene RPII over the course of time of patients without treatment success are shown on a logarithmic scale.

For A20 there was no clear direction of development like in the rest of the cohort. The median of A20 did not differ significantly between these groups. P02 had a peak of 2.69 at week 8. However, there was no striking peak of any other experimental value at week 8 and clinical data were not available for P02 at this time point.
IP-10 levels did not show a homogeneous tendency in the patients who failed to achieve sustained viral response, either. P02 had a relatively high IP-10 starting value of 2.20 and showed an increase in IL-10 levels at week 2 (5.28), then IP-10 fell drastically to a level of 0.07 at week 4 and stayed at a low level at week 8 with a relative transcript level of 0.06. P08 showed an increase in IP-10 from week 2 (0.02) to the last time point measured at week 8 (0.63).

While all three patients showed relative HERV-K HML2 expression levels of more than 1 at baseline, they started out with low IL-10 levels which increased over time in all patients. An increase in HERV-K HML2 levels could be observed between the last two time points in each of these patients respectively. Thus, high expression levels at baseline and/or rising HERV-K HML2 levels may be predictive of the outcome of DAA treatment.

4.9 Analysis of the influence of liver cirrhosis

HCV infection can lead to liver cirrhosis (World Health Organization, 2020). Liver cirrhosis signals preexisting damage to liver tissue prior to start of treatment. In total there were 10 patients with liver cirrhosis in this cohort, including the three patients who failed to clear the virus (P02, P08 and P10). The administration of Ribavirin was significantly associated with pre-existing liver cirrhosis (Chi-square $p < 0.001$, Cramer's V 0.553, Fisher's Exact Test p = 0.001). The odds ratio for liver cirrhosis patients to be administered Ribavirin was 15.750 (95 % CI 2.842 - 87.280). The addition of Ribavirin to the respective treatment regimen is common in patients with advanced liver disease or patients who have failed to achieve sustained viral response in previous treatment attempts (Mathur et al., 2018).

Patients with liver cirrhosis were 1.131 as likely to have an ASAT baseline value of one unit higher (binary logistic regression: p = 0.022). They were, however, less likely to have a by one unit higher ALAT baseline level (p = 0.029 , odds ratio 0.882). This corresponded well with the higher De-Ritis quotient observed in these patients.

A comparison of clinical parameters at baseline, EOT and SVR 12 can be found in table 4.8. ASAT levels were significantly higher in liver cirrhosis patients at EOT. De-Ritis quotient used to classify liver damage was significantly higher at baseline ($p < 0.001$) and SVR 12 (p = 0.006) in these patients. DAA treatment might be the cause for the lack of a significant difference at EOT and the following relapse in liver cirrhosis patients twelve weeks later. Bilirubin levels were, as expected, higher in liver cirrhosis patients, but the difference was only statistically significant at baseline (p = 0.008). Albumin, hemoglobin and thrombocyte levels were significantly different at all of the aforementioned time points. Quick levels showed a significant difference, while INR levels did not.
HCV RNA baseline levels were not significantly different between the two groups. However, both patients who showed a rebound of quantitative HCV RNA at SVR 12 had liver cirrhosis.

Clinical parameter	no liver cirrhosis	liver cirrhosis	p-value
ASAT baseline	69.60 IU/l	109.70 IU/l	n.s.
ASAT EOT	28.90 IU/l	45.44 IU/l	p = 0.013
ASAT SVR 12	28.21 IU/l	62.00 IU/l	n.s.
De-Ritis quotient baseline	0.787	1.348	$p < 0.001$
De-Ritis quotient EOT	1.155	1.870	n.s.

De-Ritis quotient SVR 12	1.181	1.565	p = 0.006
Bilirubin baseline	0.78 mg/dl	1.61 mg/dl	p = 0.008
Bilirubin EOT	0.77 mg/dl	2.02 mg/dl	n.s.
Bilirubin SVR 12	0.73 mg/dl	1.36 mg/dl	n.s.
Albumin baseline	38.53 g/l	31.30 g/l	p = 0.001
Albumin EOT	38.63 g/l	32.00 g/l	$p < 0.001$
Albumin SVR 12	38.86 g/l	34.33 g/l	p = 0.015
Quick baseline	100.87 %	73.10 %	p = 0.001
Quick EOT	100.30 %	75.67 %	p = 0.004
Quick SVR 12	100.31 %	74.22 %	p = 0.002
Hemoglobin baseline	14.95 g/dl	12.81 g/dl	p = 0.001
Hemoglobin EOT	14.50 g/dl	11.60 g/dl	$p < 0.001$
Hemoglobin SVR 12	14.63 g/dl	12.90 g/dl	p = 0.001
Thrombocytes baseline	212.20 /nl	104.40 /nl	p = 0.001
Thrombocytes EOT	213.17 /nl	97.67 /nl	$p < 0.001$
Thrombocytes SVR 12	213.59 /nl	105.33 /nl	$p < 0.001$

Table 4.8 Patients with liver cirrhosis were characterized by a higher baseline De-Ritis quotient, higher baseline bilirubin levels as well as lower serum albumin, lower Quick, lower hemoglobin and thrombocyte counts at baseline, EOT and SVR12. Overview of the means of clinical parameters of patients with and without liver cirrhosis. At baseline there were 30 patients without and 10 patients with liver cirrhosis. At EOT only 9 patients without liver cirrhosis were left. SVR 12 values were available for 29 patients without liver cirrhosis, except for HCV RNA (n = 30). Test used: t-test, Bonferroni-correction was applied, p < 0.0167 can be considered statistically significant to maintain the level of significance at 5 %. LC = liver cirrhosis, n.s. = not significant.

Liver cirrhosis has been shown to be associated with higher levels of HERV-K (Ma et al., 2016). Comparing the median values of HERV-K HML2 of the patients with and without liver cirrhosis, the HERV-K HML2 levels at baseline (U = 207.00, p = 0.003, n = 37), EOT (U = 142.00, p = 0.010, n = 30) and SVR 12 (U = 138.00, p = 0.009, n = 31) were significantly higher in patients suffering from liver cirrhosis. Patients with liver cirrhosis were also more likely to have relative HERV-K HML2 transcript levels of above 1 at baseline (chi-square 9.475, p = 0.002, Cramer's V 0.506, odds ratio 12.000, 95 % CI 2.098 - 68.635) as well as SVR 12 (chi-square 8.272, p =

0.004, Cramer's V 0.517, odds ratio 14.667, 95 % CI 1.828 - 117.675).

Presence of liver cirrhosis was positively correlated with HERV-K HML2 levels at SVR 12 (0.410, p = 0.022, n = 31, figure 4.14). It was also positively correlated with the HCV RNA levels at SVR 12 (correlation coefficient 0.358, p = 0.025 , n = 39) as well as clinical parameters for liver function at SVR 12 (ASAT: 0.554, $p < 0.001$, n = 38; GGT 0.498, p = 0.001, n = 38, bilirubin 0.456, p = 0.004, n = 38). Strikingly, these correlations were either stronger at SVR 12 than at baseline or EOT or significant for SVR 12 only.

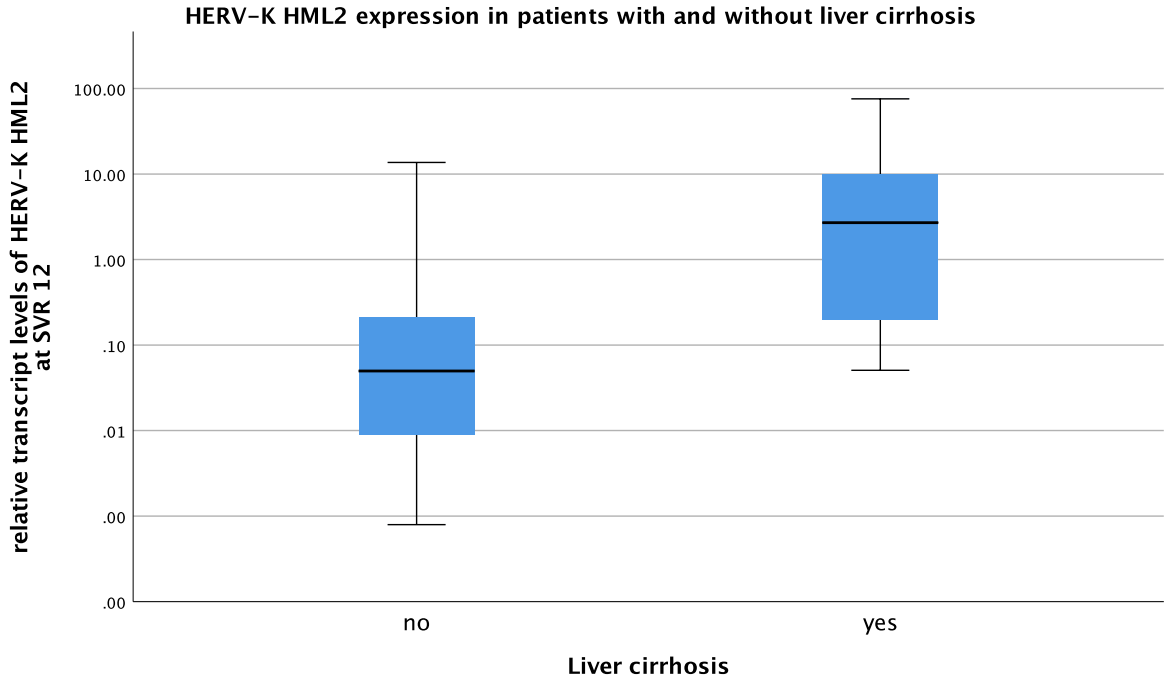

Figure 4.14 Patients with liver cirrhosis showed significantly higher expression levels of HERV-K HML2 at SVR 12 (p = 0.009, n = 27). Boxplots of HERV-K HML2 transcript levels at SVR 12 relative to the house keeping gene RPII in patients with and without liver cirrhosis are shown on a logarithmic scale.

At SVR 12, not only HERV-K HML2, but also IL-10 was higher (U = 116.00, p = 0.009, n = 27) in liver cirrhosis patients. HERV-K HML2 induced IL-10 release had been described before (Morozov et al., 2013). Subsequently, IL-10 expression may have been triggered by HERV-K HML2 in this subset of patients.

As expected, liver cirrhosis patients performed worse when it came to liver related clinical parameters. The drop in mean hemoglobin by more than one point at EOT may have been due to the higher percentage of Ribavirin administration as this drug is known to induce hemolysis and a consequent drop in hemoglobin (Karasawa et al., 2013). All patients whose treatment was unsuccessful had liver cirrhosis. Interestingly, liver cirrhosis patients showed higher levels of HERV-K HML2 and were more likely to have HERV-K HML2 expression levels of above 1.

4.10 Influence of baseline serum albumin levels

Albumin levels are one of the default parameters monitored in patients with liver disease. Many clinical scores for liver cirrhosis include albumin levels. The Child Pugh Score is used widely for an estimate of liver cirrhosis mortality (Child & Turcotte, 1964; Pugh et al., 1973). Albumin levels below normal range ($\leq$ 35 g/l) add points to the score. Accordingly, a cutoff at 35 g/l was chosen to define high or low albumin levels at baseline.

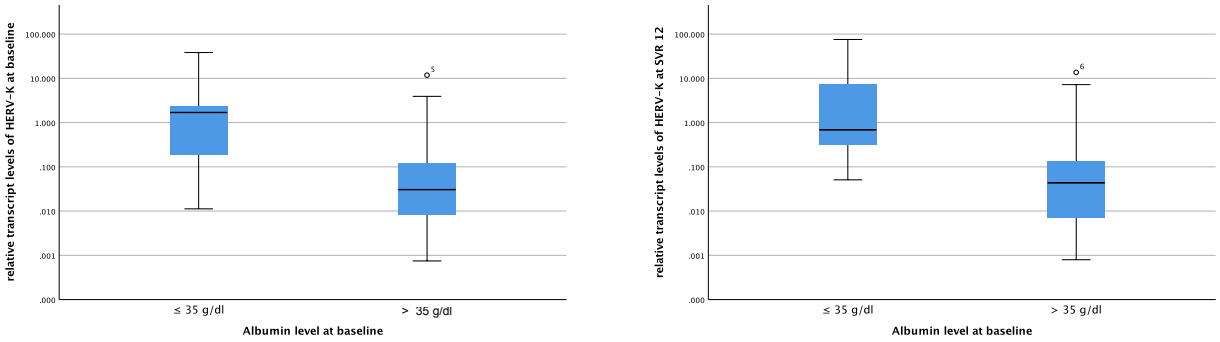

(a) HERV-K HML2 at baseline

(b) HERV-K HML2 at SVR 12

Figure 4.15 HERV-K HML2 expression at baseline (p = 0.004, n = 36) and SVR 12 (p = 0.006, n = 30) was significantly higher in patients with baseline albumin levels of $\leq$ 35 g/l. Relative expression levels of HERV-K HML2 at baseline and SVR 12 relative to the housekeeping gene RPII between patients with high (> 35 g/l) and low ($\leq$ 35 g/l) albumin levels at baseline are depicted as boxplots on a logarithmic scale.

HERV-K HML2 levels at baseline were significantly higher in patients with low albumin starting levels (p = 0.004, n = 36). Even though this difference was not significant at EOT (p = 0.104, n = 30), a highly significant difference could be detected at SVR 12 (p = 0.006, n = 30) (see figure 4.15). High HERV-K HML2 expression - defined by relative transcript levels of 1 or higher - was strongly correlated with albumin levels below 35 g/l at baseline and vice versa (chi-square 10.153, p = 0.001, Cramer's V 0.531). The odds of baseline HERV-K HML2 levels above 1 are much lower for patients with albumin starting levels of > 35 g/l (odds ratio 0.078, 95 % CI 0.014 - 0.436).

Patients who showed lower albumin levels also had higher bilirubin levels (figure 4.16), both indicating liver damage. At baseline, patients with low albumin started out with approximately double the mean bilirubin compared to patients with baseline albumin levels within normal range, however the difference was not significant at that time point (p = 0.016). During treatment bilirubin levels differed significantly (week 2 p = 0.001, week 4 p = 0.004). After treatment respective mean values converged as they declined in both groups (EOT p = 0.018, SVR 12 p = 0.062).
De-Ritis quotient was higher in patients with albumin starting levels of $\leq$ 35 g/l (baseline p < 0.001, EOT p = 0.017, SVR 12 p = 0.003).

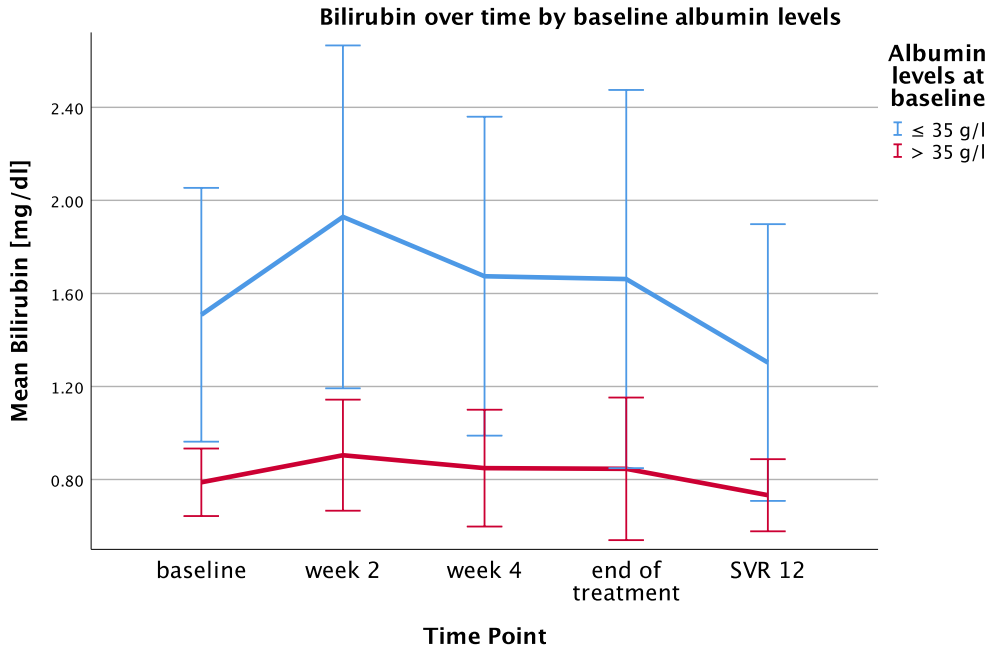

Figure 4.16 Patients with low albumin levels ($\leq$ 35 g/l) tend to have higher bilirubin levels. The development of mean bilirubin levels over time for patients with different albumin starting ranges is depicted. Error bars show the 95 % confidence intervals.

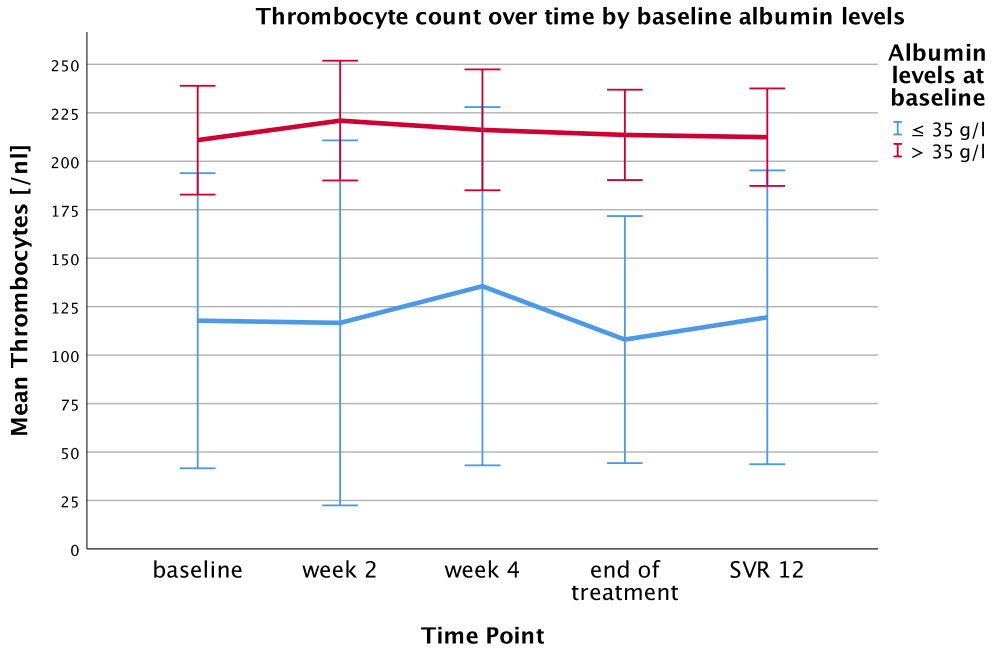

Figure 4.18 Patients with albumin baseline levels of > 35 g/l tended to have higher mean thrombocyte counts. Error bars show the 95 % confidence intervals.

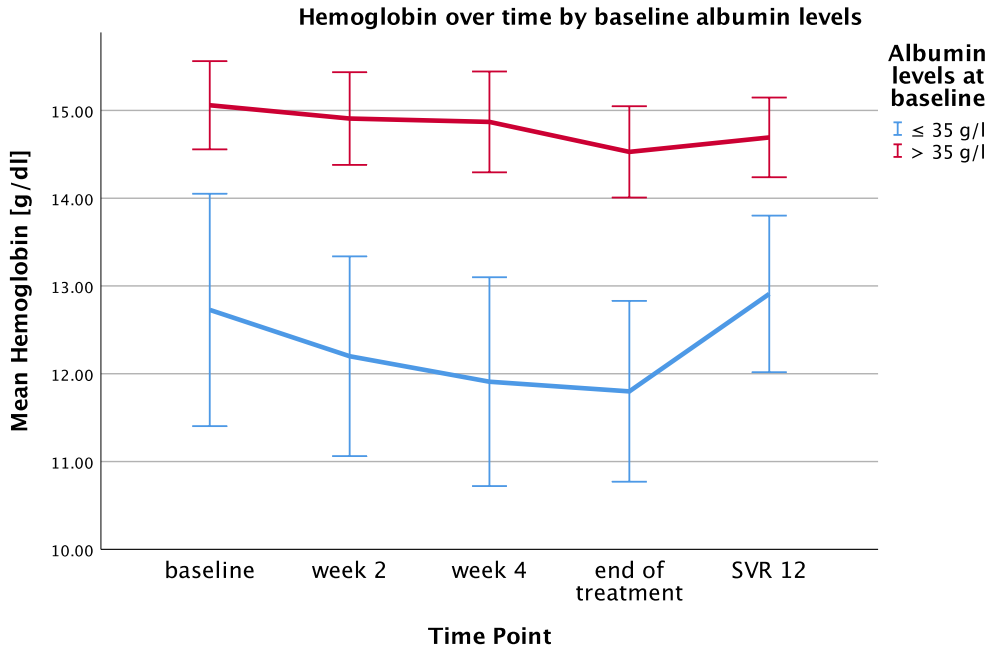

Figure 4.17 Patients with albumin levels of above 35 g/l at baseline showed significantly a higher hemoglobin count at all time points. Mean hemoglobin count for patient groups characterized by albumin levels of below or above 35 g/l over time is depicted in the graph. Error bars show the 95 % confidence intervals.

Hematology in patients with low (left) or high (right) serum albumin levels at baseline						
Time point	Mean hemoglobin			Mean thrombocyte count		
	$\leq$ 35 g/l	> 35 g/l	p-value	$\leq$ 35 g/l	> 35 g/l	p-value
baseline	12.73 g/dl	15.06 g/dl	p = 0.003	117.73 /nl	210.86 /nl	p = 0.004
week 2	12.20 g/dl	14.91 g/dl	p < 0.001	116.60 /nl	220.96 /nl	p = 0.005
week 4	11.91 g/dl	14.87 g/dl	p < 0.001	135.50 /nl	216.19 /nl	p = 0.027
EOT	11.80 g/dl	14.53 g/dl	p < 0.001	108.00 /nl	213.59 /nl	p < 0.001
SVR 12	12.91 g/dl	14.69 g/dl	p < 0.001	119.50 /nl	212.39 /nl	p = 0.002

Table 4.9 Patients with baseline serum albumin levels of $\leq$ 35 g/l showed lower hemoglobin levels and a lower thrombocyte count. P-values were calculated by independent samples t-tests.

Mean hemoglobin was about two to three points lower in patients with low albumin starting levels (figure 4.17, table 4.9). A gender bias between the groups could be ruled out (chi-square 0.25, p = 0.873). The lower mean hemoglobin levels were not worryingly low as the mean was still three points above the relative indication for transfusion of erythrocyte concentrates. Hemoglobin of less than 6 g/dl is considered an absolute indication for transfusion according to German guidelines (Vorstand der Bundesärztekammer auf Empfehlung des Wissenschaftlichen Beirats, 2014), which is much lower than the levels seen in these patients. P08 was the only patient with

hemoglobin levels of under 10 g/dl.

Not only did thrombocyte count differ significantly between the two groups at all time points except week 4 (table 4.9, figure 4.18), but for some patients the count was low enough that the risk for thrombocytopenic bleeding was increased (Kreuzer et al., 2019). Four patients (P08, P13, P15, P19) had thrombocyte counts of below 100 /nl and thrombocyte counts of P02, P07 and P17 were even below 50 /nl. Only three patients (P09, P14 and P40) with albumin levels below 35 g/l at baseline showed thrombocyte counts within normal range.

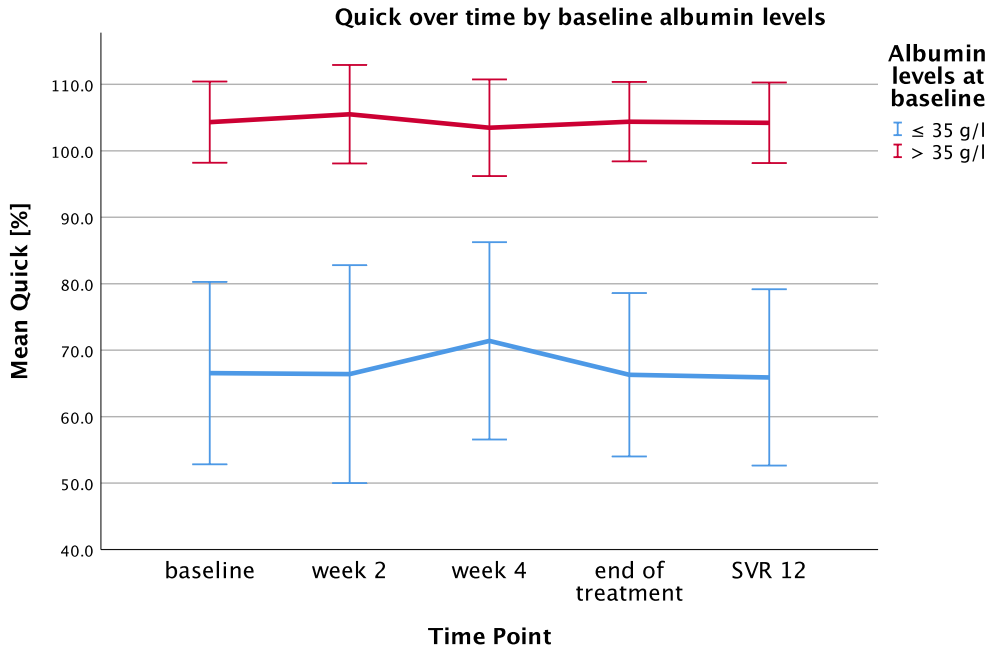

Figure 4.19 Mean Quick differed between patients with high and low baseline albumin levels at all time points. This difference was highly significant for any of the time points ($p < 0.001$). Error bars show the 95 % confidence intervals.

Hemostaseology in patients with low (left) or high (right) serum albumin levels at baseline						
Time point	Mean Quick			Mean INR		
	$\leq$ 35 g/l	> 35 g/l	p-value	$\leq$ 35 g/l	> 35 g/l	p-value
baseline	66.55 %	104.31 %	$p < 0.001$	1.38	1.01	$p = 0.007$
week 2	66.40 %	105.50 %	$p < 0.001$	1.46	1.02	$p = 0.036$
week 4	71.40 %	103.46%	$p < 0.001$	1.37	1.03	$p = 0.014$
EOT	66.30 %	104.38 %	$p < 0.001$	1.41	0.99	$p = 0.008$
SVR 12	65.90 %	104.21 %	$p < 0.001$	1.44	1.01	$p = 0.010$

Table 4.10 Patients with baseline serum albumin levels of $\leq$ 35 g/l showed a lower Quick and higher INR. P-values were calculated by independent samples t-tests.

Coagulation was impaired in patients with low albumin levels at baseline (figure 4.19, table 4.10). This may be due to defective liver function, but anticoagulatory drugs might have acted

as confounding variable. No information about anticoagulation itself or secondary diseases was obtained, thus an impact of these factors cannot be ruled out. However, albumin levels drop in advanced liver disease as it is synthesized in this location (Carvalho & Machado, 2018) and there was a clear correlation between albumin levels of $\leq$ 35 g/l at baseline and liver cirrhosis in this cohort (chi-square 18.433, p < 0.001, Cramer's V 0.679).

Even though leukocyte count did not show drastic differences between the groups (figure 4.20), it was significantly lower in patients who started out with low albumin levels at week 4 (p = 0.008), EOT (p = 0.002) and SVR 12 (p = 0.004). Mean leukocyte count was within normal range for both groups and CRP did not show a significant difference at any time point.

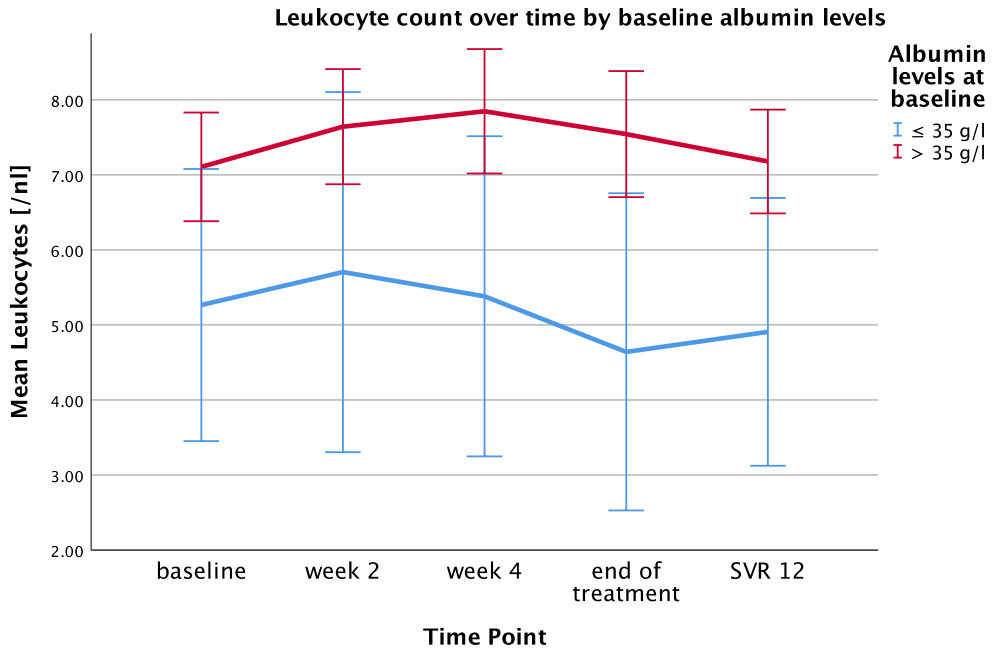

Figure 4.20 Patients with low baseline albumin levels ($\leq$ 35 g/l) showed significantly lower leukocyte counts at week 4, EOT and SVR 12. Error bars show the 95 % confidence intervals.

Albumin levels seemed to play an important role for a variety of clinical parameters including blood count and parameters for coagulation as well as cholestasis. Baseline levels of albumin below normal range were indicative of high HERV-K HML2 levels.

4.11 HERV-K HML2

4.11.1 HERV-K HML2 expression in HCV patients and healthy controls

Even though there are associations of HERV-K with a variety of viruses (see introduction) and HERV-K HML2 with liver disease (Ma et al., 2016), a role of HERV-K HML2 in hepatitis C has yet to be revealed. To shed light on this, HERV-K HML2 expression levels of healthy blood donors

were compared with those of a cohort of HCV positive patients undergoing DAA therapy. Additionally, clinical data as well as HERV-K HML2 expression levels of the hepatitis C patients were obtained throughout treatment as well as 12 weeks after the end of treatment. This way the association between HERV-K HML2 and clinical development as well as outcome of these patients could be studied.

HERV-K HML2 levels in hepatitis C patients at baseline and SVR 12 are visualized in figure 4.21. The majority of patients had relative transcript levels of HERV-K HML2 below 1 at baseline as well as SVR 12. Yet, there were some patients whose HERV-K HML2 levels were especially high at baseline or SVR 12 respectively. Overall, HERV-K HML2 expression seemed to be distributed very heterogeneously among hepatitis C patients.

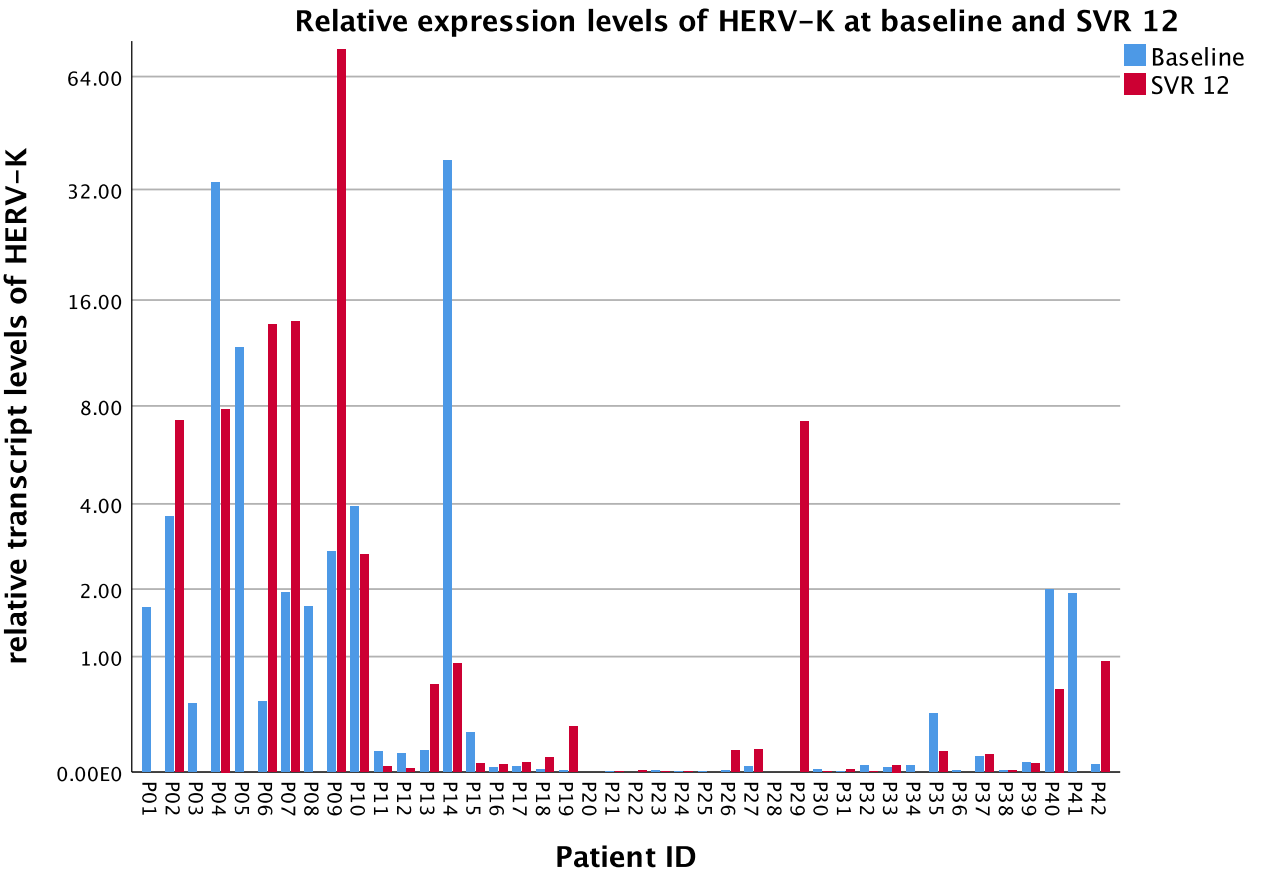

Figure 4.21 HERV-K HML2 expression levels at baseline and SVR 12 showed a heterogeneous pattern for hepatitis C patients. The distribution of HERV-K HML2 expression levels relative to the housekeeping gene RPII in 42 hepatitis C patients at baseline and SVR 12 is depicted as a barchart on a logarithmic scale.

Four healthy controls were screened for HERV-K HML2 expression levels. They showed a median HERV-K HML2 expression of 0.958. HC01 had a HERV-K HML2 expression level of 1.057, HC02 of 0.859, HC 03 of 1.165 and HC04 of 0.678. There was much less variation of HERV-K HML2 expression in this group. However, only four people were screened. Considering

the high degree of variation within the group of HCV positive patients, more healthy volunteers need to be screened for a better comparison.

Subgroup	baseline	p-value	SVR 12	p-value
all patients	0.077	p = 0.184	0.100	p = 0.128
liver cirrhosis	1.705	p = 0.414	2.694	p = 0.648
no liver cirrhosis	0.035	p = 0.020	0.050	p = 0.015
albumin > 35 g/l	0.032	p = 0.013	0.044	p = 0.038
albumin $\leq$ 35 g/l	1.705	p = 0.489	0.688	p = 0.71
Simeprevir	1.945	p = 0.226	7.835	p = 0.073
no Simeprevir	0.032	p = 0.010	0.051	p = 0.006

Table 4.11 Patients with albumin levels of > 35 g/l or without liver cirrhosis showed significantly lower HERV-K HML2 expression levels at baseline. Median relative expression of HERV-K HML2 for subgroups compared to healthy controls is depicted. Healthy controls showed a median HERV-K HML2 expression of 0.958. P-values were calculated by Mann-Whitney-U tests.

Comparing the cohort of HCV infected patients with the healthy controls, no significant difference in HERV-K HML2 expression levels could be detected at baseline or SVR 12. However, as depicted in table 4.11, patients without liver cirrhosis as well as patients with albumin levels within normal range at baseline had significantly lower HERV-K HML2 levels at baseline compared to the healthy controls. For both aforementioned conditions median HERV-K HML2 levels were low at SVR 12 as well. The boxplots of baseline HERV-K HML2 expression levels compared to HC clearly depicted the wider range of HERV-K HML2 expression in hepatitis C patients. Yet, for both subgroups the whole span of the interquartile range projected below the HERV-K HML2 levels found in healthy controls in the graphs.

Patients infected with HCV, but without severe liver damage, showed suppressed HERV-K HML2 expression. In patients with severe liver damage - e.g. liver cirrhosis or albumin levels below the normal range as indicator of impaired liver synthesis function - median HERV-K HML2 levels at baseline were above 1 (figure 4.22). For patients with liver cirrhosis the median stayed at a high level at SVR 12, whereas it dropped in patients with baseline albumin levels of $\leq$ 35 g/l. Interestingly, IP-10 levels were significantly elevated in the same subgroups at baseline (table 4.14).

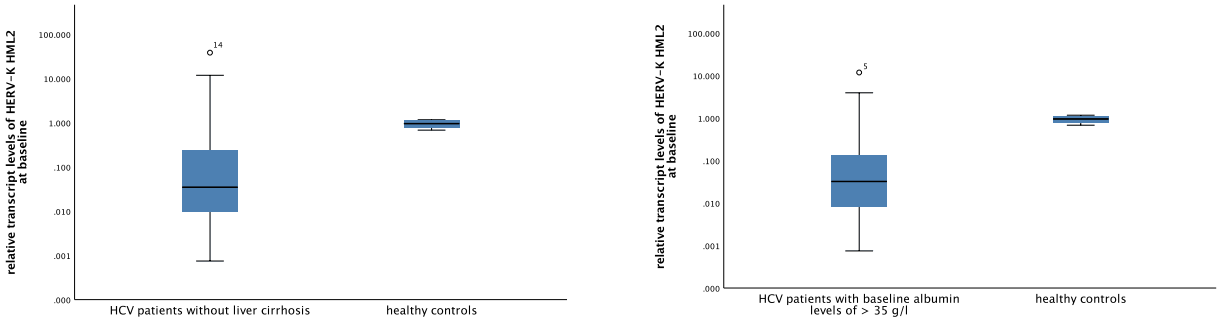

(a) No liver cirrhosis

(b) Albumin levels of > 35 g/l

Figure 4.22 Healthy controls showed higher median baseline HERV-K HML2 levels than hepatitis C patients without liver cirrhosis or baseline albumin within normal range. Boxplot of median HERV-K HML2 expression levels at baseline of hepatitis C patients a) without liver cirrhosis (n = 28) and b) with baseline albumin levels of > 35 g/l (n = 25) compared to healthy controls (n = 4).

4.11.2 Correlation of HERV-K HML2 expression at different time points

To examine the dynamics of HERV-K HML2 expression levels more closely, the development of parameters over time and correlations between different time points were examined.
Generally, HERV-K HML2 levels were positively correlated with each other at almost all time points except for week 2. An overview of the correlation matrix can be found in Table 4.12. HERV-K HML2 levels at week 2 did not correlate significantly with the other time points. Baseline HERV-K HML2 levels showed strong correlations (correlation coefficient of > 0.5) with HERV-K HML2 levels at any of the later time points, though. This means that high baseline expression levels were indicative of high HERV-K HML2 levels after week 2 and vice versa. Looking at the development of HERV-K HML2 levels in each patient depicted in Figure 4.23 there was either a spike or a dent visible for many patients at week 2. Start of treatment may influence expression levels at first. The correlation coefficient of HERV-K HML2 between EOT and SVR 12 was lower than between other time points. Thus, stopping DAA treatment may also have had an influence on HERV-K HML2 expression. The time difference between EOT and SVR 12 was twelve weeks, whereas week 2 was measured two weeks after the beginning of treatment. So HERV-K HML2 levels might already have partially recovered from DAA treatment by SVR 12. At EOT HERV-K HML2 expression levels also seemed to be much less spread out between patients than at other time points, which might be a hint that DAA treatment might have influenced HERV-K HML2 levels. Mixed model analysis showed a significant increase in HERV-K HML2 levels ($p = 0.039$) of 0.2667 to 9.869 (95 % confidence interval) between EOT and SVR 12. As liver cirrhosis was positively correlated with HERV-K HML2 levels at SVR 12, it was added to the model as a fixed effect. However, liver cirrhosis did not have a significant influence on this model (mixed model analysis, Type III Test of fixed effects: $F = 4.467$, $p = 0.062$).

	baseline	week 2	week 4	EOT	SVR 12
baseline	1	0.281 (p = 0.103)	0.660 (p < 0.001)	0.556 (p < 0.001)	0.540 (p < 0.001)
week 2	0.281 (p = 0.103)	1	0.283 (p = 0.126)	0.495 (p = 0.014)	0.257 (p = 0.181)
week 4	0.660 (p < 0.001)	0.283 (p = 0.126)	1	0.516 (p = 0.010)	0.486 (p = 0.012)
EOT	0.566 (p < 0.001)	0.495 (p = 0.014)	0.516 (p = 0.010)	1	0.399 (p = 0.006)
SVR 12	0.540 (p < 0.001)	0.257 (p = 0.181)	0.486 (p = 0.012)	0.399 (p = 0.006)	1

Table 4.12 Baseline expression levels of HERV-K HML2 did not correlate with those at week 2, but with week 4, EOT and SVR 12. A correlation matrix of HERV-K HML2 for five time points with correlation coefficients (kendall's tau) and respective p-values are shown.

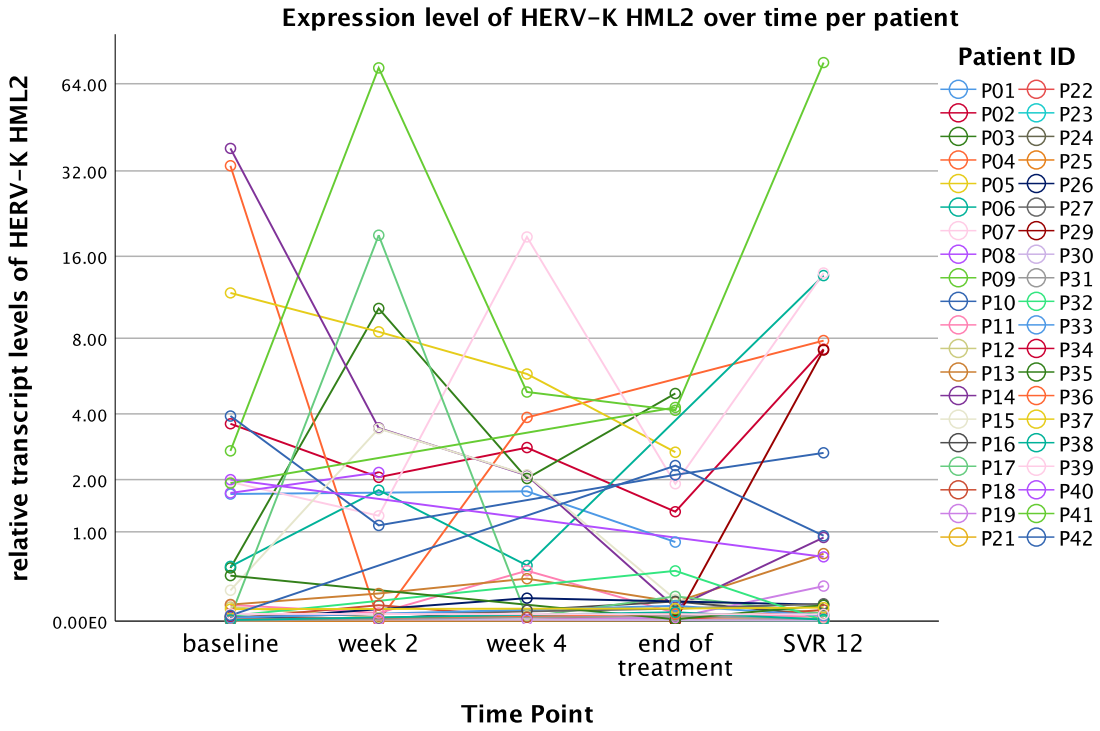

Figure 4.23 HERV-K HML2 expression levels showed the least spread between individual patients at EOT. Expression levels of HERV-K HML2 over time per patient are depicted on a logarithmic scale.

HERV-K HML2 expression levels showed a dynamic throughout the study. The start of DAA treatment seemed to alter HERV-K HML2 levels as seen at week 2. At end of treatment, levels of HERV-K HML2 expression showed the least variability and at that point there were no patients with relative expression levels above 5. This effect most likely caused by drug administration could not be seen at SVR 12 as HERV-K HML2 levels spread out again (figure 4.23).

4.11.3 Correlations of HERV-K HML2 with clinical parameters

To explore if HERV-K HML2 played a role in hepatitis C, baseline values of clinical parameters were correlated with HERV-K HML2 expression levels. Above that, end of treatment as well as

SVR 12 were taken a closer look at to evaluate if HERV-K HML2 levels either influence the outcome of DAA treatment or if treatment changed HERV-K HML2 expression levels.
HERV-K HML2 baseline transcript levels were compared with HCV RNA at SVR 12 to assess if HERV-K HML2 expression at baseline might affect treatment outcome. As no HCV RNA was detectable for any patient at EOT, statistical analysis of this time point was not reasonable. There was a significant correlation of 0.273 (p = 0.049) between baseline and SVR 12 in this cohort. A pairwise comparison of HERV-K HML2 levels at baseline revealed a tendency of higher starting levels of HERV-K HML2 in patients who did not achieve sustained viral response (p = 0.051, figure 4.24). As there were only two patients who did not achieve sustained viral response, however, more data on patients without treatment success are needed to conclude if HERV-K HML2 could be a predictor for HCV levels at SVR 12.

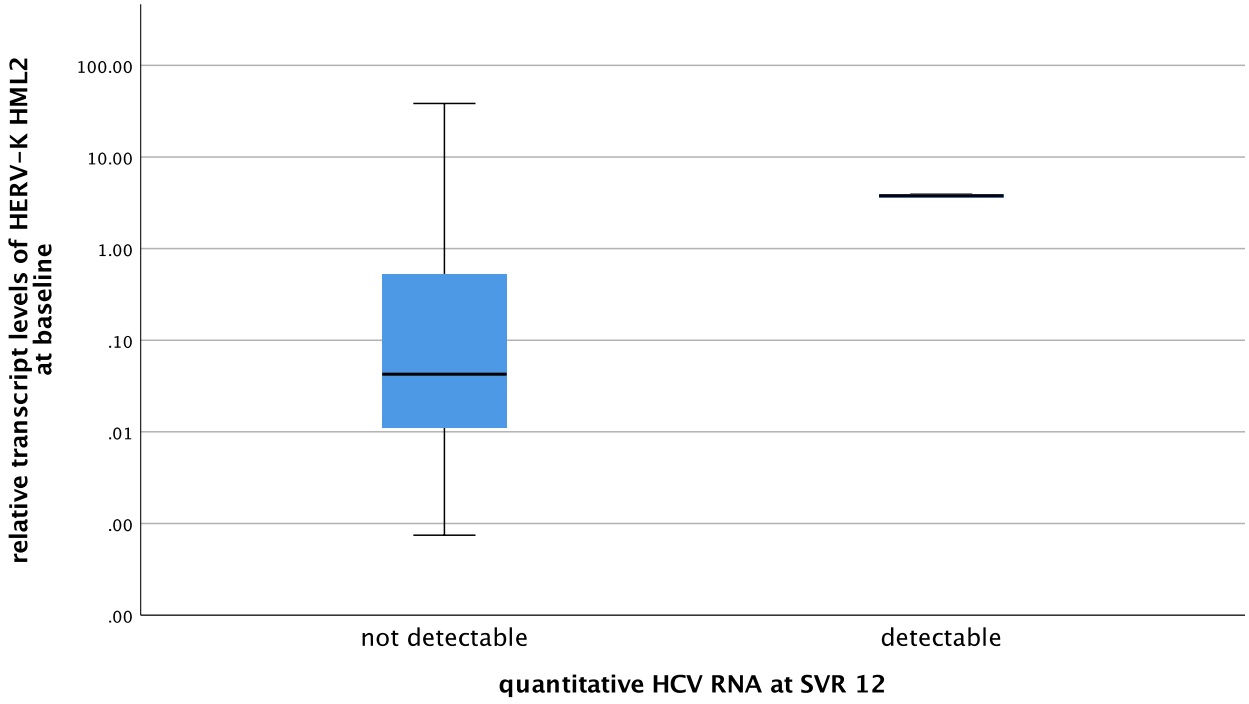

Figure 4.24 Patients without sustained viral response showed a tendency to higher HERV-K HML2 expression levels at baseline. HERV-K HML2 expression levels at baseline for patients for patients with (n = 36) and without (n = 2) sustained viral response are depicted as boxplots on a logarithmic scale.

There was a positive correlation between HERV-K HML2 at EOT and ASAT at SVR 12 (0.416, p = 0.002). HERV-K HML2 levels at SVR 12 correlated positively with the De-Ritis quotient at baseline (0.343, p = 0.008, n = 30), end of treatment (0.342, p = 0.007, n = 31) as well as SVR 12 (0.333, p = 0.010, n = 30). The positive correlation can be visually identified by taking a glance at the respective scatterplots (figures 4.25 and 4.26). There was no statistically significant correlation between HERV-K HML2 and ALAT.

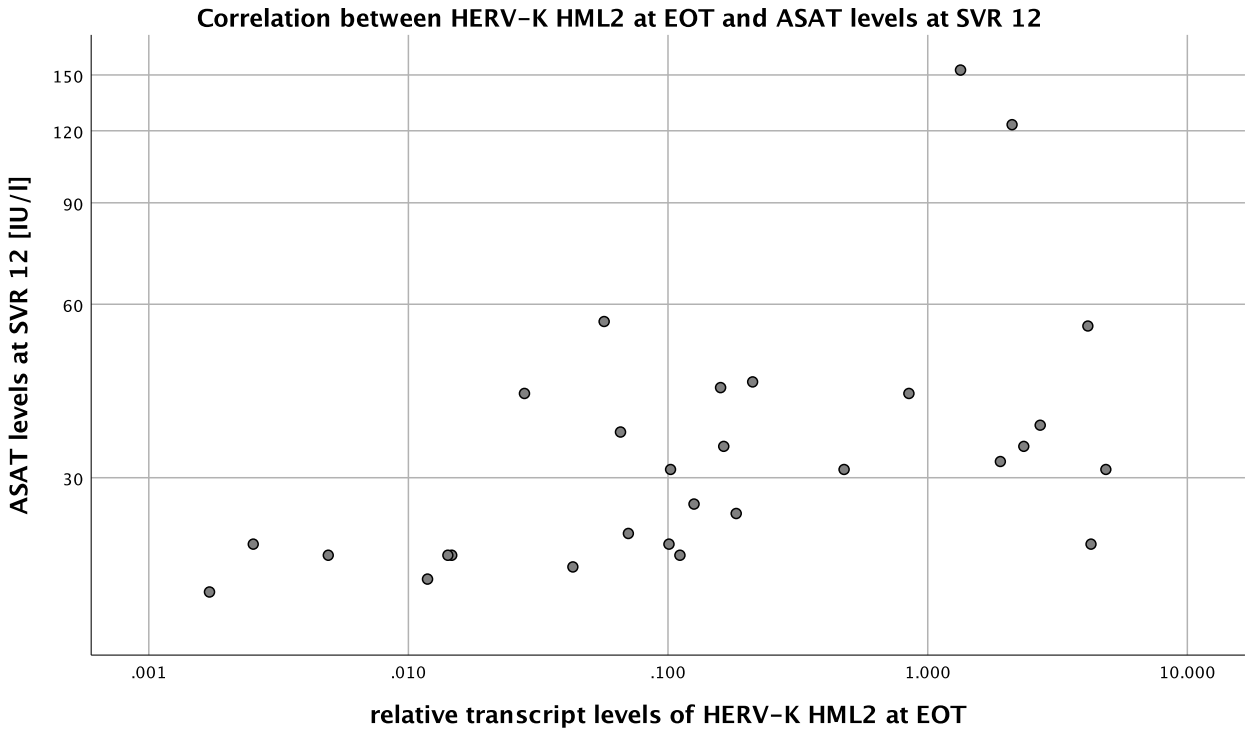

Figure 4.25 Higher levels of HERV-K HML2 at EOT correlated with higher ASAT levels at SVR 12. The correlation between ASAT at SVR 12 and HERV-K HML2 at EOT is shown as a scatter plot on a logarithmic scale.

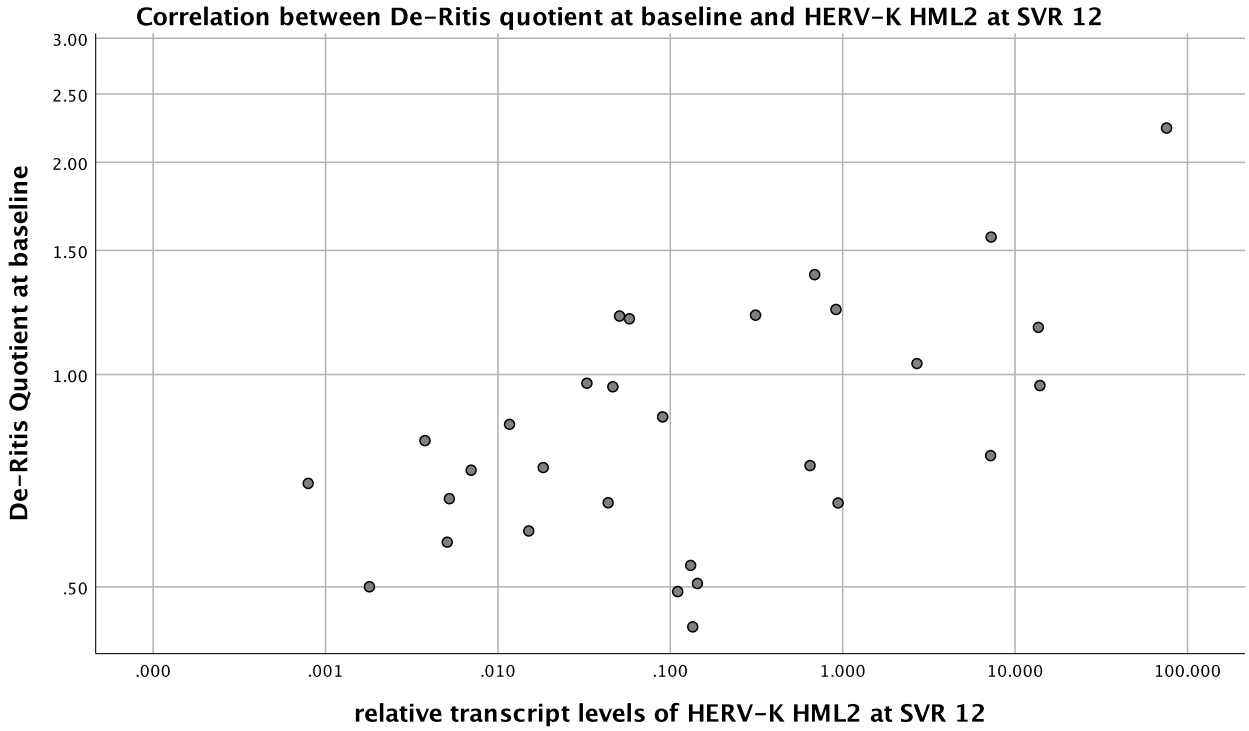

Figure 4.26 Higher levels of HERV-K HML2 at SVR 12 correlated with a higher De-Ritis quotient at baseline. The correlation between HERV-K HML2 at SVR 12 and De-Ritis quotient at baseline is shown as a scatter plot on a logarithmic scale.

Higher HERV-K HML2 levels at baseline correlated with lower albumin levels at EOT (-0.331, p = 0.006, n = 36). HERV-K HML2 expression levels at SVR 12 inversely correlated with albumin levels at baseline (-0.347, p = 0.009, n = 30) and EOT (-0.435, p = 0.001, n = 31). In the scatter plot (figure 4.27) patients with high albumin levels at baseline or EOT tended to have low HERV-K HML2 expression levels at SVR 12 and vice versa.

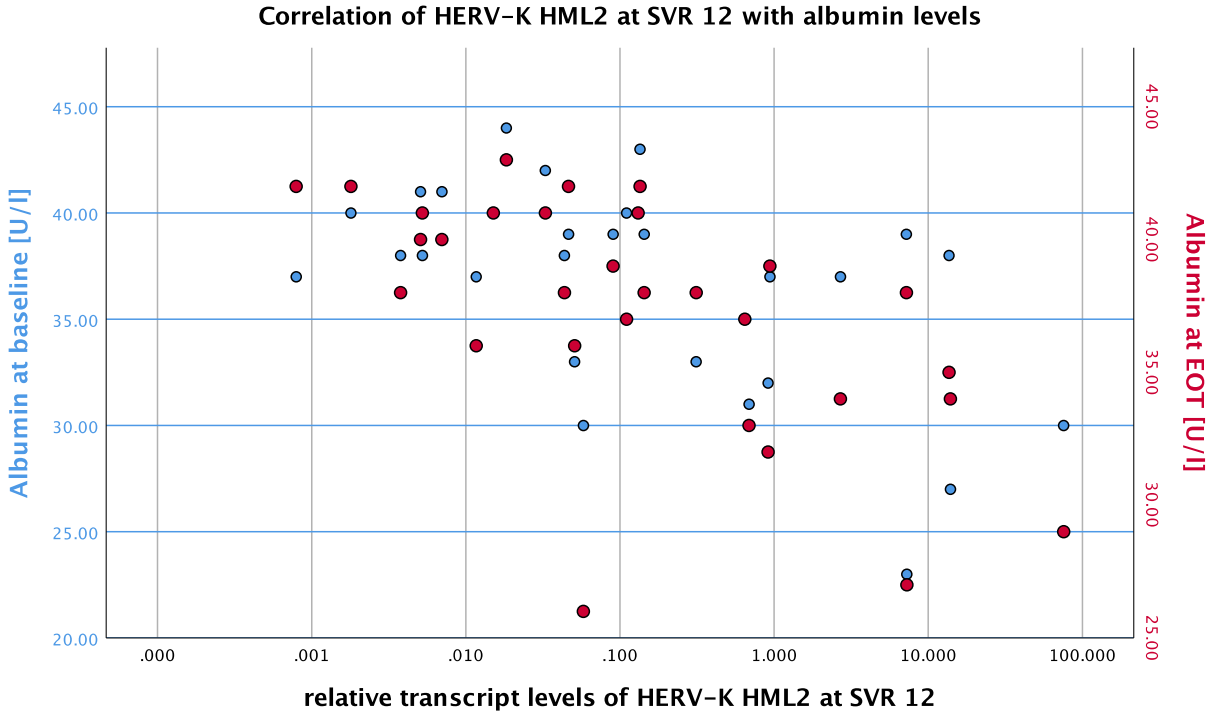

Figure 4.27 Higher levels of HERV-K HML2 at SVR 12 correlated with lower albumin levels at baseline and EOT. The correlation between HERV-K HML2 at SVR 12 and albumin levels at baseline as well as EOT is shown as a scatter plot on a logarithmic scale.

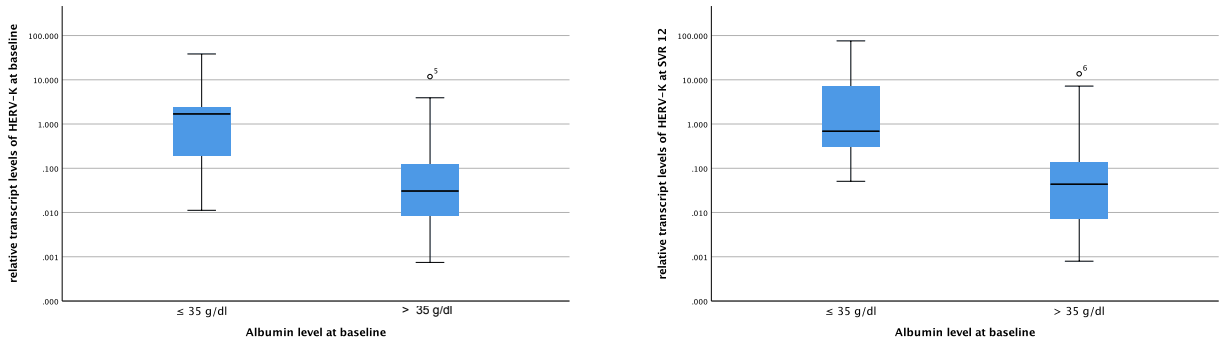

(a) baseline **(b)** SVR 12

Figure 4.28 Patients with baseline serum albumin levels of $\leq$ 35 g/l showed higher median expression levels of HERV-K HML2 at baseline (p = 0.004) as well as SVR 12 (p = 0.006) compared to patients with higher albumin levels before the start of treatment. Boxplots of HERV-K HML2 expression levels at a) baseline ($\leq$ 35 g/l: n = 13, > 35 g/l: n = 25) and b) SVR 12 ($\leq$ 35 g/l: n = 11, > 35 g/l: n = 21) for patients with baseline serum albumin levels of either $\leq$ 35 g/l or > 35 g/l are depicted.

Patients with albumin levels of $\leq$ 35 g/l at baseline had higher HERV-K HML2 levels at baseline (p = 0.004) as well as SVR 12 (p = 0.006) (figure 4.28). Above, at baseline, HERV-K HML2 transcript levels of above 1 and low albumin levels correlated as well (p = 0.001). There was an inverse correlation between albumin levels and HERV-K HML2 expression levels. Patients with low albumin levels, possibly due to an impairment of liver synthesis function, had higher HERV-K HML2 expression levels.
Except for a negative correlation between HERV-K HML2 at baseline and the respective leukocyte count (-0.276, p = 0.016, n = 37), there were no significant correlations between HERV-K HML2 levels and blood count. Quick at baseline showed negative correlation with HERV-K HML2 levels at baseline (-0.323, p = 0.006, n = 36). The INR at baseline was positively correlated with HERV-K HML2 expression at baseline (0.312, p = 0.013, n = 36), which complemented the correlation seen with Quick.
Liver cirrhosis patients had a higher De-Ritis quotient, lower albumin levels and lower Quick levels at baseline. Each of those parameters separately corresponded with higher levels of HERV-K HML2 expression at baseline and/or SVR 12. The presence of liver cirrhosis also positively correlated with HERV-K HML2 expression levels at SVR 12 (0.410, p = 0.022).

HERV-K HML2 expression levels were significantly higher or showed significant correlations with many parameters indicating worse liver function or liver damage in hepatitis C patients.

4.11.4 Analysis of the influence of baseline HERV-K HML2 expression on gene expression of experimental parameters

High HERV-K HML2 expression was defined as an expression level of at least the same level as the housekeeping gene RPII, so numerically > 1. At EOT, IL-6 expression was significantly lower in patients with high expression levels of HERV-K HML2 at baseline (p = 0.006, figure 4.29 (a)). Due to IL-6 being a pro-inflammatory marker, leukocyte and CRP levels at SVR 12 were compared between the groups. While leukocyte count was lower at SVR 12 (in HERV-K HML2 > 1, p = 0.041), there was no significant difference in CRP levels. IP-10 levels at SVR 12 were significantly higher in patients with HERV-K HML2 expression at baseline (p = 0.003, figure 4.29 (b)). No significant difference in IP-10 levels was observed between the two groups at any other time point.
There were no significant differences of expression levels of A20 or IL-10 at any time point when comparing the two groups of HERV-K HML2 expression levels at baseline.

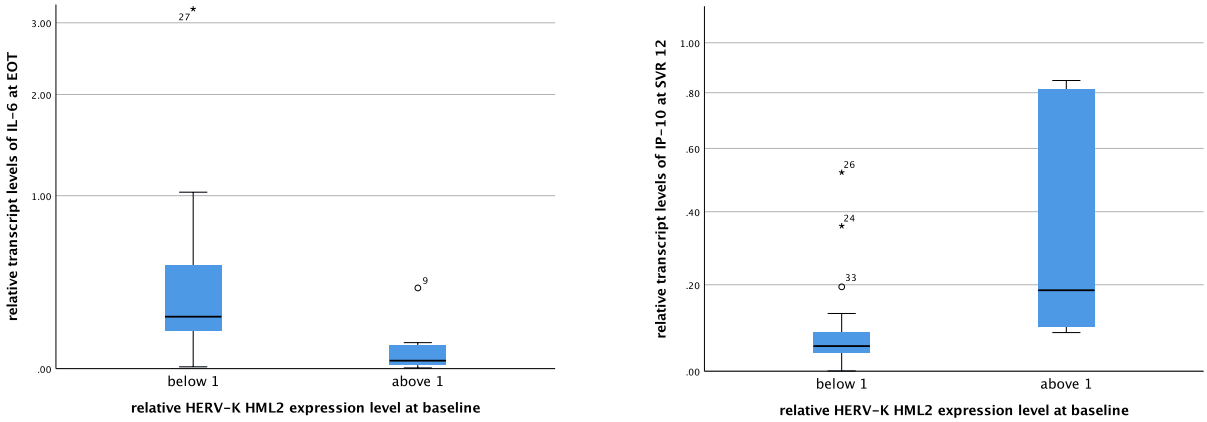

(a) IL-6 at EOT

(b) IP-10 at SVR 12

Figure 4.29 Patients with HERV-K HML2 expression levels of above 1 showed significantly lower IL-6 levels at EOT (p = 0.006) and significantly higher IP-10 levels at SVR 12 (p = 0.003). The boxplots show the relative expression levels of IL-6 at EOT (below 1: n = 23, above 1: n = 8) and IP-10 at SVR 12 (below 1: n = 24, above 1: n = 6) relative to the housekeeping gene RPII between patients with HERV-K HML2 expression levels of below or above 1 at baseline.

HERV-K HML2 expression at baseline was associated with the De-Ritis quotient at baseline (chi-square 5.639, p = 0.018, Cramer's V 0.396, Mann-Whitney-U: p = 0.011). Apart from this, at baseline Quick was higher in patients with low HERV-K HML2 levels (p = 0.006), but INR was not. Albumin levels were also significantly higher at all time points except for SVR 12. SVR 12 was the only time point when mean albumin levels were within normal range for patients with high baseline expression levels of HERV-K HML2. For patients with low relative transcript levels of HERV-K HML2 at baseline, mean albumin was within normal range for all time points. DAA treatment might have lead to a recovery of albumin levels in patients with baseline HERV-K HML2 levels above 1 (table 4.13).

Mean albumin levels by HERV-K HML2 expression at baseline			
Time point	HERV-K HML2 < 1	HERV-K HML2 > 1	p-value
baseline	38.04 g/l	32.10 g/l	p = 0.005
week 2	37.52 g/l	31.89 g/l	p = 0.003
week 4	38.45 g/l	32.56 g/l	p = 0.001
EOT	38.35 g/l	34.10 g/l	p = 0.004
SVR 12	38.68 g/l	35.30 g/l	p = 0.048

Table 4.13 Mean albumin levels were significantly lower for patients with HERV-K HML2 expression levels of > 1 at baseline, but recovered throughout DAA treatment. P-values were calculated by independent samples t-tests.

Many of the correlations described in the previous chapter could be supported by pairwise comparison of the two groups defined by their HERV-K HML2 expression level at baseline. A

cutoff at a relative expression level of 1 could be useful to assess the development of clinical and experimental parameters at baseline and possibly for the development of a predictive score for clinical outcome of DAA treatment in hepatitis C patients.

4.12 Analysis of IP-10, IL-6, A20 and IL-10 expression

An short introduction for each of the experimental parameters is provided in section 4.4.2. All of the parameters in this section are inflammation markers linked to the NF-kB pathway.

4.12.1 IP-10

Levels of IP-10 expression showed a broad distribution among patients at baseline. These baseline levels correlated strongly with the IP-10 levels at week 2 (0.668, p = 0.002, n = 13). There seemed to be a drop in IP-10 levels after week 2. At SVR 12, IP-10 levels spread out again, but not quite as much as at baseline (figure 4.30). Correspondingly IP-10 levels at week 2 were by 0.459 to 3.181 (95 % confidence interval) higher than at SVR 12 (mixed model analysis, p = 0.018). At SVR 12 median IP-10 levels were about half as high compared to baseline for patients without liver cirrhosis and patients with high baseline albumin levels. This means that after completion of treatment they approached the median expression level of healthy controls which was 0.063. HCV infection was associated with high IP-10 expression levels in patients without liver cirrhosis (p = 0.020) or albumin levels of > 35 g/l at baseline (p = 0.026). The difference in HCV expression level compared to healthy controls was also significant for all patients (p = 0.020), but not for those with liver cirrhosis (p = 0.171) or low albumin levels (p = 0.109) when analyzed separately. During DAA treatment IP-10 levels normalized and at SVR 12 there was no significant difference between healthy blood donors and any of the groups, even though patients with liver cirrhosis and patients with low albumin starting levels maintained a higher median value of IP-10 at SVR 12.

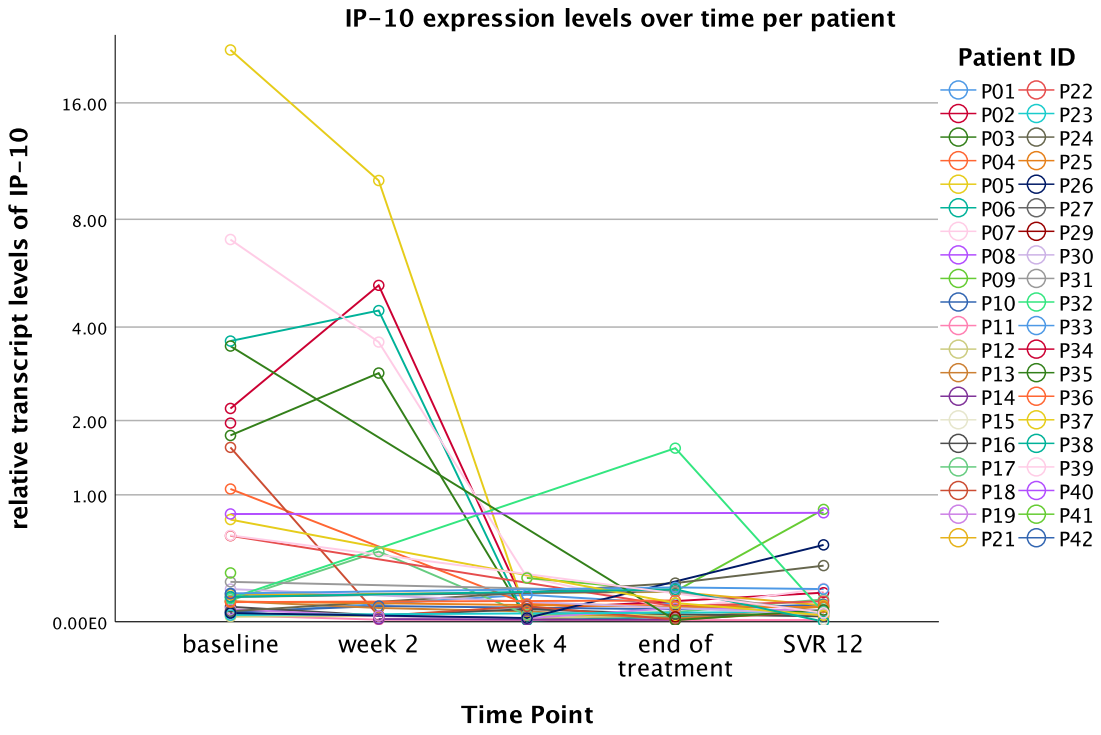

Figure 4.30 A decline of IP-10 expression levels after the start of DAA treatment could be observed. Relative IP-10 transcript levels for each patient by time point are depicted on a logarithmic scale.

Median IP-10 expression levels				
Subgroup	baseline	p-value	SVR 12	p-value
all patients	0.166	p = 0.020	0.066	p = 0.439
liver cirrhosis	0.121	p = 0.171	0.129	p = 0.109
no liver cirrhosis	0.167	p = 0.020	0.056	p = 0.748
albumin $>$ 35 g/l	0.163	p = 0.026	0.056	p = 0.725
albumin $\leq$ 35 g/l	0.123	p = 0.109	0.151	p = 0.154

Table 4.14 IP-10 expression differed between hepatitis C patients and healthy controls at baseline, but not at SVR 12. Median relative IP-10 expression levels for each subgroup of hepatitis C patients were compared to healthy controls. Healthy controls showed a median IP-10 expression level of 0.063. P-values were calculated by Mann-Whitney-U tests.

IP-10 levels at week 2 strongly correlated with bilirubin levels at EOT (0.516, p = 0.010, n = 14) and SVR 12 (0.508, p = 0.012, n = 14) (figure 4.31). IP-10 levels at EOT, when the median of IP-10 was at a very low level of 0.082, positively correlated with with leukocyte levels (0.311, p = 0.026, n = 26) and CRP (0.312, p = 0.026, n = 26) at the same time point.

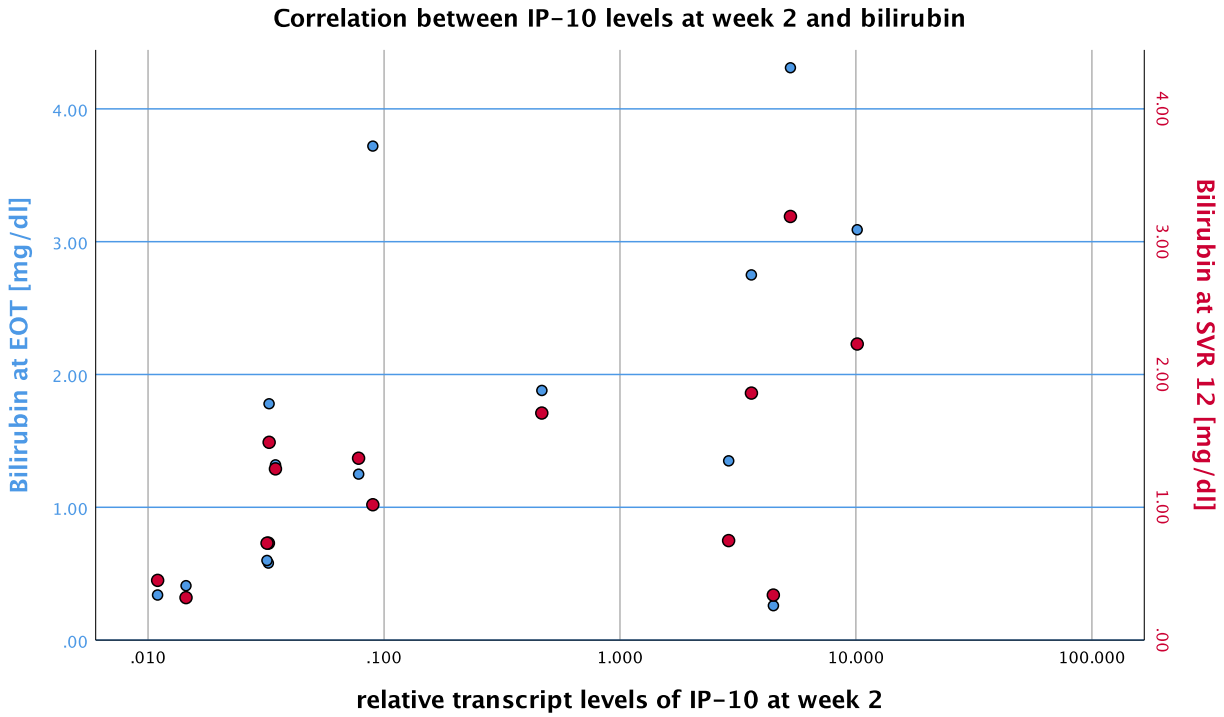

Figure 4.31 IP-10 levels at week 2 showed a strong positive correlation with bilirubin levels at EOT and SVR 12. A scatter plot of the relative transcript levels of IP-10 at week 2 and bilirubin levels at EOT (blue dots) and SVR 12 (red dots) is depicted. Logarithmic scale.

IP-10 baseline levels correlated with HERV-K HML2 levels at baseline (0.312, p = 0.009, n = 34) and IP-10 levels at week 2 correlated strongly with HERV-K HML2 levels at EOT (0.636, p = 0.004, n = 12). Baseline IP-10 expression levels showed a negative correlation with A20 levels at SVR 12 (-0.409, p = 0.003, n = 26). IP-10 at EOT correlated with IL-6 levels at EOT (0.345, p = 0.014) and for both parameters the expression levels seemed to be less spread out at EOT than at other time points. So, IP-10 showed positive correlations with rather pro-inflammatory markers (IL-6 and HERV-K HML2), whereas it was negatively correlated with A20, an anti-inflammatory agent.

There was evidence that IP-10 levels were elevated in hepatitis C patients compared to healthy controls. This observation could be reversed by DAA treatment. IP-10 levels at early time points showed positive correlations with bilirubin and HERV-K HML2 levels at EOT. At EOT, IP-10 levels were positively correlated with leukocytes, CRP and IL-6, all markers for inflammation, at the same time point.

4.12.2 IL-6

Even though IL-6 is a pro-inflammatory cytokine, no significant correlation between IL-6 and leukocyte count or CRP levels could be detected. Hemoglobin at week 2 (-0.527, p = 0.005, n = 16), week 4 (-0.542, p = 0.005, n = 15) and EOT (-0.505, p = 0.009, n = 15) showed strong in-

verse correlations with IL-6 levels at week 2. This correlation was not significant at SVR 12. While hemoglobin levels decreased from baseline to EOT, mean hemoglobin showed an increase after treatment was finished, which might have caused the loss of correlation at SVR 12. Drug administration might have caused IL-6 expression and contributed to lower hemoglobin levels, especially as IL-6 was not correlated with hemoglobin levels at baseline and SVR 12. IL-6 levels at week 2 were also positively correlated with the De-Ritis quotient at baseline (0.517, p = 0.005, n = 16). So patients with more severe pre-existing liver damage seemed to induce greater expression of IL-6 upon start of treatment.

IL-6 levels at different time points were positively correlated with each other. Especially IL-6 levels at EOT showed statistically significant correlations with expression levels at baseline (0.401, p = 0.004, n = 26), week 2 (0.769, p < 0.001, n = 13) and SVR 12 (0.408, p = 0.008, n = 22). IL-6 levels at week 4 showed a significant positive correlation with those at SVR 12 (0.590, p = 0.005, n = 13). However, no significant trend in development of IL-6 over time could be identified (mixed model analysis, figure 4.32). Strikingly, the correlation between IL-6 at week 2 and EOT was by far the strongest.

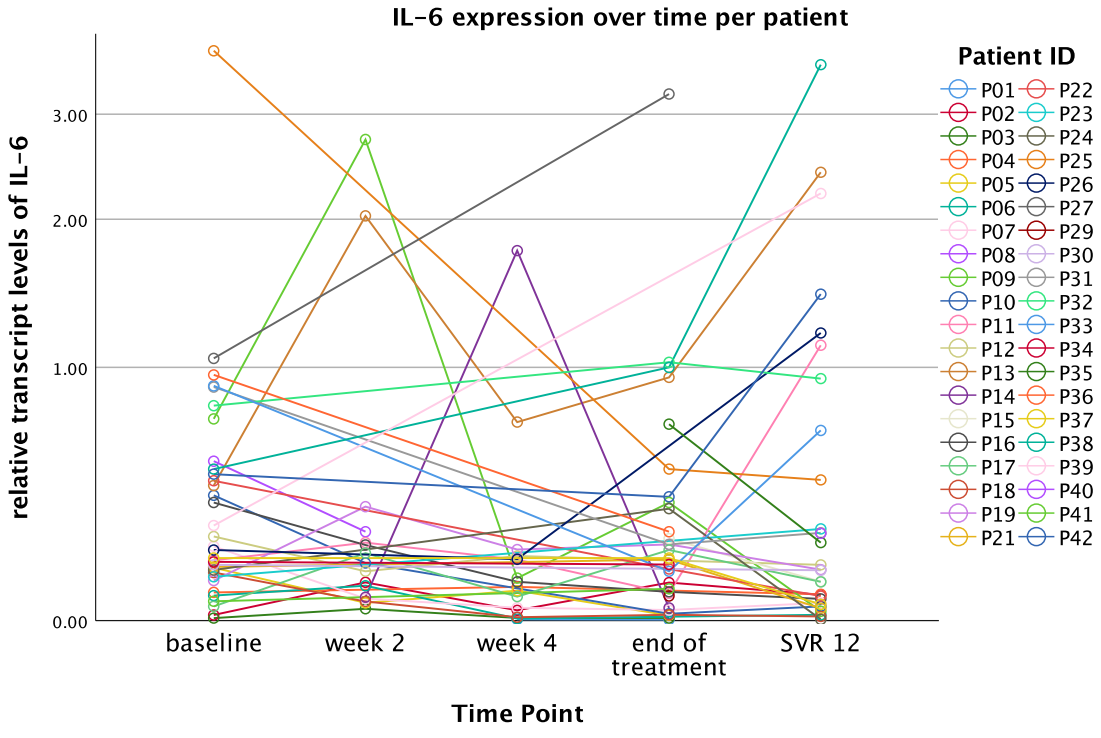

Figure 4.32 IL-6 expression seemed to be affected by the start of DAA treatment and IL-6 levels at week 2 strongly correlated with those at EOT (correlation coefficient 0.769, n = 13). The expression level of IL-6 over time per patient is shown on a logarithmic scale.

Comparing IL-6 levels to other experimental parameters at baseline, EOT and SVR 12, correlations with HERV-K HML2, IP-10 and IL-10 could be found. IL-6 expression levels at baseline correlated with IL-10 levels at baseline (0.371, p = 0.003, n = 32). At EOT, IL-6 showed a neg-

ative correlation with HERV-K HML2 baseline levels (-0.313, p = 0.017, n = 29) and a positive correlation with EOT IP-10 levels (0.345, p = 0.014, n = 26).

IL-6 expression might have been induced by drug administration and lead to a fall in hemoglobin. The interactions with other pro- and anti-inflammatory cytokines seemed to be too sophisticated to deduct a clear motive from these data.

4.12.3 A20

A20 expression levels at baseline showed a positive correlation with ALAT levels at EOT (0.327, p = 0.005, n = 37). Apart from that, CRP at week 4 was correlated with A20 levels at EOT (0.430, p = 0.003, n = 25). A20 levels only correlated with each other at week 4 and SVR 12 (0.604, p = 0.003, n = 14) and there was no significant change in A20 levels over time (mixed model analysis). Apart from that A20 at baseline correlated with IL-6 levels at week 4 (0.559, p = 0.002, n = 17) and A20 at SVR 12 showed an inverse correlation with baseline expression levels of IP-10 (-0.409, p = 0.003, n = 26).
For P14, the patient with a peak in relative A20 transcript levels at week 4 (5.938), quantitative HCV RNA was still detectable at that time point. At week 4, HCV RNA could only be detected in a total of 7 patients. However, there was no other peculiarity for any clinical or experimental parameter that might be associated with this peak in A20.

No clear pattern for the development of A20 expression levels in this cohort nor the association with other experimental or clinical parameters could be identified (figure 4.33).

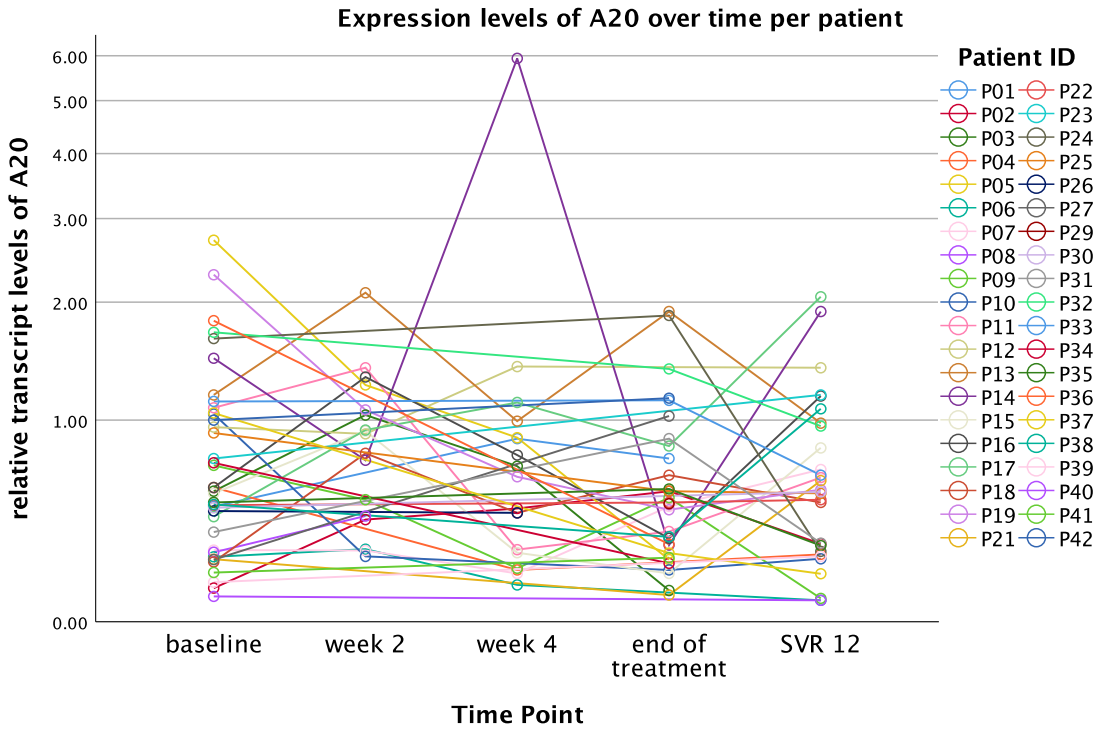

Figure 4.33 No clear pattern of the development of A20 over time could be found. The expression level of A20 over time per patient is depicted on a logarithmic scale.

4.12.4 IL-10

Clinical parameters from earlier time points tended to correlate with IL-10 levels at SVR 12. This might have been due to decreasing inflammation and a rise of IL-10 levels as a consequence. Albumin (-0.409, p = 0.005, n = 25) and hemoglobin (-0.376, p = 0.009, n = 25) levels at week 2 correlated negatively with IL-10 levels at SVR 12. ASAT at EOT showed a positive correlation with IL-10 levels at SVR 12 (0.358, p = 0.010, n = 27). Interestingly, IL-10 at EOT was positively correlated with leukocyte count at EOT (0.342, p = 0.007, n = 31) as well as SVR 12 (0.416, p = 0.001, n = 30). It would be interesting to characterize the leukocytes immunologically at EOT and SVR 12 to see if there was a change triggered by IL-10.

IL-10 expression levels at week 2 correlated inversely with HERV-K HML2 expression levels at week 4 (-0.560, p = 0.005, n = 14). Baseline levels of IL-10 showed a positive correlation with baseline levels of IL-6 (0.371, p = 0.003, n = 32) and this positive correlation between the two parameters was even stronger at week 2 (0.600, p = 0.001, n = 16). After week 2, IL-6 levels and IL-10 levels did not correlate significantly anymore. There was a significant rise in IL-10 levels between baseline and SVR 12 (mixed model analysis, p = 0.047, 95 % CI 0.007 - 0.950, figure 4.34). This may be an indication of healing liver damage as IL-10 is known to be hepatoprotective (Louis et al., 1997).

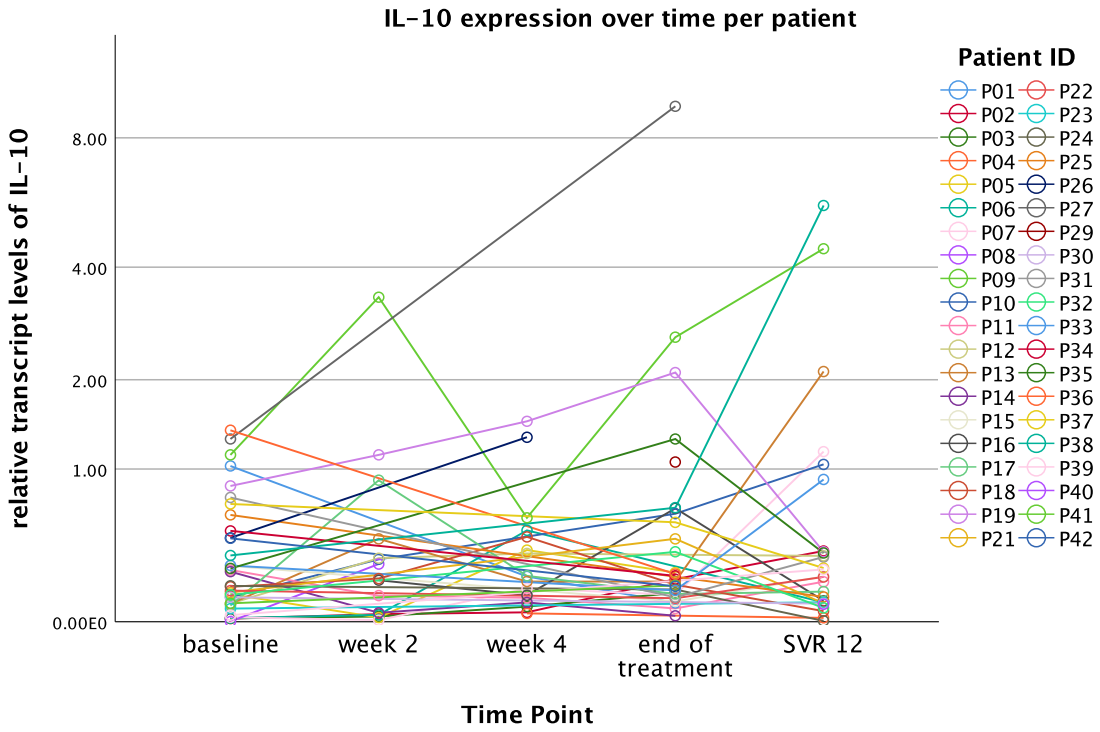

Figure 4.34 There was a rise in IL-10 expression between baseline and SVR 12. Relative expression levels of IL-10 over time per patient are depicted on a logarithmic scale.

The role of IL-10 in hepatitis C patients under DAA therapy seemed to be elaborate. Medical intervention had an effect on IL-10 expression after treatment completion. Patients with lower albumin and hemoglobin levels after the start of treatment as well as those with higher ASAT levels at EOT had higher IL-10 levels at SVR 12. Experimentally, lower IL-10 expression at week 2 was strongly associated with higher HERV-K HML2 expression at week 4 and vice versa. There is a possibility that IL-10 might have had a regulatory effect on HERV-K HML2 expression after start of treatment.

5 Discussion

5.1 Clinical outcome

The main parameter to monitor treatment success is the viral load. To determine if HCV RNA is detectable at any time point, quantitative HCV RNA is measured in serum. We could observe a significant decrease at week 2 already. At week 2, HCV RNA was still detectable in 26 patients, but at week 4 in 7 patients only. The majority of patients (92.86 %) achieved a sustained viral response defined by a non-detectable amount of HCV RNA 12 weeks after end of treatment. In HCV infected patients treated with various DAAs studies reported a SVR above 90 % (Spengler, 2018; Zoratti et al., 2020), which was consistent with this cohort.
Liver function improved over the course of treatment as ASAT, ALAT and GGT decreased. At baseline, a mean De-Ritis quotient of below 1 (mean value: 0.92) was coherent with the expected quotient for viral hepatitis. As most patients had ASAT and ALAT levels within normal range at SVR 12, the De-Ritis quotient did not produce meaningful outcome at that time point and was therefore not used for evaluation of clinical outcome.
In this cohort only two patients failed to achieve sustained viral response at SVR 12 and one patient, P08, died after week 8. What these patients had in common were high ASAT and ALAT levels, low albumin levels and a low thrombocyte count. So the patients seemed to have worse liver function. Interestingly, bilirubin only differed significantly between these patients and the rest of the cohort at EOT. Apart from that, the three patients experienced a rise in HERV-K HML2 and IL-10 expression levels from their respective second to last to the last measured time point. Additionally, HERV-K HML2 levels at baseline were significantly higher than in the rest of the cohort ($p = 0.029$) and above 1 for all three patients at all time points, which was the cutoff used at baseline to determine if HERV-K HML2 was expressed or suppressed in this study. These findings need to be further validated by expanding the number of patients.
All in all, DAA treatment was successful and a normalization of liver function in general as well as liver synthesis function could be achieved.

5.2 Possibilities by expansion of sample size

To strengthen the observed results bigger cohorts of HCV patients under DAA therapy are necessary to capture more patients without sustained viral response. More patients without successful

treatment would lead to a higher power of the statistical analysis regarding treatment failure. However, this is a hard task to achieve as DAA treatment results in a very high percentage of SVR and consequently healed patients. Yet with only three patients who were not treated successfully in total and two patients who did not accomplish to clear the virus, the influence of HERV-K HML2 levels at baseline on HCV RNA at SVR 12 was not strong enough to determine whether HERV-K HML2 could be reliably used as a biomarker for sustained viral response.
Furthermore, the influence of specific DAAs on the course of treatment could be analyzed better if there were more patients per DAA group. Especially big differences could be seen when comparing patients who received Simeprevir with patients who received any NS5A inhibitor. A lot of these differences were already present at baseline when medication had not been started yet meaning that the differences already present at baseline cannot be attributed to the respective drugs. Interestingly, bilirubin and albumin levels as well as the De-Ritis quotient were not significantly different between Simeprevir and the other aforementioned DAAs at SVR 12 anymore. A significant difference in HERV-K HML2 expression remained when comparing Ledipasvir and/or Daclatasvir with Simeprevir at SVR 12, whereas the significant difference in HERV-K HML2 expression levels between Ledipasvir and Daclatasvir at baseline was not detectable at SVR 12. Ledipasvir and Daclatasvir are both NS5A inhibitors, while Simeprevir targets NS3-4. It would be interesting to look at the interaction of the drugs with the viral proteins and study if this influenced HERV-K HML2 expression.

5.3 Albumin levels as stronger predictor for the development of clinical parameters during DAA treatment than liver cirrhosis

Liver cirrhosis has been shown to be linked to HCV infection (World Health Organization, 2020), so naturally a comparison between patients with and without liver cirrhosis was conducted first. Disease progression in hepatitis C patients treated with DAAs has been shown to be associated with advanced liver cirrhosis, portal hypertension and baseline albumin levels below 35 g/l (Mendizabal et al., 2020). Patients with different albumin levels at baseline differed more strongly in our cohort than patients grouped by their state of liver cirrhosis. Since information about dialysis was missing, the respective model of end stage liver disease score (Kamath et al., 2001; Wiesner et al., 2003) could not be calculated. To assess liver cirrhosis mortality one would resort to the Child-Pugh score (Child & Turcotte, 1964; Pugh et al., 1973) which takes bilirubin, albumin and INR into account. Due to the lack of clinical information about ascites and encephalopathy this score could not be calculated for patients in this cohort, either. However, bilirubin, INR and albumin were taken a closer look at. Classifying patients by their baseline bilirubin and INR levels did not yield very striking results as there were not many significant differences between the respec-

tive groups. However, patients with baseline albumin levels of either $\leq$ 35 g/l or above did have notably different levels of other parameters. The cutoff used in this study was chosen according to the Child-Pugh score. When this score is applied, patients with albumin levels above 35 g/l receive one point only. If albumin levels are between 28 and 35 g/l two points are added and below this, three points are assigned (Child & Turcotte, 1964; Pugh et al., 1973).
Associations with clinical parameters were much stronger when grouping by baseline albumin levels than by the state of liver cirrhosis. For both groups Quick, hemoglobin and thrombocyte count differed significantly. Bilirubin levels were significantly different at baseline when grouping by liver cirrhosis, whereas they did not show a significant difference at that time point when grouped by albumin levels. However, mean bilirubin levels were not different anymore once treatment was started in patients with different starting levels of albumin. Furthermore, no significant difference in leukocyte levels could be found when grouping by presence of liver cirrhosis, while leukocyte count was significantly lower in patients with albumin starting levels of $\leq$ 35 g/l from week 4 on.

5.4 HERV-K HML2 expression in hepatitis C patients

Patients with HCV infection who did not have liver cirrhosis or did not have low albumin levels ($\leq$ 35 g/l) at baseline showed significantly lower HERV-K HML2 expression levels than healthy controls. This remained true at SVR 12, after treatment had been completed. It would be interesting to explore how HCV silenced HERV-K HML2 expression and which factors inhibited this mechanism as this effect did not apply for patients with liver cirrhosis or low albumin starting levels, so patients with impaired liver function. There is evidence that HERV-K HML2 expression was associated with liver cirrhosis (Ma et al., 2016), but an association of HERV-K HML2 and albumin had not been studied yet.

5.4.1 HERV-K HML2 as a marker for liver damage in hepatitis C patients

In a recent study, HCV positive children were screened for HERV-H, HERV-K and HERV-W expression compared to healthy controls as well as throughout DAA treatment (Tovo et al., 2020). HERV-K expression was higher in hepatitis C patients than in healthy controls, but no information about liver cirrhosis or other clinical parameters was obtained. In my thesis the opposite was true for HERV-K HML2 in patients without liver cirrhosis or albumin levels within normal range. However, it was not specified which subtype of HERV-K was analyzed and consequently it remains unclear if a direct comparison to data of my thesis can be conducted.
My study provides the first evidence for an association between albumin levels and HERV-K HML2 expression in hepatitis C patients. At baseline, there was a strong correlation between HERV-K HML2 expression levels and baseline serum albumin levels. Relative HERV-K HML2 expression levels of below 1 were associated with significantly lower albumin levels throughout

treatment. Albumin levels for this group recovered to a mean within normal range at SVR 12. Patients with liver cirrhosis showed significantly higher levels of HERV-K HML2 at baseline, EOT as well as SVR 12. The De-Ritis quotient calculated by ASAT divided by ALAT was used to estimate the severity of liver damage. This quotient was highly associated with HERV-K HML2 levels at baseline. At baseline, Quick showed a negative and INR a positive association with HERV-K HML2 levels. All of these clinical parameters were indicators of impaired liver function.

This study provides strong evidence that HERV-K HML2 is a marker for the severity of liver damage in hepatitis C patients.

Once more patients who failed treatment could be included, a score to predict the presence of detectable HCV RNA at SVR 12 could be developed. This score could possibly include baseline albumin levels, liver cirrhosis and HERV-K HML2 expression levels. Thus, HERV-K HML2 might serve either as a biomarker alone or as part of a score predicting the outcome of DAA treatment.

5.4.2 The role of IP-10 in HCV infection

IP-10 was upregulated in hepatitis C patients compared to healthy controls, but this could be reversed by DAA treatment. After week 2, there was a drop in IP-10 levels. The normalization of IP-10 expression levels may be an indicator for treatment success. Several studies have shown a decrease of IP-10 expression in response to treatment as well (Tabll et al., 2019; Anthony et al., 2020). There was a positive correlation between IP-10 levels at week 2 and bilirubin levels, a marker for cholestasis, for the last two time points. Except for that there were no significant correlations between IP-10 and clinical parameters. However, IP-10 levels showed significant correlations with HERV-K HML2 expression levels. Induction of IP-10 expression by stimulation of breast cancer PBMC with HERV-K antigen has been achieved before (Wang-Johanning et al., 2008). However, no other evidence of an association or interaction of IP-10 expression and HERV-K could be found, so the evidence presented here is the first evidence of an association between IP-10 and HERV-K HML2 in hepatitis C patients. An induction of IP-10 expression by stimulation of HCV PBMC with HERV-K HML2 could be tackled to see if this effect could be achieved in HCV as well.

5.5 Reverse transcriptase inhibitors as additional therapy

HERV-K HML2 can be classified as retrovirus. To treat retroviral diseases, e.g. caused by human immunodeficiency virus (HIV), reverse transcriptase inhibitors are in clinical use. Raltegravir is one of them in clinical use to treat HIV. Reverse transcriptase as well as integrase inhibitors used in HIV treatment have demonstrated their ability to inhibit human endogenous retroviruses (Tyagi et al., 2017). If HERV-K HML2 plays an integral role in treatment success of antiviral therapy of

HCV, Raltegravir or other reverse transcriptase inhibitors could be used in an effort to improve treatment for patients with high HERV-K HML2 levels before the start of treatment in addition to DAA treatment. For patients with high HERV-K HML2 expression levels who have failed to achieve sustained viral response in the past, an addition of a reverse transcriptase inhibitor might improve the chances of treatment success. Furthermore, a case study described resolution of autoimmune thrombocytopenia in an HCV/HIV co-infected patient after addition of Raltegravir to his treatment scheme (Gentile et al., 2013). This observation may be a hint to investigate a possible relationship between the use of reverse-transcriptase inhibitors in HCV, HIV and related autoimmune diseases as the involvement of human endogenous retroviruses in the development of the respective associated autoimmune disease may contribute to its resolution after introduction of Raltegravir.

5.6 Mixed cyroglobulinemia - an autoimmune disease associated with HCV

HCV infection is associated with mixed cryoglobulinemia, a cutaneous and systemic autoimmune disease. Only few HCV positive patients develop cryoglobulinemia, yet a large percentage of cryoglobulinemia patients, e.g. up to 90 % in Italy, are HCV-positive (Ramos-Casals et al., 2012). Cardinal symptoms of mixed cryoglobulinemia include a cutaneous vasculitic rash, peripheral nerve involvement as well as membranoproliferative glomerulonephritis, a condition which may lead to lethal renal failure (Ferri et al., 2004). There are less common, but possibly life threatening, manifestations like gastrointestinal ischemia or alveolar haemorrhage. Additionally, mixed cryoglobulinemia may lead to neoplasia.

HERV-K is known to be associated with autoimmune diseases, specifically rheumatoid arthritis (RA). RA patients showed a significantly higher IgG antibody response to HERV-K10 Gag matrix peptide (Nelson et al., 2014) and on the transcriptional level a significant upregulation of HERV-K10 Gag in RA patients compared to controls was detected (Ejtehadi et al., 2006). Controls were healthy individuals or patients with other autoimmune conditions, e.g. osteoarthritis, in these studies. Molecular mimicry may explain these findings. HERV-K HML2 shows molecular mimicry with key regions of the target of rheumatoid factor (RF). A peptide sequence homology between KVSTKNI on HERV-K HML2 Gag and KVSNKAL on IgG1Fc has been detected. In addition, the viral segment GKELK showed similarity to the sequence GKEYK of IgG1Fc being a key target (Trela et al., 2016).

Thus, it would be interesting to investigate whether HERV-K HML2 was associated with the development of mixed cryoglobulinemia in HCV patients and whether it was the factor keeping the balance between immunity and autoimmunity. The molecular mimicry of RF may induce

the formation of immune complexes and consecutive activation of the complement system. As HERV-K has an integration site within the complement C4 gene (Tassabehji et al., 1994), there is a possibility of misactivation. TLR stimulation through HERV-K (Dembny et al., 2020; Yu et al., 2012) can lead to B-cell stimulation and consecutive production of proinflammatory cytokines and auto-antibodies leading to the development of autoimmune conditions like mixed cryoglobulinemia. None of the patients in the cohort of this study were affected by mixed cryoglobulinemia. However, it would be interesting to experimentally validate the role of HERV-K HML2 in the development of mixed cryoglobulinemia in HCV patients in the future.

5.7 A possible role of HERV-K in other diseases associated with HCV infection

Hepatic diseases associated with HCV	
Liver steatosis, fibrosis and cirrhosis	HCC
Extrahepatic diseases associated with hepatitis C	
Immune-related extrahepatic manifestations	Inflammatory-related extrahepatic manifestations
Mixed cryoglobulinemia	Type 2 diabetes mellitus type 2
Cryoglobulinemic vasculitis	Insulin resistance
B-cell NHL	NHL, non-Hodgkin's lymphoma
Sicca syndrome	Glomerulonephritis, renal insufficiency
Arthralgia/myalgia	Fatigue, depression
Autoantibody production (i.e. cryoglobulins, rheumatoid factor, and antinuclear, anticardiolipin, antithyroid and anti-smooth muscle antibodies)	Cognitive impairment
Polyarteritis nodosa	Cardiovascular disorders (e.g. stroke, ischemic heart disease)
Monoclonal gammopathies	Impaired quality of life
Immune thrombocytopenia	Polyarthritis/fibromyalgia

Table 5.1 Hepatitis C is associated with hepatic as well as extrahepatic diseases as reviewed by (Cacoub et al., 2016). A potential link between some of these diseases and HERV-K HML2 is plausible and could be investigated in the future.

Many of the aforementioned diseases associated with hepatitis C (see table 5.1) are linked to HERVs as well. Liver cirrhosis and HCC are associated with higher levels of HERV-K HML2 (Ma et al., 2016). Within the complex of autoimmune diseases an association between HERVs and certain disease are well studied. Sjögren's disease whose patients usually develop a sicca syndrome with dry eyes and mouth (Moyes et al., 2005). HERV-R is associated with polyarteritis nodosa as endothelial vascular disease (Katsumata et al., 1999). HERV-K is supposed to contribute to multiple myeloma (Schmidt et al., 2015) and HERV H, K and W are overexpressed in immune cells of fibromyalgia patients (Ovejero et al., 2020). HERV-K 18 polymorphisms were found in schizophrenia patients with diabetes mellitus type 2 (Dickerson et al., 2008). There are many studies showing associations between HERVs and neurological disorders. A reduction of HERV-W expression within the central nervous system was shown in patients with major depres-

sion (Weis et al., 2007).

These common associations between HCV and HERV related diseases highlight the necessity to unravel the pathways HERVs are involved in as this could help understand the pathogenesis of hepatitis C as well as various other diseases.

5.8 Interaction of biochemical pathways with HERV-K and hepatitis C

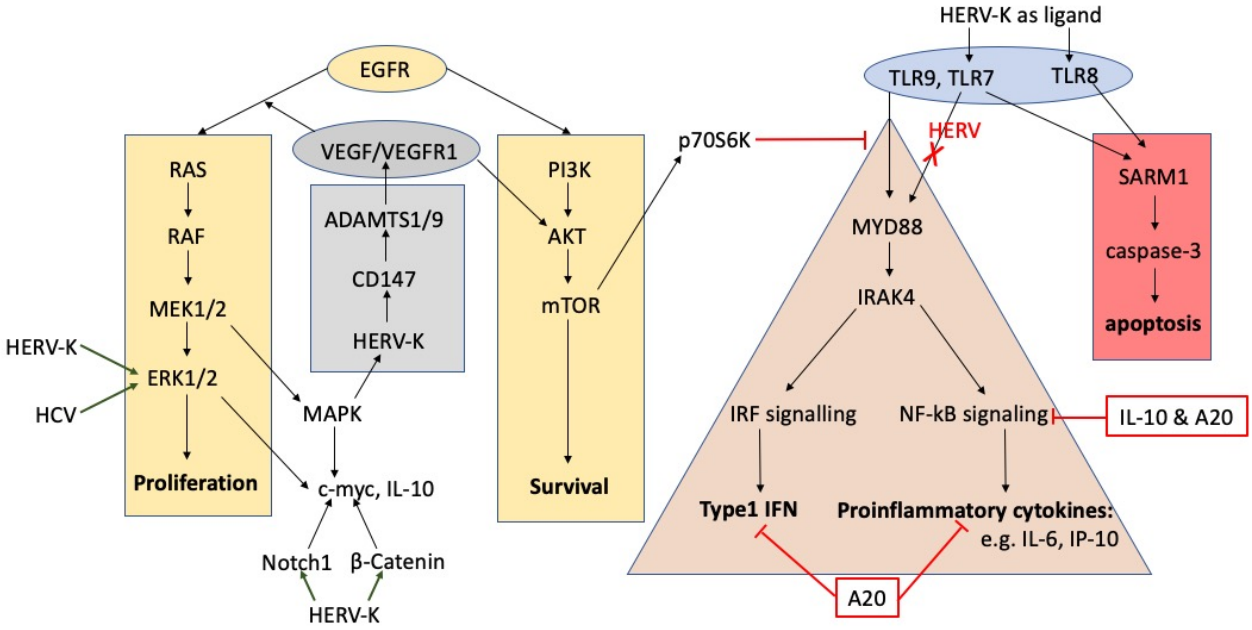

Figure 5.1 Possible points of interaction of HERV-K with major biochemical pathways. EGFR promotes proliferation by the RAS-RAF-MEK-ERK pathway as well as survival by the PI3K-AKT-mTOR pathway. TLR signalling leads to production of Type 1 interferon and proinflammatory cytokines as well as apoptosis. Abbreviations: EGFR = epidermal growth factor receptor, RAS: proto-oncogene, RAF: proto-oncogene, MEK = mitogen-activated protein kinase kinase, ERK = extracellular signal-regulated kinases, VEGF(R) = vascular endothelial growth factor (receptor), ADAMTS = A disintegrin and metalloproteinase with thrombospondin motifs, CD = cluster of differentiation, MAPK = mitogen activated protein kinases, c-myc: regulator gene, proto-oncogene , Notch1: transmembrane protein , beta-catenin: intracellular signal transducer , PI3K = Phosphoinositide 3-kinase, AKT = protein kinase B, mTOR = mammalian target of rapamycin, p70S6K = Ribosomal protein S6 kinase beta-1, TLR = toll like receptor, MYD88 = myeloid differentiation primary response 88, IRAK4 = interleukin-1 receptor-associated kinase 4, IRF = interferon regulatory factor, NF-kB = nuclear factor kappa-light-chain-enhancer of activated B cells, SARM1 = sterile alpha and TIR motif containing 1.

Figure 5.1 shows an overview of the major pathways HERV-K is involved in. EGFR activates the ERK pathway which leads to proliferation as well as the PI3K-AKT-mTOR pathway promoting cell survival. ERK1/2 could be activated by HERV-K HML2 and lead to the transcription of

early response proteins like myc, FOSL1 and EGR1 (Lemaître et al., 2017). Overexpression of HERV-K Np9 was observed to lead to an upregulation of β-catenin, phospho-ERK, c-myc, and cleaved Notch1 (Chen et al., 2013). In Kaposi sarcoma, MAPK lead to upregulation of HERV-K env which then lead to VEGF/VEGFR1 induction resulting in anchorage independent growth thus tumorogenesis (Dai et al., 2018). VEGF prompted the same pathways as EGFR. These data suggest that the ERK- as well as AKT-pathway are highly important for the influence of HERV-K on pathogenesis of diseases.
HERV-K contributed to axonal degeneration and neurodegeneration by activation of toll like receptors (TLRs) (Dembny et al., 2020). ERV dsRNA could activate TLR7 (Strick et al., 2016) and there is evidence that an immune system lacking certain TLRs (TLR3, TLR7, TLR9) was not capable of keeping the expression of endogenous retroviruses in check (Yu et al., 2012). TLR 7 and TLR9 activated Myd88 which then activated IRAK4. Consequently, IRF signaling leading to the production of type 1 interferon (IFN) as well as NF-kB signaling which leads to the production of proinflammatory cytokines could be activated (Kawai & Akira, 2010). In neurodegenerative diseases HERV-K HML2 did not show an effect on the downstream Myd88 pathway and therefore did not induce NF-kB. However, another pathway was activated leading to apoptosis via Sterile alpha and TIR domain-containing 1 (SARM1) and caspase-3 signaling (Dembny et al., 2020). In ALS, HERV-K envelope protein showed paracrine neurotoxicity (Küry et al., 2018). mTor, part of the PI3K-AKT-mTOR pathway, can activate p70S6K which then blocks TLR9 and Myd88 interaction and thus causes an inhibition of IRF and NF-kB signaling (Kawai & Akira, 2010). This crosslink might be of importance in HERV-K related pathogenesis of diseases as an activation of the EGFR-related pathways might contribute to a downregulation of NF-kB. A20 inhibited antiviral response through type 1 IFN and proinflammatory cytokines (Catrysse et al., 2014). IL-10 and A20 inhibited NF-kB signaling (Yoshimura et al., 2003), whereas IL-6 and IP-10 are pro-inflammatory cytokines stimulated by activation of this pathway (Wang et al., 1995). So the experimental parameters used in this study are all either a product of NF-kB signaling or have an influence on this pathway.

Activation of the EGFR-ERK pathway was described to be involved in progression of hepatitis C to HCC (Benkheil et al., 2018). According to the same study, AKT signaling did not have an impact on the gene expression profile leading to transformation. Another study confirmed this by reporting decreased mTOR and AKT in HCV related HCC (Golob-Schwarzl et al., 2017). HERV-K also activated ERK1/2 (Lemaître et al., 2017) and therefore might contribute to uncontrolled proliferation. A downregulation of IRF5 in HCV-positive versus HCV negative HCC patients or healthy donor livers could be found (Cevik et al., 2017). If HERV-related TLR signaling did not induce MYD88, IRF would not be upregulated, either. Thus, there could be a link between HERV expression and HCC development in hepatitis C patients, which needs to be further investigated.

As HCV infection and hepatitis C related HCC development play a role in the regulation of certain elements within these pathways, an effect of HERV-K, possibly even HERV-K HML2,

expression on hepatitis C might be mechanistically explained by studying these pathways in depth.

5.9 Implications for further research

My data show that there was a dynamic of HERV-K HML2 expression in hepatitis C patients. Expression of HERV-K HML2 was associated with clinical parameters and should be considered as a possible candidate for a biomarker for sustained viral response. More in depth research is required to unravel the function of HERV-K HML2 in HCV patients. On the one hand the size of the cohort needs to be extended and on the other hand the biochemical pathways and mechanisms leading to these associations need to be studied. As there is evidence that HERV-K did not activate NF-kB signaling (Dembny et al., 2020) and the associations of HERV-K HML2 with the gene expression of A20, IL-6 and IL-10 were inconclusive, I would propose focusing on SARM1 mediated apoptosis induced by TLR-signaling as well as the ERK- and AKT-pathways. Furthermore, the expression of IP-10 in hepatitis C patients as well as its associations with HERV-K HML2 expression over time yielded highly interesting results which should be studied more in depth.

The number of healthy controls as well as the number of patients without treatment success needs to be expanded to increase the statistical power of the comparison between these groups and the HCV patients who achieved sustained viral response. Once a significant difference in HERV-K HML2 expression levels between those groups is confirmed in a larger cohort, the biochemical mechanisms underlying these differences need to be investigated. Key pathways to tackle would be the EGFR-ERK pathway, the AKT pathway as well as TLR-induced IRF and SARM1 signaling. HERV-K shows an influence on various positions within these pathways as outlined in the previous chapter. Some of them are shown to contribute to malignant transformation in hepatitis C patients. So HCV positive HCC patients should be taken a closer look at as well. Ideally, the patients would be followed up in a longitudinal setting to see if HERV-K HML2 expression levels were predictive of HCC development. As this may take several decades, in the meantime a cohort of HCC patients with and without hepatitis C could be analyzed to see if there were differences in HERV-K HML2 expression between those groups.

One could identify loci within HERV-K HML2 that are up- or downregulated in hepatitis C patients. Then, more targeted studies of these loci could be accomplished. An introduction of HERV-K HML2 in healthy cells as well as cells from HCV positive donors via a vector could be achieved in vitro. To conduct immunological studies, it would be interesting to see if the loci within HERV-K HML2 could be translated into functional proteins of human endogenous retroviruses, specifically Env or Gag. Once the loci are identified one could try to overexpress HERV-K HML2 in HCV-PBMC as well as PBMC from healthy donors by introducing HERV-K HML2. This way

one could check if pro- and anti-inflammatory cytokine expression changed through introduction of HERV-K HML2. Ideally, this would be done without IL-2 stimulation to prohibit T cell stimulation by IL-2. Furthermore, an HCV PBMC culture could be stimulated with HERV-K HML2 proteins and cytokine expression as well as cytokines in the supernatant could be monitored. Morozov et al. stimulated PBMC of healthy donors with HERV-K and as a result IL-10 expression rose (Morozov et al., 2013). It would be interesting to see if the same happened for PBMC of HCV patients and if the other parameters behaved accordingly. Additionally, with this approach one could identify if HERV-K HML2 overexpression induced IP-10 as seen by stimulation of PBMC with HERV-K antigen before (Wang-Johanning et al., 2008).
Injection of HERV-K HML2 deoxyuridine nucleotidohydrolase has been performed in a rat model of pulmonal arterial hypertension (PAH). IL-6 expression increased following treatment in this setting (Saito et al., 2017). The same substance could be used for injection into an animal model for HCV to see if effects from in vitro experiments remain true in vivo. With these experiments, the influence of HERV-K HML2 on cytokine production within a physiological environment could be elucidated.

A great advantage of PBMC is the easy accessibility as whole blood donation is sufficient to harvest PBMC. However, apart from this, it would be interesting to have a look at liver tissue. Liver tissue from HCV positive patients could be stained for HERV-K HML2 expression. This could be compared to HCV positive patients with HCC as well as tissue from HCC patients who were HCV negative. This way, one could determine whether HERV-K HML2 is expressed in liver tissue and whether a difference between patients with and without HCC could be observed. HERV-K HML2 expression in HCV positive as well as HCV negative liver cirrhosis could be investigated using this approach as well. A comparison with tissue from healthy controls would be hard to achieve due to ethical reasons.
My study highlights that HERV-K HML2 had an influence on HCV infection and outcome of DAA treatment. There are numerous implications for further research.

6 Conclusion

This study provides evidence for suppression of HERV-K HML2 expression in hepatitis C patients without liver cirrhosis or with baseline albumin levels of at least 35 g/l. It also shows elevated IP-10 expression in hepatitis C patients at baseline which declined after week 2 of medical treatment. The association between IP-10 and HERV-K HML2 expression levels at baseline suggests an interaction between these parameters before the start of DAA treatment.

Start of drug administration altered HERV-K HML2 expression levels. At the end of treatment, HERV-K HML2 levels showed the least variety between patients. HERV-K HML2 levels were strongly correlated with albumin levels and the presence of liver cirrhosis in HCV positive patients. In this study, HERV-K HML2 levels at baseline were the only parameter that significantly correlated with quantitative HCV RNA at SVR 12. HERV-K HML2 may be considered as a candidate for a predictive biomarker to assess outcome of DAA treatment, but as only two patients showed a relapse of quantitative HCV RNA levels at SVR 12 an expansion of cohort size is necessary to confirm these results.

Liver cirrhosis and baseline albumin levels were the strongest factors separating the cohort into two distinct groups differing from each other with respect to clinically relevant parameters. Liver cirrhosis and albumin levels of $\leq$ 35 g/l were correlated with clinical parameters indicating worse liver function.

This is the first study to investigate HERV-K HML2 expression in hepatitis C patients treated with DAAs while taking baseline characteristics as well as clinical routine blood parameters for liver function into account. It provides indications of HERV-K HML2 as a plausible biomarker candidate for hepatitis C treatment success. However, further studies are necessary to unravel the possible functional role of HERV-K HML2 in HCV infection.

List of Tables

List of Figures

A Acknowledgements

I would like to thank my parents who have showed continuous support throughout my personal academic path. They never doubted that I would be successful. I am incredibly thankful for every encouraging word and being able to talk to them whenever I did not feel great or something did not go as planned, no matter how small the issue.

Moreover, I would like to thank my close friends for always supporting me. I am exceptionally grateful to have such wonderful people in my life.

Thank you, Ulrike Protzer, for giving me the opportunity to complete my dissertation with you as my supervisor. You are a true role model for me and my professional path.
Last, but not least, I would like to thank Michelle Vincendeau. It is incredible that even during your complicated pregnancy you did an incredible job supervising me. I highly appreciate being able to talk to you at any time and I have the utmost respect for your resilience - you are amazing.

B Supplementary material

Hepatitis C patient characteristics													
Patient ID	Gender	Age	HCV genotype	Way of infection	Liver cirrhosis	Drug duration	Simeprevir	Sofosbuvir	Ribavirin	Daclatasvir	Ledipasvir	Viekirax	Exviera
P01	female	45	1B	unknown	yes	12	yes	yes	yes	no	no	no	no
P02	male	35	1A	drugs	yes	12	yes	yes	no	no	no	no	no
P03	female	70	1A	unknown	no	12	yes	yes	no	no	no	no	no
P04	male	49	1	unknown	12	yes	yes	no	no	no	no	no	
P05	male	55	1B	unknown	no	12	yes	yes	no	no	no	no	no
P06	female	61	1B	native of high risk country	no	12	yes	yes	no	no	no	no	no
P07	male	56	1B	unknown	yes	24	yes	yes	yes	no	no	no	no
P08	female	53	1	transfusion	yes	not applicable	yes	yes	yes	no	no	no	no
P09	female	48	1A	drugs	yes	12	yes	yes	no	no	no	no	no
P10	male	59	1	unknown	yes	24	yes	yes	yes	no	no	no	no
P11	female	54	1A	unknown	no	12	no	yes	no	yes	no	no	no
P12	female	63	1A	unknown	no	12	no	yes	no	yes	no	no	no
P13	male	44	1B	drugs	yes	24	no	yes	no	yes	no	no	no
P14	male	69	1B	unknown	no	12	no	yes	no	yes	no	no	no
P15	male	74	1B		yes	12	no	yes	yes	yes	no	no	no
P16	female	62	1A	unknown	no	12	no	yes	no	yes	no	no	no
P17	female	54	1B	unknown	yes	24	yes	yes	yes	no	no	no	no
P18	female	60	1A	drugs	no	12	no	yes	no	yes	no	no	no
P19	female	55	1	unknown	no	24	no	yes	yes	yes	no	no	no
P20	female	74	1B	transfusion	yes	24	no	yes	yes	yes	no	no	no
P21	male	57	1	unknown	no	12	no	yes	no	no	yes	no	no
P22	female	46	1B	transfusion	no	12	no	no	no	no	no	yes	yes
P23	male	41	1A	unknown	no	12	no	yes	no	no	yes	no	no
P24	female	46	1B	transfusion	no	8	no	yes	no	no	yes	no	no
P25	female	56	1	unknown	no	12	no	no	no	no	no	yes	yes
P26	male	34	1B	drugs	no	12	no	yes	yes	no	yes	no	no
P27	male	45	3	native of high risk country	no	12	no	yes	no	yes	no	no	no
P28	female	64	4	native of high risk country	no	12	no	yes	yes	no	yes	no	no
P29	male	66	1B	unknown	no	12	no	yes	no	no	yes	no	no
P30	male	54	4	native of high risk country	no	12	no	no	yes	no	no	yes	no
P31	male	55	1B	unknown	no	12	no	no	no	no	no	yes	yes
P32	male	44	1A	unknown	no	12	no	yes	no	no	yes	no	no
P33	male	50	3	drugs	no	12	no	yes	no	yes	no	no	no
P34	female	64	1B	unknown	no	12	no	no	no	no	no	yes	yes
P35	male	48	3	drugs	no	12	no	yes	no	yes	no	no	no
P36	female	52	3	drugs	no	12	no	yes	no	yes	no	no	no
P37	male	52	3	native of high risk country	no	12	no	yes	no	yes	no	no	no
P38	female	45	3	drugs	no	12	no	yes	no	yes	no	no	no
P39	male		3a		no	12	no	yes	no	yes	no	no	no
P40	female	50	3	unknown	no	12	no	yes	no	yes	no	no	no
P41	female	59	3	unknown	no	12	no	yes	no	yes	no	no	no
P42	male	56	3	drugs	no	12	no	yes	no	yes	no	no	no

References

Abdelrazik, A. M., Abozaid, H. E., & Montasser, K. A. (2018). Role of Hepatitis C Virus (HCV) core antigen in improving blood transfusion safety in high prevalence, resource limited countries, a step forward. *Transfusion and Apheresis Science*, *57*(4), 566–568. doi: 10.1016/j.transci.2018.06.006

Alfahad, T., & Nath, A. (2013). Retroviruses and amyotrophic lateral sclerosis. *Antiviral Research*, *99*(2), 180–187. doi: 10.1016/j.antiviral.2013.05.006

Alter, M. J., Margolis, H. S., Krawczynski, K., Judson, F. N., Mares, A., james Alexander, W., ... Beach, M. J. (1992). The Natural History of Community-Acquired Hepatitis C in the United States. *New England Journal of Medicine*, *327*(27), 1899–1905. doi: 10.1056/NEJM199212313272702

Anthony, D. D., Sulkowski, M. S., Smeaton, L. M., Damjanovska, S., Shive, C. L., Kowal, C. M., ... Wyles, D. L. (2020). HCV DAA Therapy in Persons with HIV-HCV Genotype 1 Coinfection Results in High Rate of Sustained Virologic Response and Heterogeneity in Normalization of Soluble Markers of Immune Activation. *The Journal of Infectious Diseases*. doi: 10.1093/infdis/jiaa254/5836999

Armbruester, V., Sauter, M., Krautkraemer, E., Meese, E., Kleiman, A., Best, B., ... Mueller-Lantzsch, N. (2002). A novel gene from the human endogenous retrovirus K expressed in transformed cells. *Clinical Cancer Research*, *8*(6), 1800–1807.

Baum, H. (2019). Thrombozyten. In A. M. Gressner & T. Arndt (Eds.), *Lexikon der Medizinischen Laboratoriumsdiagnostik* (pp. 2295–2296). Berlin, Heidelberg: Springer Berlin Heidelberg. doi: 10.1007/978-3-662-48986-4_3027

Baust, C., Seifarth, W., Schön, U., Hehlmann, R., & Leib-Mösch, C. (2001). Functional Activity of HERV-K-T47D-Related Long Terminal Repeats. *Virology*. doi: 10.1006/viro.2001.0898

Bazin, R., & Lemieux, R. (1987). Role of the macrophage-derived hybridoma growth factor in the in vitro and in vivo proliferation of newly formed B cell hybridomas. *Journal of immunology (Baltimore, Md. : 1950)*, *139*(3), 780–7.

Behrens, S. E., Tomei, L., & De Francesco, R. (1996). Identification and properties of the RNA-dependent RNA polymerase of hepatitis C virus. *The EMBO Journal*, *15*(1), 12–22. doi: 10.1002/j.1460-2075.1996.tb00329.x

Bender, R., Grouven, U., & Ziegler, A. (2007). Analysis of variance for repeated measurements. *Deutsche medizinische Wochenschrift (1946)*, *132 Suppl 1*. doi: 10.1055/s-2007-959045

Benkheil, M., Paeshuyse, J., Neyts, J., Van Haele, M., Roskams, T., & Liekens, S. (2018). HCV-induced EGFR-ERK signaling promotes a pro-inflammatory and pro-angiogenic signature contributing to liver cancer pathogenesis. *Biochemical Pharmacology*, *155*, 305–315. doi: 10.1016/j.bcp.2018.07.011

Benova, L., Mohamoud, Y. A., Calvert, C., & Abu-Raddad, L. J. (2014). Vertical transmission of hepatitis C virus: Systematic review and meta-analysis. *Clinical Infectious Diseases*, *59*(6), 765–773. doi: 10.1093/cid/ciu447

Bhardwaj, N., Maldarelli, F., Mellors, J., & Coffin, J. M. (2014). HIV-1 Infection Leads to Increased Transcription of Human Endogenous Retrovirus HERV-K (HML-2) Proviruses In Vivo but Not to Increased Virion Production. *Journal of Virology*, *88*(19), 11108–11120. doi: 10.1128/jvi.01623-14

Brass, V., Berke, J. M., Montserret, R., Blum, H. E., Penin, F., & Moradpour, D. (2008). Structural determinants for membrane association and dynamic organization of the hepatitis C virus NS3-4A complex. *Proceedings of the National Academy of Sciences of the United States of America*, *105*(38), 14545–14550. doi: 10.1073/pnas.0807298105

Brinzevich, D., Young, G. R., Sebra, R., Ayllon, J., Maio, S. M., Deikus, G., ... Mulder, L. C. F. (2014). HIV-1 Interacts with Human Endogenous Retrovirus K (HML-2) Envelopes Derived from Human Primary Lymphocytes. *Journal of Virology*, *88*(11), 6213–6223. doi: 10.1128/jvi.00669-14

Buzdin, A., Ustyugova, S., Khodosevich, K., Mamedov, I., Lebedev, Y., Hunsmann, G., & Sverdlov, E. (2003). Human-specific subfamilies of HERV-K (HML-2) long terminal repeats: Three master genes were active simultaneously during branching of hominoid lineages. *Genomics*, *81*(2), 149–156. doi: 10.1016/S0888-7543(02)00027-7

Büscher, K., Hahn, S., Hofmann, M., Trefzer, U., Özel, M., Sterry, W., ... Denner, J. (2006). Expression of the human endogenous retrovirus-K transmembrane envelope, Rec and Np9 proteins in melanomas and melanoma cell lines. *Melanoma Research*, *16*(3), 223–234. doi: 10.1097/01.cmr.0000215031.07941.ca

Büscher, K., Trefzer, U., Hofmann, M., Sterry, W., Kurth, R., & Denner, J. (2005). Expression of human endogenous retrovirus K in melanomas and melanoma cell lines. *Cancer Research*, *65*(10), 4172–4180. doi: 10.1158/0008-5472.CAN-04-2983

Cacoub, P., Comarmond, C., Domont, F., Savey, L., Desbois, A. C., & Saadoun, D. (2016). Extrahepatic manifestations of chronic hepatitis C virus infection. *Therapeutic Advances in Infectious Disease*, *3*(1), 3. doi: 10.1177/2049936115585942

Carvalho, J. R., & Machado, M. V. (2018). New insights about albumin and liver disease. *Annals of Hepatology*, *17*(4), 547-560. doi: https://doi.org/10.5604/01.3001.0012.0916

Catrysse, L., Vereecke, L., Beyaert, R., & van Loo, G. (2014). A20 in inflammation and autoimmunity. In *Trends in immunology* (Vol. 35, pp. 22–31). Elsevier. doi: 10.1016/j.it.2013.10.005

Cevik, O., Li, D., Baljinnyam, E., Manvar, D., Pimenta, E. M., Waris, G., ... Kaushik-Basu, N. (2017). Interferon regulatory factor 5 (IRF5) suppresses hepatitis C virus (HCV) replication and HCV-associated hepatocellular carcinoma. *Journal of Biological Chemistry*, *292*(52), 21676–21689. doi: 10.1074/jbc.M117.792721

Chan, S. M., Sapir, T., Park, S.-S., Rual, J.-F., Contreras-Galindo, R., Reiner, O., & Markovitz, D. M. (2019). The HERV-K accessory protein Np9 controls viability and migration of teratocarcinoma cells. *PLOS ONE*, *14*(2), e0212970. doi: 10.1371/journal.pone.0212970

Chen, T., Meng, Z., Gan, Y., Wang, X., Xu, F., Gu, Y., ... Xu, R. (2013). The viral oncogene np9 acts as a critical molecular switch for co-activating β-catenin, erk, akt and notch1 and promoting the growth of human leukemia stem/progenitor cells. *Leukemia*, *27*, 1469-1478.

Child, C., & Turcotte, J. (1964). Surgery and portal hypertension. *Major Probl Clin Surg*, *1*, 1-85.

Chong, W. M., Hsu, S. C., Kao, W. T., Lo, C. W., Lee, K. Y., Shao, J. S., ... Yu, M. J. (2016). Phosphoproteomics identified an NS5A phosphorylation site involved in hepatitis C virus replication. *Journal of Biological Chemistry*, *291*(8), 3918–3931. doi: 10.1074/jbc.M115.675413

Cnaan, A., Laird, N. M., & Slasor, P. (1997). Using the general linear mixed model to analyse unbalanced repeated measures and longitudinal data. *Statistics in Medicine*, *16*(20), 2349–2380. doi: 10.1002/(SICI)1097-0258(19971030)16:20<2349::AID-SIM667>3.0.CO;2-E

Coffin, J., Hughes, S., & Varmus, H. (1997). Genetic organization. In *Retroviruses.* Cold Spring Harbor Laboratory Press.

Colombo, M., Choo, Q. L., Del Ninno, E., Dioguardi, N., Kuo, G., Donato, M. F., ... Houghton, M. (1989). Prevalence of antibodies to hepatitis C virus in Italian patients with hepatocellular carcinoma. *The Lancet*, *334*(8670), 1006–1008. doi: 10.1016/S0140-6736(89)91016-7

Contreras-Galindo, R., Almodóvar-Camacho, S., González-Ramírez, S., Lorenzo, E., & Yamamura, Y. (2007). Short Communication Comparative Longitudinal Studies of HERV-K and HIV-1 RNA Titers in HIV-1-Infected Patients Receiving Successful versus Unsuccessful Highly Active Antiretroviral Therapy. *AIDS Research And Human Retroviruses*, *23*(9), 1083–1086. doi: 10.1089/aid.2007.0054

Contreras-Galindo, R., Dube, D., Fujinaga, K., Kaplan, M. H., & Markovitz, D. M. (2017). Susceptibility of Human Endogenous Retrovirus Type K to Reverse Transcriptase Inhibitors. *Journal of Virology*, *91*(23). doi: 10.1128/jvi.01309-17

Contreras-Galindo, R., Kaplan, M. H., Markovitz, D. M., Lorenzo, E., & Yamamura, Y. (2006). Detection of HERV-K(HML-2) Viral RNA in Plasma of HIV Type 1-Infected Individuals. , *22*(10), 979–984.

Cox, A. L., Netski, D. M., Mosbruger, T., Sherman, S. G., Strathdee, S., Ompad, D., ... Thomas, D. L. (2005). Prospective Evaluation of Community-Acquired Acute-Phase Hepatitis C Virus Infection. *Clinical Infectious Diseases*, *40*(7), 951–958. doi: 10.1086/428578

Curtin, F., & Schulz, P. (1998). Multiple correlations and Bonferroni's correction. *Biological Psychiatry*, *44*(8), 775–777. doi: 10.1016/S0006-3223(98)00043-2

Dai, L., Del Valle, L., Miley, W., Whitby, D., Ochoa, A. C., Flemington, E. K., & Qin, Z. (2018). Transactivation of human endogenous retrovirus K (HERV-K) by KSHV promotes Kaposi's sarcoma development. *Oncogene*, *37*(33), 4534–4545. doi: 10.1038/s41388-018-0282-4

de Martel, C., Maucort-Boulch, D., Plummer, M., & Franceschi, S. (2015). World-wide relative contribution of hepatitis B and C viruses in hepatocellular carcinoma. *Hepatology*, *62*(4), 1190–1200. doi: 10.1002/hep.27969

Dembny, P., Newman, A. G., Singh, M., Hinz, M., Szczepek, M., Krüger, C., ... Lehnardt, S. (2020). Human endogenous retrovirus HERV-K(HML-2) RNA causes neurodegeneration through Toll-like receptors. *JCI Insight*, *5*(7). doi: 10.1172/jci.insight.131093

Denner, J. (1998). Immunosuppression by retroviruses: Implications for xenotransplantation. In *Annals of the new york academy of sciences* (Vol. 862, pp. 75–86). New York Academy of Sciences. doi: 10.1111/j.1749-6632.1998.tb09119.x

Denolly, S., Mialon, C., Bourlet, T., Amirache, F., Penin, F., Lindenbach, B., ... Cosset, F. L. (2017). The amino-terminus of the hepatitis C virus (HCV) p7 viroporin and its cleavage from glycoprotein E2-p7 precursor determine specific infectivity and secretion levels of HCV particle types. *PLoS Pathogens*, *13*(12). doi: 10.1371/journal.ppat.1006774

Devos, M., Mogilenko, D. A., Fleury, S., Gilbert, B., Becquart, C., Quemener, S., ... Dombrowicz, D. (2019). Keratinocyte Expression of A20/TNFAIP3 Controls Skin Inflammation Associated with Atopic Dermatitis and Psoriasis. *Journal of Investigative Dermatology*, *139*(1), 135–145. doi: 10.1016/j.jid.2018.06.191

Dewannieux, M., Blaise, S., & Heidmann, T. (2005). Identification of a Functional Envelope Protein from the HERV-K Family of Human Endogenous Retroviruses. *Journal of Virology*, *79*(24), 15573–15577. doi: 10.1128/jvi.79.24.15573-15577.2005

Dewannieux, M., Harper, F., Richaud, A., Letzelter, C., Ribet, D., Pierron, G., & Heidmann, T. (2006). Identification of an infectious progenitor for the multiple-copy HERV-K human endogenous retroelements. *Genome Research*, *16*(12), 1548–1556. doi: 10.1101/gr.5565706

Di Marco, R., Xiang, M., Zaccone, P., Leonardi, C., Franco, S., Meroni, P., & Nicoletti, F. (1999). Concanavalin A-induced Hepatitis in mice is prevented by interleukin (IL)-10 and exacerbated by endogenous IL-10 deficiency. *Autoimmunity*, *31*(2), 75–83. doi: 10.3109/08916939908994050

Dickerson, F., Rubalcaba, E., Viscidi, R., Yang, S., Stallings, C., Sullens, A., ... Yolken, R. (2008). Polymorphisms in human endogenous retrovirus K-18 and risk of type 2 diabetes in individuals with schizophrenia. *Schizophrenia Research*, *104*(1-3), 121–126. doi: 10.1016/j.schres.2008.05.005

Domanskiĭ, A., Akopov, S., Lebedev, I., Nikolaev, L., & Sverdlov, E. (2002). Enhancer Activity of Solitary Long Terminal Repeat of the Human Endogenous Retrovirus of the HERV-K Family. *Bioorganicheskaia khimiia*, *28*(4).

Douville, R., Liu, J., Rothstein, J., & Nath, A. (2011). Identification of active loci of a human endogenous retrovirus in neurons of patients with amyotrophic lateral sclerosis. *Annals of Neurology*, *69*(1), 141–151. doi: 10.1002/ana.22149

Egger, D., Wolk, B., Gosert, R., Bianchi, L., Blum, H. E., Moradpour, D., & Bienz, K. (2002). Expression of Hepatitis C Virus Proteins Induces Distinct Membrane Alterations Including a Candidate Viral Replication Complex. *Journal of Virology*, *76*(12), 5974–5984. doi: 10.1128/jvi.76.12.5974-5984.2002

Ehling, A., Gierten, B., & Arndt, T. (2019). Hepatitis C-Virus (HCV). In A. M. Gressner & T. Arndt (Eds.), *Lexikon der Medizinischen Laboratoriumsdiagnostik* (pp. 1095–1098). Berlin, Heidelberg: Springer Berlin Heidelberg. doi: 10.1007/978-3-662-48986-4_1429

Ejtehadi, H. D., Freimanis, G. L., Ali, H. A., Bowman, S., Alavi, A., Axford, J., ... Nelson, P. N. (2006). The potential role of human endogenous retrovirus K10 in the pathogenesis of rheumatoid arthritis: A preliminary study. *Annals of the Rheumatic Diseases*, *65*(5), 612–616. doi: 10.1136/ard.2004.031146

El-Zanaty, F., & Way, A. (2009). *Egypt demographic and health survey 2008.* Ministry of Health, El-Zanaty and Associates, and Macro International. Retrieved from `https://dhsprogram.com/pubs/pdf/FR220/FR220.pdf`

Evans, S., Repasky, E., & Fisher, D. (2015). Fever and the thermal regulation of immunity: the immune system feels the heat. *Nat Rev Immunol*, *15*, 335–349. doi: 10.1038/nri3843

Ferri, C., Sebastiani, M., Giuggioli, D., Cazzato, M., Longombardo, G., Antonelli, A., ... Zignego, A. L. (2004). Mixed cryoglobulinemia: demographic, clinical, and serologic features and survival in 231 patients. *Seminars in Arthritis and Rheumatism*, *33*(6), 355 - 374. doi: 10.1016/j.semarthrit.2003.10.001

Fiorentino, D. F., Bond, M. W., & Mosmann, T. R. (1989). Two types of mouse t helper cell: IV. Th2 clones secrete a factor that inhibits cytokine production by Thl clones. *Journal of Experimental Medicine*, *170*(6), 2081–2095. doi: 10.1084/jem.170.6.2081

Fraser, C., Humphries, R. K., & Mager, D. L. (1988). Chromosomal distribution of the RTVL-H family of human endogenous retrovirus-like sequences. *Genomics*, *2*(4), 280–287. doi: 10.1016/0888-7543(88)90015-8

Freimanis, G., Hooley, P., Ejtehadi, H. D., Ali, H. A., Veitch, A., Rylance, P. B., ... Nelson, P. N. (2010). A role for human endogenous retrovirus-K (HML-2) in rheumatoid arthritis: Investigating mechanisms of pathogenesis. *Clinical and Experimental Immunology*, *160*(3), 340–347. doi: 10.1111/j.1365-2249.2010.04110.x

Friebe, P., & Bartenschlager, R. (2002). Genetic Analysis of Sequences in the 3' Nontranslated Region of Hepatitis C Virus That Are Important for RNA Replication. *Journal of Virology*, *76*(11), 5326–5338. doi: 10.1128/jvi.76.11.5326-5338.2002

Friebe, P., Lohmann, V., Krieger, N., & Bartenschlager, R. (2001). Sequences in the 5' non-translated region of hepatitis C virus required for RNA replication. *Journal of virology*, *75*(24), 12047–57. doi: 10.1128/JVI.75.24.12047-12057.2001

Fuchs, N. V., Loewer, S., Daley, G. Q., Izsvák, Z., Löwer, J., & Löwer, R. (2013). Human endogenous retrovirus K (HML-2) RNA and protein expression is a marker for human embryonic and induced pluripotent stem cells. *Retrovirology*, *10*(1), 115. doi: 10.1186/1742-4690-10-115

Gavito, A. L., Bautista, D., Suarez, J., Badran, S., Arco, R., Pavón, F. J., ... Baixeras, E. (2016). Chronic IL-6 administration desensitizes IL-6 response in liver, causes hyperleptinemia and aggravates steatosis in diet-induced-obese mice. *PLoS ONE*, *11*(6). doi: 10.1371/journal .pone.0157956

Gentile, I., Bonadies, G., Buonomo, A. R., Minei, G., Borrelli, F., Foggia, M., ... Borgia, G. (2013). Resolution of autoimmune thrombocytopenia associated with raltegravir use in an HIV-positive patient. *Platelets*, *24*(7), 574–577. doi: 10.3109/09537104.2012.735721

Gerlach, J. T., Diepolder, H. M., Zachoval, R., Gruener, N. H., Jung, M. C., Ulsenheimer, A., ... Pape, G. R. (2003). Acute hepatitis C: High rate of both spontaneous and treatment-induced viral clearance. *Gastroenterology*, *125*(1), 80–88. doi: 10.1016/S0016-5085(03)00668-1

Glazko, G. V. (2003). Estimation of Divergence Times for Major Lineages of Primate Species. *Molecular Biology and Evolution*, *20*(3), 424–434. doi: 10.1093/molbev/msg050

Golob-Schwarzl, N., Krassnig, S., Toeglhofer, A. M., Park, Y. N., Gogg-Kamerer, M., Vierlinger, K., … Haybaeck, J. (2017). New liver cancer biomarkers: PI3K/AKT/mTOR pathway members and eukaryotic translation initiation factors.
doi: 10.1016/j.ejca.2017.06.003

Gosert, R., Egger, D., Lohmann, V., Bartenschlager, R., Blum, H. E., Bienz, K., & Moradpour, D. (2003). Identification of the Hepatitis C Virus RNA Replication Complex in Huh-7 Cells Harboring Subgenomic Replicons. *Journal of Virology*, *77*(9), 5487–5492. doi: 10.1128/jvi.77.9.5487-5492.2003

Gressner, A. M., & Arndt, T. (2019). Gamma-GT. In *Lexikon der Medizinischen Laboratoriumsdiagnostik* (pp. 929–929). Berlin, Heidelberg: Springer Berlin Heidelberg. doi: 10.1007/978-3-662-48986-4_311464

Gressner, A. M., & Gressner, O. A. (2019a). Alanin-Aminotransaminase. In A. M. Gressner & T. Arndt (Eds.), *Lexikon der medizinischen laboratoriumsdiagnostik* (pp. 53–55). Berlin, Heidelberg: Springer Berlin Heidelberg. doi: 10.1007/978-3-662-48986-4_128

Gressner, A. M., & Gressner, O. A. (2019b). Albumin. In A. M. Gressner & T. Arndt (Eds.), *Lexikon der Medizinischen Laboratoriumsdiagnostik* (pp. 55–58). Berlin, Heidelberg: Springer Berlin Heidelberg. doi: 10.1007/978-3-662-48986-4_130

Gressner, A. M., & Gressner, O. A. (2019c). Aspartat-Aminotransaminase. In A. M. Gressner & T. Arndt (Eds.), *Lexikon der Medizinischen Laboratoriumsdiagnostik* (pp. 212–214). Berlin, Heidelberg: Springer Berlin Heidelberg. doi: 10.1007/978-3-662-48986-4_308

Gressner, A. M., & Gressner, O. A. (2019d). Bilirubin. In A. M. Gressner & T. Arndt (Eds.), *Lexikon der Medizinischen Laboratoriumsdiagnostik* (pp. 436–440). Berlin, Heidelberg: Springer Berlin Heidelberg. doi: 10.1007/978-3-662-48986-4_557

Gressner, A. M., & Gressner, O. A. (2019e). C-reaktives Protein. In A. M. Gressner & T. Arndt (Eds.), *Lexikon der Medizinischen Laboratoriumsdiagnostik* (pp. 631–633). Berlin, Heidelberg: Springer Berlin Heidelberg. doi: 10.1007/978-3-662-48986-4_790

Gressner, A. M., & Gressner, O. A. (2019f). De-Ritis-Quotient. In A. M. Gressner & T. Arndt (Eds.), *Lexikon der Medizinischen Laboratoriumsdiagnostik* (pp. 673–673). Berlin, Heidelberg: Springer Berlin Heidelberg. doi: 10.1007/978-3-662-48986-4_852

Griffin, S. D., Beales, L. P., Clarke, D. S., Worsfold, O., Evans, S. D., Jaeger, J., … Klenk, H. D. (2003). The p7 protein of hepatitis C virus forms an ion channel that is blocked by the

antiviral drug, Amantadine. In *Febs letters* (Vol. 535, pp. 34–38). Elsevier. doi: 10.1016/S0014-5793(02)03851-6

Grow, E. J., Flynn, R. A., Chavez, S. L., Bayless, N. L., Wossidlo, M., Wesche, D. J., ... Wysocka, J. (2015). Intrinsic retroviral reactivation in human preimplantation embryos and pluripotent cells. *Nature*, *522*(7555), 221–246. doi: 10.1038/nature14308

Guder, W. G. (2019). Kreatinin. In A. M. Gressner & T. Arndt (Eds.), *Lexikon der Medizinischen Laboratoriumsdiagnostik* (pp. 1399–1401). Berlin, Heidelberg: Springer Berlin Heidelberg. doi: 10.1007/978-3-662-48986-4_1777

Hanke, K., Chudak, C., Kurth, R., & Bannert, N. (2013). The Rec protein of HERV-K(HML-2) upregulates androgen receptor activity by binding to the human small glutamine-rich tetratricopeptide repeat protein (hSGT). *International Journal of Cancer*, *132*(3), 556–567. doi: 10.1002/ijc.27693

He, K.-L., & Ting, A. T. (2002). A20 Inhibits Tumor Necrosis Factor (TNF) Alpha-Induced Apoptosis by Disrupting Recruitment of TRADD and RIP to the TNF Receptor 1 Complex in Jurkat T Cells. *Molecular and Cellular Biology*, *22*(17), 6034–6045. doi: 10.1128/mcb.22.17.6034-6045.2002

Herbst, H., Sauter, M., Kühler-Obbarius, C., Löning, T., & Mueller-Lantzsch, N. (1998). Human endogenous retrovirus (HERV)-K transcripts in germ cell and trophoblastic tumours. *APMIS : acta pathologica, microbiologica, et immunologica Scandinavica*, *106*(1), 216–20. doi: 10.1111/j.1699-0463.1998.tb01338.x

Hohenadl, C., Germaier, H., Walchner, M., Hagenhofer, M., Herrmann, M., Stürzl, M., ... Leib-Mösch, C. (1999). Transcriptional activation of endogenous retroviral sequences in human epidermal keratinocytes by UVB irradiation. *The Journal of investigative dermatology*, *113*(4), 587–94. doi: 10.1046/j.1523-1747.1999.00728.x

Hsiao, F. C., Tai, A. K., Deglon, A., Sutkowski, N., Longnecker, R., & Huber, B. T. (2009). EBV LMP-2A employs a novel mechanism to transactivate the HERV-K18 superantigen through its ITAM. *Virology*, *385*(1), 261–6. doi: 10.1016/j.virol.2008.11.025

Institut für klinische Chemie und Laboratoriumsmedizin, U. M. (2020). *Analytinformationen.* Retrieved 2020-08-16, from `https://www.unimedizin-mainz.de/index.php?id=16083`

Isken, O., Langerwisch, U., Jirasko, V., Rehders, D., Redecke, L., Ramanathan, H., ... Tautz, N. (2015). A Conserved NS3 Surface Patch Orchestrates NS2 Protease Stimulation, NS5A Hyperphosphorylation and HCV Genome Replication. *PLOS Pathogens*, *11*(3), e1004736. doi: 10.1371/journal.ppat.1004736

Jern, P., Sperber, G. O., & Blomberg, J. (2005). Use of endogenous retroviral sequences (ERVs) and structural markers for retroviral phylogenetic inference and taxonomy. *Retrovirology*, *2*, 50. doi: 10.1186/1742-4690-2-50

Kamath, P. S., Wiesner, R. H., Malinchoc, M., Kremers, W., Therneau, T. M., Kosberg, C. L., ... Kim, W. R. (2001). A model to predict survival in patients with end-stage liver disease. *Hepatology*, *33*(2), 464-470. doi: 10.1053/jhep.2001.22172

Karamitros, T., Hurst, T., Marchi, E., Karamichali, E., Georgopoulou, U., Mentis, A., ... Magiorkinis, G. (2018). Human endogenous retrovirus-K HML-2 integration within RASGRF2 is associated with intravenous drug abuse and modulates transcription in a cell-line model. *Proceedings of the National Academy of Sciences of the United States of America*, *115*(41), 10343–10439. doi: 10.1073/pnas.1811940115

Karasawa, T., Saito, T., Ueno, Y., Sugimoto, M., & Soga, T. (2013). Metabolome analysis of erythrocytes from patients with chronic hepatitis c reveals the etiology of ribavirin-induced hemolysis. *Int J Med Sci*, *10*, 1575-1577. doi: 10.7150/ijms.6436

Kato, M., Sanada, M., Kato, I., Sato, Y., Takita, J., Takeuchi, K., ... Ogawa, S. (2009). Frequent inactivation of A20 in B-cell lymphomas. *Nature*, *459*(7247), 712–716. doi: 10.1038/nature07969

Katsumata, K., Ikeda, H., Sato, M., Ishizu, A., Kawarada, Y., Kato, H., ... Yoshiki, T. (1999). Cytokine Regulation of env Gene Expression of Human Endogenous Retrovirus-R in Human Vascular Endothelial Cells. *Clinical Immunology*.

Kawai, T., & Akira, S. (2010). *The role of pattern-recognition receptors in innate immunity: Update on toll-like receptors* (Vol. 11) (No. 5). Nature Publishing Group. doi: 10.1038/ni.1863

King, A. M., Adams, M. J., Carstens, E. B., & Lefkowitz, E. J. (2012). Family - retroviridae. In *Virus taxonomy* (p. 477 - 495). San Diego: Elsevier. doi: 10.1016/B978-0-12-384684-6.00044-6

Kirkwood, T. (1983). Calibration of reference thromboplastins and standardisation of the prothrombin time ratio. *Thrombosis and haemostasis*, *49*(3), 238—244.

Kong, L., Zhou, Y., Bu, H., Lv, T., Shi, Y., & Yang, J. (2016). Deletion of interleukin-6 in monocytes/macrophages suppresses the initiation of hepatocellular carcinoma in mice. *Journal of Experimental and Clinical Cancer Research*, *35*(1). doi: 10.1186/s13046-016-0412-1

Kopf, M., Baumann, H., Freer, G., Freudenberg, M., Lamers, M., Kishimoto, T., ... Köhler, G. (1994). Impaired immune and acute-phase responses in interleukin-6-deficient mice. *Nature*, *368*(6469), 339–342. doi: 10.1038/368339a0

Kreuzer, K.-A., Gattermann, N., Gebhart, J., Goede, J., Grießhammer, M., Jost, E., & Langer, F. (2019). *Thrombozytopenien.* Retrieved 2020-08-16, from http://web.archive.org/web/20080207010024/http://www.808multimedia.com/winnt/kernel.htm

Krishnamurthy, N., & Kurzrock, R. (2018). Targeting the Wnt/beta-catenin pathway in cancer: Update on effectors and inhibitors. In *Cancer treatment reviews* (Vol. 62, pp. 50–60). W.B. Saunders Ltd. doi: 10.1016/j.ctrv.2017.11.002

Kurth, R., & Bannert, N. (2010). Beneficial and detrimental effects of human endogenous retroviruses. In *International journal of cancer* (Vol. 126, pp. 306–314). Int J Cancer. doi: 10.1002/ijc.24902

Küry, P., Nath, A., Créange, A., Dolei, A., Marche, P., Gold, J., ... Perron, H. (2018). Human Endogenous Retroviruses in Neurological Diseases. In *Trends in molecular medicine* (Vol. 24, pp. 379–394). Elsevier Ltd. doi: 10.1016/j.molmed.2018.02.007

Lander, E. S., Linton, L. M., Birren, B., Nusbaum, C., Zody, M. C., Baldwin, J., ... Morgan, M. J. (2001). Initial sequencing and analysis of the human genome. *Nature*, *409*(6822), 860–921. doi: 10.1038/35057062

Lania, L., Di Cristofano, A., Strazzullo, M., Pengue, G., Majello, B., & Mantia, G. L. (1992). Structural and functional organization of the human endogenous retroviral ERV9 sequences. *Virology*, *191*(1), 464–468. doi: 10.1016/0042-6822(92)90211-7

Lauw, F. N., Pajkrt, D., Hack, C. E., Kurimoto, M., van Deventer, S. J. H., & van der Poll, T. (2000). Proinflammatory Effects of IL-10 During Human Endotoxemia. *The Journal of Immunology*, *165*(5), 2783–2789. doi: 10.4049/jimmunol.165.5.2783

Lee, E. G., Boone, D. L., Chai, S., Libby, S. L., Chien, M., Lodolce, J. P., & Ma, A. (2000). Failure to regulate TNF-induced NF-κB and cell death responses in A20-deficient mice. *Science*, *289*(5488), 2350–2354. doi: 10.1126/science.289.5488.2350

Leib-Mösch, C., & Seifarth, W. (1996). Evolution and Biological Significance of Human Retroelements. In *Virus genes* (Vol. 11, pp. 133–145).

Lemaître, C., Tsang, J., Bireau, C., Heidmann, T., & Dewannieux, M. (2017). A human endogenous retrovirus-derived gene that can contribute to oncogenesis by activating the ERK pathway and inducing migration and invasion. *PLoS Pathogens*, *13*(6). doi: 10.1371/journal.ppat.1006451

Lentsch, A. B., Shanley, T. P., Sarma, V., & Ward, P. A. (1997). In vivo suppression of nf-kappa b and preservation of i kappa b alpha by interleukin-10 and interleukin-13. *J. Clin. Invest*, *100*(10), 2443–2448.

Li, K., Foy, E., Ferreon, J. C., Nakamura, M., Ferreon, A. C., Ikeda, M., ... Lemon, S. M. (2005). Immune evasion by hepatitis C virus NS3/4A protease-mediated cleavage of the Toll-like receptor 3 adaptor protein TRIF. *Proceedings of the National Academy of Sciences of the United States of America*, *102*(8), 2992–2997. doi: 10.1073/pnas.0408824102

Li, K. Z., Liao, Z. Y., Li, Y. X., Ming, Z. Y., Zhong, J. H., Wu, G. B., ... Zhao, Y. N. (2019). A20 rescues hepatocytes from apoptosis through the NF-κB signaling pathway in rats with acute liver failure. *Bioscience Reports*, *39*(1). doi: 10.1042/BSR20180316

Li, W., Lee, M. H., Henderson, L., Tyagi, R., Bachani, M., Steiner, J., ... Nath, A. (2015). Human endogenous retrovirus-K contributes to motor neuron disease. *Science Translational Medicine*, *7*(307). doi: 10.1126/scitranslmed.aac8201

Lichtman, M. A., Spivak, J. L., Boxer, L. A., Shattil, S. J., & Henderson, E. S. (2000). Hematology - Commentary on and reprint of Quick AJ, Stanley-Brown M, Bancroft FW, A study of the coagulation defect in hemophilia and in jaundice, in American Journal of the Medical Sciences (1935) 190:501–511. In *American journal of the medical sciences* (p. 857-867). San Diego: Academic Press. doi: 10.1016/B978-012448510-5.50171-0

Lin, C., Thomson, J. A., & Rice, C. M. (1995). A central region in the hepatitis C virus NS4A protein allows formation of an active NS3-NS4A serine proteinase complex in vivo and in vitro. *Journal of virology*, *69*(7), 4373–80.

Liu, J., Tang, W., Chen, G., Lu, Y., Feng, C., & Tu, X. M. (2016). Correlation and agreement: overview and clarification of competing concepts and measures. *Shanghai Archives of Psychiatry*, *28*(2), 115–120. doi: 10.11919/j.issn.1002-0829.216045

Liu, R. X., Wei, Y., Zeng, Q. H., Chan, K. W., Xiao, X., Zhao, X. Y., ... Kuang, D. M. (2015). Chemokine (C-X-C motif) receptor 3-positive B cells link interleukin-17 inflammation to protumorigenic macrophage polarization in human hepatocellular carcinoma. *Hepatology*, *62*(6), 1779–1790. doi: 10.1002/hep.28020

Livak, K. J., & Schmittgen, T. D. (2001). Analysis of Relative Gene Expression Data Using Real-Time Quantitative PCR and the 2 C T Method. *METHODS*, *25*, 402–408. doi: 10.1006/meth.2001.1262

Lohmann, V., Körner, F., Herian, U., & Bartenschlager, R. (1997). Biochemical properties of hepatitis C virus NS5B RNA-dependent RNA polymerase and identification of amino acid sequence motifs essential for enzymatic activity. *Journal of virology*, *71*(11), 8416–28.

Louis, H., Le Moine, O., Peny, M. O., Quertinmont, E., Fokan, D., Goldman, M., & Devière, J. (1997). Production and role of interleukin-10 in concanavalin A-induced hepatitis in mice. *Hepatology*, *25*(6), 1382–1389. doi: 10.1002/hep.510250614

Lower, R., Boller, K., Hasenmaier, B., Korbmacher, C., Muller-Lantzscht, N., Lower, J., & Kurth, R. (1993). Identification of human endogenous retroviruses with complex mRNA expression and particle formation. *Proceedings of the National Academy of Science USA*, *90*, 4480–4484.

Luster, A. D., & Ravetch, J. V. (1987). Biochemical characterization of a gamma interferon-inducible cytokine (IP-10). *Journal of Experimental Medicine*.

Löwer, R., Löwer, J., & Frank, H. (1984). Human teratocarcinomas cultured in vitro produce unique retrovirus-like viruses. *Journal of General Virology*, *65*(5), 887–898. doi: 10.1099/0022-1317-65-5-887

Löwer, R., Tönjes, R. R., Korbmacher, C., Kurth, R., & Löwer, J. (1995). Identification of a Rev-related protein by analysis of spliced transcripts of the human endogenous retroviruses HTDV/HERV-K. *Journal of virology*, *69*(1), 141–149. doi: 10.1128/jvi.69.1.141-149.1995

Ma, W., Hong, Z., Liu, H., Chen, X., Ding, L., Liu, Z., ... Yuan, Y. (2016). Human Endogenous retroviruses-k (HML-2) expression is correlated with prognosis and progress of hepatocellular carcinoma. *BioMed Research International*, *2016*. doi: 10.1155/2016/8201642

Mager, D. L., & Freeman, J. D. (1995). HERV-H Endogenous Retroviruses: Presence in the New World Branch but Amplification in the Old World Primate Lineage. *Virology*, *213*(2), 395–404. doi: 10.1006/viro.1995.0012

Mamedov, I., Lebedev, Y., Hunsmann, G., Khusnutdinova, E., & Sverdlov, E. (2004). A rare event of insertion polymorphism of a HERV-K LTR in the human genome. *Genomics*, *84*(3), 596–9. doi: 10.1016/j.ygeno.2004.04.010

Manghera, M., & Douville, R. N. (2013). *Endogenous retrovirus-K promoter: A landing strip for inflammatory transcription factors?* (Vol. 10) (No. 1). Retrovirology. doi: 10.1186/1742-4690-10-16

Mareschi, K., Montanari, P., Rassu, M., Galliano, I., Daprà, V., Adamini, A., ... Bergallo, M. (2019). Human Endogenous Retrovirus-H and K Expression in Human Mesenchymal Stem Cells as Potential Markers of Stemness. *Intervirology*, *62*(1), 9–14. doi: 10.1159/000499185

Mathur, P., Kottilil, S., & Wilson, E. (2018). Use of Ribavirin for Hepatitis C Treatment in the Modern Direct-acting Antiviral Era. *Journal of Clinical and Translational Hepatology*, *6*(4), 1–7. doi: 10.14218/jcth.2018.00007

Matsusaka, T., Fujikawa, K., Nishio, Y., Mukaida, N., Matsushima, K., Kishimoto, T., & Akira, S. (1993). Transcription factors NF-IL6 and NF-κB synergistically activate transcription of the inflammatory cytokines, interleukin 6 and interleukin 8. *Proceedings of the National Academy of Sciences of the United States of America*, *90*(21), 10193–10197. doi: 10.1073/pnas.90.21.10193

Mayer, J., Sauter, M., Racz, A., Scherer, D., Mueller-Lantzsch, N., & Meese, E. (1999). An almost-intact human endogenous retrovirus K on human chromosome 7. *Nature Genetics*, *21*(3), 257–258. doi: 10.1038/6766

McCormick, A. L., Brown, R. H., Cudkowicz, M. E., Al-Chalabi, A., & Garson, J. A. (2008). Quantification of reverse transcriptase in ALS and elimination of a novel retroviral candidate. *Neurology*, *70*(4), 278–283. doi: 10.1212/01.wnl.0000297552.13219.b4

McLauchlan, J., Lemberg, M. K., Hope, G., & Martoglio, B. (2002). Intramembrane proteolysis promotes trafficking of hepatitis C virus core protein to lipid droplets. *EMBO Journal*, *21*(15), 3980–3988. doi: 10.1093/emboj/cdf414

Medstrand, P., & Mager, D. L. (1998). Human-specific integrations of the HERV-K endogenous retrovirus family. *Journal of virology*, *72*(12), 9782–7.

Mehraein, Y., Ehlhardt, S., Seifert, M., Schneider, J., Ojak, A., & Zang, K. D. (2006). Human endogenous retrovirus HERV-K(HML-2) Rec expression and. *The Journal of Rheumatology Rheumatology The Journal*, *33*(1), 16–23.

Mendizabal, M., Piñero, F., Ridruejo, E., Wolff, F. H., Anders, M., Reggiardo, V., ... Silva, M. (2020). Disease Progression in Patients With Hepatitis C Virus Infection Treated With Direct-Acting Antiviral Agents. *Clinical Gastroenterology and Hepatology*. doi: 10.1016/j.cgh.2020.02.044

Messina, J. P., Humphreys, I., Flaxman, A., Brown, A., Cooke, G. S., Pybus, O. G., & Barnes, E. (2015). Global distribution and prevalence of hepatitis C virus genotypes. *Hepatology*, *61*(1), 77–87. doi: 10.1002/hep.27259

Meylan, E., Curran, J., Hofmann, K., Moradpour, D., Binder, M., Bartenschlager, R., & Tschopp, J. (2005). Cardif is an adaptor protein in the RIG-I antiviral pathway and is targeted by hepatitis C virus. *Nature*, *437*(7062), 1167–1172. doi: 10.1038/nature04193

Mihm, S., Schweyer, S., & Ramadori, G. (2003). Expression of the Chemokine IP-10 Correlates With the Accumulation of Hepatic IFN-g and IL-18 mRNA in Chronic Hepatitis C but not in Hepatitis B. *Journal of Medical Virology*, *70*, 562–570. doi: 10.1002/jmv.10431

Miller, A. M., Wang, H., Bertola, A., Park, O., Horiguchi, N., Hwan Ki, S., ... Gao, B. (2011). Inflammation-associated interleukin-6/signal transducer and activator of transcription 3 activation ameliorates alcoholic and nonalcoholic fatty liver diseases in interleukin-10-deficient mice. *Hepatology*, *54*(3), 846–856. doi: 10.1002/hep.24517

Ministry of Health and Population, Cairo, Egypt, El-Zanaty and Associates, Cairo, Egypt, & The DHS Program ICF International, Rockville, Maryland, USA. (2015). *Egypt Health Issues Survey 2015.* Retrieved 2020-08-16, from `https://dhsprogram.com/pubs/pdf/FR313/FR313.pdf`

Mohd Hanafiah, K., Groeger, J., Flaxman, A. D., & Wiersma, S. T. (2013). Global epidemiology of hepatitis C virus infection: New estimates of age-specific antibody to HCV seroprevalence. *Hepatology*, *57*(4), 1333–1342. doi: 10.1002/hep.26141

Moradpour, D., Penin, F., & Rice, C. M. (2007). Replication of hepatitis C virus. *Nature Reviews Microbiology*, *5*(6), 453–463. doi: 10.1038/nrmicro1645

Moreno, A., Bárcena, R., García-Garzón, S., Muriel, A., Quereda, C., Moreno, L., ... Moreno, S. (2005). HCV clearance and treatment outcome in genotype 1 HCV-monoinfected, HIV-coinfected and liver transplanted patients on peg-IFN-α-2b/ribavirin. *Journal of Hepatology*, *43*(5), 783–790. doi: 10.1016/j.jhep.2005.05.019

Morozov, V. A., Dao Thi, V. L., & Denner, J. (2013). The Transmembrane Protein of the Human Endogenous Retrovirus - K (HERV-K) Modulates Cytokine Release and Gene Expression. *PLoS ONE*, *8*(8), e70399. doi: 10.1371/journal.pone.0070399

Moyes, D. L., Martin, A., Sawcer, S., Temperton, N., Worthington, J., Griffiths, D. J., & Venables, P. J. (2005). The distribution of the endogenous retroviruses HERV-K113 and HERV-K115 in health and disease. *Genomics*, *86*(3), 337–341. doi: 10.1016/j.ygeno.2005.06.004

Murphy, D. G., Sablon, E., Chamberland, J., Fournier, E., Dandavino, R., & Tremblay, C. L. (2015). Hepatitis C virus genotype 7, a new genotype originating from Central Africa. *Journal of Clinical Microbiology*, *53*(3), 967–972. doi: 10.1128/JCM.02831-14

Muster, T., Waltenberger, A., Grassauer, A., Hirschl, S., Caucig, P., Romirer, I., ... Wolff, K. (2003). An Endogenous Retrovirus Derived from Human Melanoma Cells. *Cancer Research*, *63*, 8735–8741.

Nakamichi, K., Saiki, M., Sawada, M., Takayama-Ito, M., Yamamuro, Y., Morimoto, K., & Kurane, I. (2005). Rabies Virus-Induced Activation of Mitogen-Activated Protein Kinase and NF-κB Signaling Pathways Regulates Expression of CXC and CC Chemokine Ligands in Microglia. *Journal of Virology*, *79*(18), 11801–11812. doi: 10.1128/jvi.79.18.11801-11812.2005

Ndlovu, M. N., Van Lint, C., Van Wesemael, K., Callebert, P., Chalbos, D., Haegeman, G., & Vanden Berghe, W. (2009). Hyperactivated NF-κB and AP-1 Transcription Factors Promote Highly Accessible Chromatin and Constitutive Transcription across the Interleukin-6 Gene Promoter in Metastatic Breast Cancer Cells. *Molecular and Cellular Biology*, *29*(20), 5488–5504. doi: 10.1128/mcb.01657-08

Nellåker, C., Yao, Y., Jones-Brando, L., Mallet, F., Yolken, R. H., & Karlsson, H. (2006). Transactivation of elements in the human endogenous retrovirus W family by viral infection. *Retrovirology*, *3*, 44. doi: 10.1186/1742-4690-3-44

Nelson, D. R., Lauwers, G. Y., Lau, J. Y., & Davis, G. L. (2000). Interleukin 10 treatment reduces fibrosis in patients with chronic hepatitis C: A pilot trial of interferon nonresponders. *Gastroenterology*, *118*(4), 655–660. doi: 10.1016/S0016-5085(00)70134-X

Nelson, P. N., Lever, A. M., Smith, S., Pitman, R., Murray, P., Perera, S. A., ... Booth, J. C. (1999). Molecular investigations implicate human endogenous retroviruses as mediators of anti-retroviral antibodies in autoimmune rheumatic disease. *Immunological Investigations*, *28*(4), 277–289. doi: 10.3109/08820139909060862

Nelson, P. N., Roden, D., Nevill, A., Freimanis, G. L., Trela, M., Ejtehadi, H. D., ... Rylance, P. B. (2014). Rheumatoid arthritis is associated with IgG antibodies to human endogenous retrovirus Gag matrix: A potential pathogenic mechanism of disease? *Journal of Rheumatology*, *41*(10), 1952–1960. doi: 10.3899/jrheum.130502

Neufeldt, C. J., Joyce, M. A., Van Buuren, N., Levin, A., Kirkegaard, K., Gale Jr., M., ... Wozniak, R. W. (2016). The Hepatitis C Virus-Induced Membranous Web and Associated Nuclear Transport Machinery Limit Access of Pattern Recognition Receptors to Viral Replication Sites. *PLOS Pathogens*, *12*(2), e1005428. doi: 10.1371/journal.ppat.1005428

Neumann, A. U., Lam, N. P., Dahari, H., Gretch, D. R., Wiley, T. E., Layden, T. J., & Perelson, A. S. (1998). Hepatitis C viral dynamics in vivo and the antiviral efficacy of interferon-α therapy. *Science*, *282*(5386), 103–107. doi: 10.1126/science.282.5386.103

Novak, U., Rinaldi, A., Kwee, I., Nandula, S. V., Rancoita, P. M., Compagno, M., ... Bertoni, F. (2009). The NF-κB negative regulator TNFAIP3 (A20) is inactivated by somatic mutations and genomic deletions in marginal zone lymphomas. *Blood*, *113*(20), 4918–4921. doi: 10.1182/blood-2008-08-174110

Ono, M., Kawakami, M., & Ushikubo, H. (1987). Stimulation of expression of the human endogenous retrovirus genome by female steroid hormones in human breast cancer cell line T47D. *Journal of Virology*, *61*(6), 2059–2062. doi: 10.1128/jvi.61.6.2059-2062.1987

Ono, M., Yasunaga, T., Miyata, T., & Ushikubo, H. (1986). Nucleotide Sequence of Human Endogenous Retrovirus Genome Related to the Mouse Mammary Tumor Virus Genome. *Journal of Virology*, *60*(2), 589–598.

Ormsby, C. E., SenGupta, D., Tandon, R., Deeks, S. G., Martin, J. N., Jones, R. B., ... Nixon, D. F. (2012). Human endogenous retrovirus expression is inversely associated with chronic immune activation in HIV-1 infection. *PLoS ONE*, *7*(8). doi: 10.1371/journal.pone.0041021

Ovejero, T., Sadones, O., Sánchez-Fito, T., Almenar-Pérez, E., Espejo, J. A., Martín-Martínez, E., ... Oltra, E. (2020). Activation of Transposable Elements in Immune Cells of Fibromyalgia Patients. *International Journal of Molecular Sciences*, *21*(4), 1366. doi: 10.3390/ijms21041366

Pavlovic, D., Neville, D. C., Argaud, O., Blumberg, B., Dwek, R. A., Fischer, W. B., & Zitzmann, N. (2003). The hepatitis C virus p7 protein forms an ion channel that is inhibited by long-alkyl-chain iminosugar derivatives. *Proceedings of the National Academy of Sciences of the United States of America*, *100*(10), 6104–6108. doi: 10.1073/pnas.1031527100

Pawlotsky, J.-M. (2002). Use and Interpretation of Virological Tests for Hepatitis C. *Hepatology*. doi: 10.1053/jhep.2002.36815

Petruzziello, A., Marigliano, S., Loquercio, G., & Cacciapuoti, C. (2016). Hepatitis C virus (HCV) genotypes distribution: an epidemiological up-date in Europe. *Infectious Agents and Cancer*, *11*(1), 53. doi: 10.1186/s13027-016-0099-0

Pugh, R. N. H., Murray-Lyon, I. M., Dawson, J. L., Pietroni, M. C., & Williams, R. (1973). Transection of the oesophagus for bleeding oesophageal varices. *BJS (British Journal of Surgery)*, *60*(8), 646-649. doi: 10.1002/bjs.1800600817

Ramos-Casals, M., Stone, J. H., Cid, M. C., & Bosch, X. (2012). The cryoglobulinaemias. In *The lancet* (Vol. 379, pp. 348–360). Lancet. doi: 10.1016/S0140-6736(11)60242-0

Rao, M. R., Naficy, A. B., Darwish, M. A., Darwish, N. M., Schisterman, E., Clemens, J. D., & Edelman, R. (2002). Further evidence for association of hepatitis C infection with parenteral schistosomiasis treatment in Egypt. *BMC Infectious Diseases*, *2*. doi: 10.1186/1471-2334-2-29

Robert Koch Institut. (2019). *Infektionsepidemiologisches Jahrbuch meldepflichtiger Krankheiten für 2018.* Retrieved 2020-08-16, from `https://www.rki.de/DE/Content/Infekt/Jahrbuch/Jahrbuch_2018.pdf?__blob=publicationFile`

Rubbia-Brandt, L., Quadri, R., Abid, K., Giostra, E., Malé, P. J., Mentha, G., ... Negro, F. (2000). Hepatocyte steatosis is a cytopathic effect of hepatitis C virus genotype 3. *Journal of hepatology*, *33*(1), 106–15. doi: 10.1016/s0168-8278(00)80166-x

Ruda, V. M., Akopov, S. B., Trubetskoy, D. O., Manuylov, N. L., Vetchinova, A. S., Zavalova, L. L., ... Sverdlov, E. D. (2004). Tissue specificity of enhancer and promoter activities of a HERV-K(HML-2) LTR. *Virus Research*, *104*(1), 11–16. doi: 10.1016/j.virusres.2004.02.036

Rustgi, V. K. (2007). The epidemiology of hepatitis C infection in the United States. *Journal of Gastroenterology*, *42*(7), 513–521. doi: 10.1007/s00535-007-2064-6

Saito, T., Miyagawa, K., Chen, S. Y., Tamosiuniene, R., Wang, L., Sharpe, O., ... Rabinovitch, M. (2017). Upregulation of human endogenous retrovirus-K is linked to immunity and inflammation in pulmonary arterial hypertension. *Circulation*, *136*(20), 1920–1935. doi: 10.1161/CIRCULATIONAHA.117.027589

Sarrazin, C., Zimmermann, T., Berg, T., Neumann, U. P., Schirmacher, P., Schmidt, H., ... Zeuzem, S. (2018). Prophylaxis, diagnosis and therapy of hepatitis-C-virus (HCV) infection: The German guidelines on the management of HCV infection: AWMF-Register-No: 021/012. *Zeitschrift für Gastroenterologie*, *56*(7), 756–838. doi: 10.1055/a-0599-1320

Schanab, O., Humer, J., Gleiss, A., Mikula, M., Sturlan, S., Grunt, S., ... Waltenberger, A. (2011). Expression of human endogenous retrovirus K is stimulated by ultraviolet radiation in melanoma. *Pigment Cell and Melanoma Research*, *24*(4), 656–665. doi: 10.1111/j.1755-148X .2011.00860.x

Schmidt, K. L., Vangsted, A. J., Hansen, B., Vogel, U. B., Hermansen, N. E. U., Jensen, S. B., ... Nexø, B. A. (2015). Synergy of two human endogenous retroviruses in multiple myeloma. *Leukemia Research*, *39*(10), 1125–1128. doi: 10.1016/j.leukres.2015.06.014

Schmitt, K., Heyne, K., Roemer, K., Meese, E., & Mayer, J. (2015). HERV-K(HML-2) rec and np9 transcripts not restricted to disease but present in many normal human tissues. *Mobile DNA*, *6*(1), 4. doi: 10.1186/s13100-015-0035-7

Schmitt, K., Reichrath, J., Roesch, A., Meese, E., & Mayer, J. (2013). Transcriptional profiling of human endogenous retrovirus group herv-k(hml-2) loci in melanoma. *Genome biology and evolution*, *5(2)*, 307–328.

Schuijs, M. J., Willart, M. A., Vergote, K., Gras, D., Deswarte, K., Ege, M. J., ... Hammad, H. (2015). Farm dust and endotoxin protect against allergy through A20 induction in lung epithelial cells. *Science*, *349*(6252), 1106–1110. doi: 10.1126/science.aac6623

Seifarth, W., Frank, O., Zeilfelder, U., Spiess, B., Greenwood, A. D., Hehlmann, R., & Leib-Mösch, C. (2005). Comprehensive Analysis of Human Endogenous Retrovirus Transcriptional Activity in Human Tissues with a Retrovirus-Specific Microarray. *Journal of Virology*, *79*(1), 341–352. doi: 10.1128/jvi.79.1.341-352.2005

Seifarth, W., Skladny, H., Krieg-Schneider, F., Reichert, A., Hehlmann, R., & Leib-Mösch, C. (1995). Retrovirus-like particles released from the human breast cancer cell line T47-D display type B- and C-related endogenous retroviral sequences. *Journal of virology*, *69*(10), 6408–6416. doi: 10.1128/jvi.69.10.6408-6416.1995

Shembade, N., Ma, A., & Harhaj, E. W. (2010). Inhibition of NF-kB signaling by A20 through disruption of ubiquitin enzyme complexes. *Science*, *327*(5969), 1135–1139. doi: 10.1126/ science.1182364

Shiryaev, S. A., Thomsen, E. R., Cieplak, P., Chudin, E., Cheltsov, A. V., Chee, M. S., ... Strongin, A. Y. (2012). New details of HCV NS3/4A proteinase functionality revealed by a high-throughput cleavage assay. *PLoS ONE*, *7*(4). doi: 10.1371/journal.pone.0035759

Sokhi, U. K., Liber, M. P., Frye, L., Park, S., Kang, K., Pannellini, T., ... Gong, S. (2018). Dissection and function of autoimmunity-associated TNFAIP3 (A20) gene enhancers in humanized mouse models. *Nature Communications*, *9*(1), 1–15. doi: 10.1038/s41467-018-03081-7

Spengler, U. (2018). Direct antiviral agents (DAAs) - A new age in the treatment of hepatitis C virus infection. In *Pharmacology and therapeutics* (Vol. 183, pp. 118–126). Elsevier Inc. doi: 10.1016/j.pharmthera.2017.10.009

Steele, A. J., Al-Chalabi, A., Ferrante, K., Cudkowicz, M. E., Brown, R. H., & Garson, J. A. (2005). Detection of serum reverse transcriptase activity in patients with ALS and unaffected blood relatives. *Neurology*, *64*(3), 454–458. doi: 10.1212/01.WNL.0000150899.76130.71

Strick, R., Strissel, P. L., Baylin, S. B., & Chiappinelli, K. B. (2016). Unraveling the molecular pathways of DNA-methylation inhibitors: human endogenous retroviruses induce the innate immune response in tumors. *OncoImmunology*, *5*(5), e1122160. doi: 10.1080/2162402X.2015.1122160

Subramanian, R. P., Wildschutte, J. H., Russo, C., & Coffin, J. M. (2011). Identification, characterization, and comparative genomic distribution of the HERV-K (HML-2) group of human endogenous retroviruses. *Retrovirology*, *8*, 90. doi: 10.1186/1742-4690-8-90

Sugimoto, J., Matsuura, N., Kinjo, Y., Takasu, N., Oda, T., & Jinno, Y. (2001). Transcriptionally active HERV-K genes: Identification, isolation, and chromosomal mapping. *Genomics*, *72*(2), 137–144. doi: 10.1006/geno.2001.6473

Sutkowski, N., Conrad, B., Thorley-Lawson, D. A., & Huber, B. T. (2001). Epstein-Barr virus transactivates the human endogenous retrovirus HERV-K18 that encodes a superantigen. *Immunity*, *15*(4), 579–589. doi: 10.1016/S1074-7613(01)00210-2

Suwanthawornkul, T., Anothaisintawee, T., Sobhonslidsuk, A., Thakkinstian, A., & Teerawattananon, Y. (2015). Efficacy of second generation direct-acting antiviral agents for treatment naïve hepatitis C genotype 1: A systematic review and network meta-analysis. *PLoS ONE*, *10*(12). doi: 10.1371/journal.pone.0145953

Tabll, A., El Shenawy, R., Elsharkawy, H., & Mohamed, F. Z. (2019). Serum inducible protein-10 chemokine as a biomarker for clearance of HCV with and without treatment in Egyptian patients. *Human Antibodies*, *27*(4), 265–273. doi: 10.3233/HAB-190381

Tai, A. K., Luka, J., Ablashi, D., & Huber, B. T. (2009). HHV-6A infection induces expression of HERV-K18-encoded superantigen. *Journal of Clinical Virology*, *46*(1), 47–48. doi: 10.1016/j.jcv.2009.05.019

Takahata, N., & Satta, Y. (1997). Evolution of the primate lineage leading to modern humans: Phylogenetic and demographic inferences from DNA sequences. *Proceedings of the National*

Academy of Sciences of the United States of America, *94*(9), 4811–4815. doi: 10.1073/pnas.94.9.4811

Tassabehji, M., Strachan, T., Anderson, M., Duncan Campbell, R., Collier, S., & Lako, M. (1994). Identification of a novel family of human endogenous retroviruses and characterization of one family member, HERV-K(C4), located in the complement C4 gene cluster. *Nucleic Acids Research*, *22*(24), 5211-5217. doi: 10.1093/nar/22.24.5211

Tavakolian, S., Goudarzi, H., & Faghihloo, E. (2019). Evaluating the expression level of HERV-K env, np9, rec and gag in breast tissue. *Infectious Agents and Cancer*, *14*(1), 42. doi: 10.1186/s13027-019-0260-7

Tavakolian, S., Goudarzi, H., Lak, E., & Faghihloo, E. (2019). The evaluation of HERV-K env, np9, rec, gag expression in normal, polyp and cancerous tissues of gastric and colon. *Future Virology*, *14*(12), 805–812. doi: 10.2217/fvl-2019-0114

Tosato, G., Seamon, K., Goldman, N., Sehgal, P., May, L., Washington, G., ... Pike, S. (1988). Monocyte-derived human B-cell growth factor identified as interferon-beta 2 (BSF-2, IL-6). *Science*, *239*(4839), 502–504. doi: 10.1126/science.239.4839.502

Tovo, P.-A., Garazzino, S., Daprà, V., Alliaudi, C., Silvestro, E., Calvi, C., ... Bergallo, M. (2020). Chronic hcv infection is associated with overexpression of human endogenous retroviruses that persists after drug-induced viral clearance. *International Journal of Molecular Sciences*, *21*(11). doi: 10.3390/ijms21113980

Trela, M., Nelson, P. N., & Rylance, P. B. (2016). The role of molecular mimicry and other factors in the association of Human Endogenous Retroviruses and autoimmunity. *APMIS*, *124*(1-2), 88–104. doi: 10.1111/apm.12487

Tyagi, R., Li, W., Parades, D., Bianchet, M. A., & Nath, A. (2017). Inhibition of human endogenous retrovirus-K by antiretroviral drugs. *Retrovirology*, *14*(1), 21. doi: 10.1186/s12977-017-0347-4

Vincendeau, M., Göttesdorfer, I., Schreml, J. M. H., Wetie, A. G. N., Mayer, J., Greenwood, A. D., ... Leib-Mösch, C. (2015). Modulation of human endogenous retrovirus (HERV) transcription during persistent and de novo HIV-1 infection. *Retrovirology*, *12*(1), 27. doi: 10.1186/s12977-015-0156-6

Viola, M. V., Frazier, M., White, L., Brody, J., & Spiegelman, S. (1975). RNA instructed DNA polymerase activity in a cytoplasmic particulate fraction in brains from Guamanian patients. *Journal of Experimental Medicine*, *142*(2), 483–494. doi: 10.1084/jem.142.2.483

Vorstand der Bundesärztekammer auf Empfehlung des Wissenschaftlichen Beirats. (2014). *Querschnitts-Leitlinien (BÄK) zur Therapie mit Blutkomponenten und Plasmaderivaten.* Re-

trieved 2020-08-17, from https://www.bundesaerztekammer.de/fileadmin/user_upload/downloads/QLL_Haemotherapie_2014.pdf

Wallace, T. A., Downey, R. F., Seufert, C. J., Schetter, A., Dorsey, T. H., Johnson, C. A., ... Glynn, S. A. (2014). Elevated HERV-K mRNA expression in PBMC is associated with a prostate cancer diagnosis particularly in older men and smokers. *Carcinogenesis*, *35*(9), 2074–2083. doi: 10.1093/carcin/bgu114

Wan, S., Kuo, N., Kryczek, I., Zou, W., & Welling, T. H. (2015). Myeloid cells in hepatocellular carcinoma. *Hepatology*, *62*(4), 1304-1312. doi: 10.1002/hep.27867

Wang, P., Wu, P., Siegel, M. I., Egan, R. W., & Billah, M. M. (1995). Interleukin (IL)-10 inhibits nuclear factor kappa B (NF kappa B) activation in human monocytes. IL-10 and IL-4 suppress cytokine synthesis by different mechanisms. *The Journal of biological chemistry*, *270(16)*, 9558-9563.

Wang-Johanning, F., Liu, J., Rycaj, K., Huang, M., Tsai, K., Rosen, D. G., ... Johanning, G. L. (2007). Expression of multiple human endogenous retrovirus surface envelope proteins in ovarian cancer. *International Journal of Cancer*, *120*(1), 81–90. doi: 10.1002/ijc.22256

Wang-Johanning, F., Radvanyi, L., Rycaj, K., Plummer, J. B., Yan, P., Sastry, K. J., ... Johanning, G. L. (2008). Human endogenous retrovirus K triggers an antigen-specific immune response in breast cancer patients. *Cancer Research*, *68*(14), 5869–5877. doi: 10.1158/0008-5472.CAN-07-6838

Wardell, A. D., Errington, W., Ciaramella, G., Merson, J., & McGarvey, M. J. (1999). Characterization and mutational analysis of the helicase and NTPase activities of hepatitis C virus full-length NS3 protein. *Journal of General Virology*, *80*(3), 701–709. doi: 10.1099/0022-1317-80-3-701

Wedemeyer, H., Dore, G. J., & Ward, J. W. (2015). Estimates on HCV disease burden worldwide - Filling the gaps. *Journal of Viral Hepatitis*, *22*(s1), 1–5. doi: 10.1111/jvh.12371

Wei, B., Ji, F., Yeo, Y. H., Ogawa, E., Stave, C. D., Dang, S., ... Nguyen, M. H. (2018). Systematic review and meta-analysis: Real-world effectiveness of direct-acting antiviral therapies in chronic hepatitis C genotype 3 in Asia. *BMJ Open Gastroenterology*, *5*(1). doi: 10.1136/bmjgast-2018-000209

Weis, S., Llenos, I. C., Sabunciyan, S., Dulay, J. R., Isler, L., Yolken, R., & Perron, H. (2007). Reduced expression of human endogenous retrovirus (HERV)-W GAG protein in the cingulate gyrus and hippocampus in schizophrenia, bipolar disorder, and depression. *Journal of Neural Transmission*, *114*(5), 645–655. doi: 10.1007/s00702-006-0599-y

Wiegand, J., Kaiser, T., Lobstein, S., Brand, F., Wojan, M., Stölzel, U., ... Tillmann, H. L. (2006). Low prevalence of chronic hepatitis C, but high prevalence of elevated aminotransferases in

a cohort of 2026 patients referred for orthopaedic surgery in the eastern part of Germany. *Zeitschrift für Gastroenterologie*, *44*(1), 11–14. doi: 10.1055/s-2005-858876

Wiesner, R., Edwards, E., Freeman, R., Harper, A., Kim, R., Kamath, P., ... Krom, R. (2003). Model for end-stage liver disease (meld) and allocation of donor livers. *Gastroenterology*, *124 (1)*, 91-96. doi: https://doi.org/10.1053/gast.2003.50016

World Health Organization. (2017). *Global Hepatitis Report, 2017.* Retrieved 2020-08-16, from `https://apps.who.int/iris/bitstream/handle/10665/255016/9789241565455-eng.pdf;jsessionid=911F0535FB77693EE806532E03CB3E96?sequence=1`

World Health Organization. (2020). *Hepatitis C.* Retrieved 2020-08-16, from `https://www.who.int/news-room/fact-sheets/detail/hepatitis-c`

Yoshimura, A., Mori, H., Ohishi, M., Aki, D., & Hanada, T. (2003). Negative regulation of cytokine signaling influences inflammation. *Current Opinion in Immunology*, *15*(6), 704 - 708. doi: 10.1016/j.coi.2003.09.004

You, S., Stump, D. D., Branch, A. D., & Rice, C. M. (2004). A cis-Acting Replication Element in the Sequence Encoding the NS5B RNA-Dependent RNA Polymerase Is Required for Hepatitis C Virus RNA Replication. *Journal of Virology*, *78*(3), 1352–1366. doi: 10.1128/jvi.78.3.1352-1366.2004

Yu, H. L., Zhao, Z. K., & Zhu, F. (2013). The role of human endogenous retroviral long terminal repeat sequences in human cancer (Review). *International Journal of Molecular Medicine*, *32*(4), 755–762. doi: 10.3892/ijmm.2013.1460

Yu, P., Lübben, W., Slomka, H., Gebler, J., Konert, M., Cai, C., ... Bauer, S. (2012). Nucleic Acid-Sensing Toll-like Receptors Are Essential for the Control of Endogenous Retrovirus Viremia and ERV-Induced Tumors. *Immunity*, *37*(5), 867–879. doi: 10.1016/j.immuni.2012.07.018

Zaidi, D., Huynh, H. Q., Carroll, M. W., Baksh, S., & Wine, E. (2018). Tumor necrosis factor α-induced protein 3 (A20) is dysregulated in pediatric Crohn disease. *Clinical and Experimental Gastroenterology*, *11*, 217–231. doi: 10.2147/CEG.S148217

Zeuzem, S. (2017). Treatment options in hepatitis C - The current state of the art. *Deutsches Ärzteblatt International*, *114*(1-2), 11–21. doi: 10.3238/arztebl.2017.0011

Zoratti, M. J., Siddiqua, A., Morassut, R. E., Zeraatkar, D., Chou, R., van Holten, J., ... Druyts, E. (2020). Pangenotypic direct acting antivirals for the treatment of chronic hepatitis C virus infection: A systematic literature review and meta-analysis. *EClinicalMedicine*, *18*, 100237. doi: 10.1016/j.eclinm.2019.12.007